JAN. - APR. 1998
Volume IV Number I

ISSN 0859 144X

THE ASEAN JOURNAL OF RADIOLOGY

Published by The Radiological Society and
The Royal College of Radiologists of Thailand,
Bangkok, Thailand

Supported through an educational grant from

TOSHIBA

GLOBAL IMAGING ▪ MEDICAL SYSTEMS

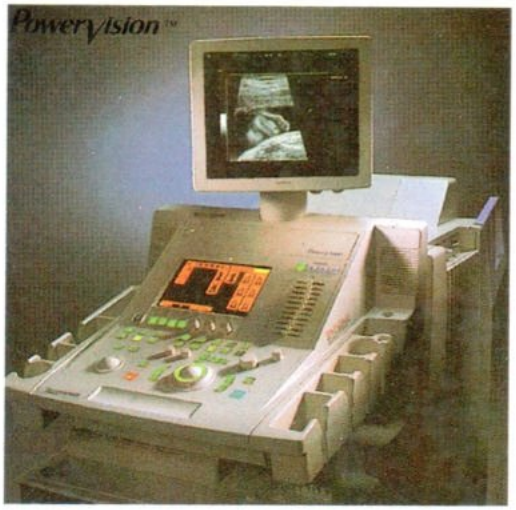

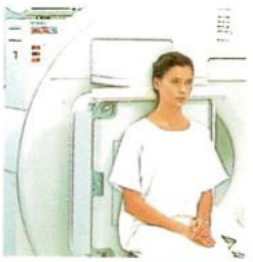

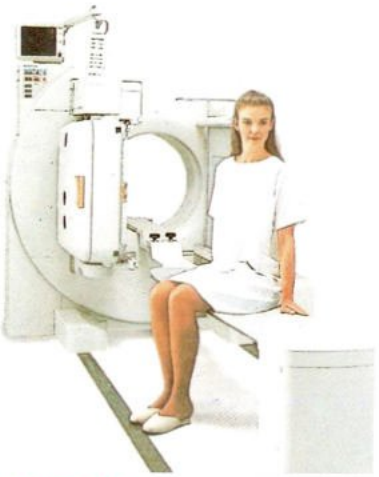

DIGITAL GAMMACAMERA SYSTEM

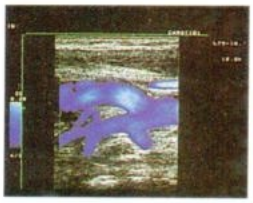

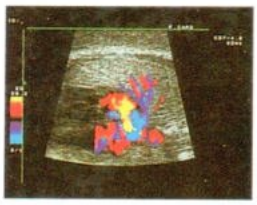

FULLY-DIGITAL ULTRASOUND SYSTEM

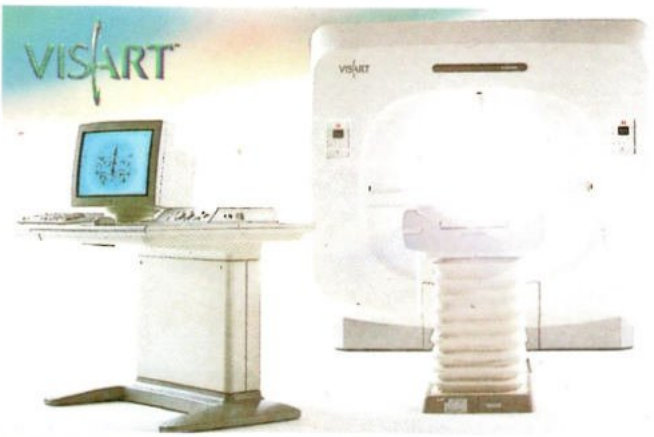

MAGNETIC RESONANCE IMAGING SYSTEM

Xtension

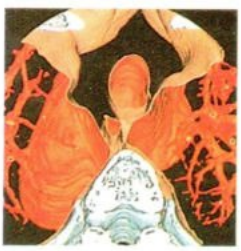

WORKSTATION

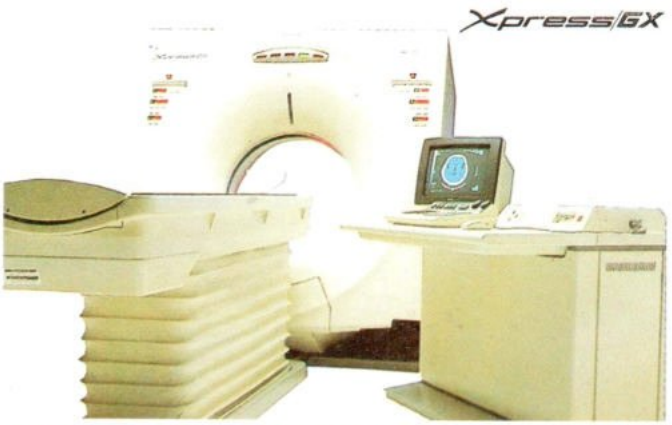

COMPUTED TOMOGRAPHY SYSTEM

CMC BIOTECH

(SOLE DISTRIBUTOR)

CMC BIOTECH CO., LTD.
HEAD OFFICE : 364 LADPHRAO 94, WANGTHONGLANG, BANGKOK 10310
TEL: 530-4995-6, 559-3261-2 FAX : 539-6903
NORTH EASTERN BRANCH :
301/155 MUBAN KHON KAEN VILLA, MITTRAPAB ROAD, AMPHUR MUANG, KHON KAEN 40000
TEL: (043) 246-210 FAX : (043) 244-729 PAGER 151, 152 CALL 759823
SOUTHERN BRANCH :
306 PRACHAYINDEE ROAD, KHORHONG HADYAI, SONGKHLA 90110
TEL: (074) 356259 FAX : (074) 364-004 MOBILE PHONE : 01-445-3755 PAGER 151, 152 CALL 653571
NORTHERN BRANCH :
27 NIMMANHAEMIN ROAD, SOI 11 SUTHEP, AMPHUR MUANG, CHIANGMAI 50000
TEL: (053) 894-807 MOBILE PHONE : 01-914-8292 PAGER 151, 152 CALL 759803

JAN. - APR. 1998
Volume IV Number I

ISSN 0859 144X

THE ASEAN JOURNAL OF RADIOLOGY

Published by The Radiological Society and
The Royal College of Radiologists of Thailand,
Bangkok, Thailand

Supported through an educational grant from

THE ASEAN JOURNAL OF RADIOLOGY

Volume IV Number I JAN. - APR. 1998

CONTENTS

THE ASEAN JOURNAL OF RADIOLOGY

Volume IV Number I JAN. - APR. 1998

CONTENTS

RADIOPHARMACEUTICAL FOR IMAGING OF LIVER, GALL BLADDER AND BILIARY DUCTS(^{99m}TC-DISIDA)

Nisarut RUKSAWIN M.S.

ABSTRACT

The cholescintigraphic procedures have played a significant role in diagnosis of hepatobiliary disorder in Thailand. Especially ^{99m}Tc-DISIDA scintigrams of infants are the diagnosis procedures of choice for biliary atresia because it is difficult to diagnose by other means for examples CT and ultrasonography. The synthesis of DISIDA (2,6-diisopropylacetanilide iminodiacetic acid), was prepared successfully since 1983 at Section of Nuclear Medicine, Siriraj Hospital. The DISIDA compound was made into DISIDA instant kits by adding appropriate amount of stannous chloride. Each kit contained 10 mg of DISIDA and 0.25 mg of $SnCl_2.2H_2O$. Radiochemical purity was good at 2-4 ml of Na $^{99m}TcO_4$ (activity of 1 to 50 mCi) and lasted for 6 hours. The Lyophilized form of DISIDA-kit had stability not less than 1 year. No reports of unfavorable effects on patients with this product during the past 14 years.

INTRODUCTION

It is unfavourable to use ^{131}I compound for liver diagnosis especially with scinticamera imaging because of its high gamma energy . The absorbed radiation dose of ^{131}I is too high when comparing with ^{99m}Tc. ^{99m}Tc is one of the ideal radionuclides for the diagnostic purpose. It is carrier free and its isotopic abundance is 100%. The chemical mass is negligible and the binding sites of such compound as DISIDA (2,6-diisopropylacetanilide iminodiacetic acid) should be able to bind relatively large quantities of ^{99m}Tc. This radionuclide also decay to give a high photon yield of good energy (90%,140 KeV). The advantages of this radiopharmaceutical include its safety and accuracy with low radiation dose[1] and decreased dependence on hepatic function. A unique feature is their ability to depict the physiology and dynamics of biliary excretion.[2,3,4]

MATERIALS AND METHODS

Analytical grade or equivalent reagent chemicals, water, sterilized and pyrogen free, as well as sterile disposible syringes were used in all procedures. Sodium pertechnetate ($Na^{99m}TcO_4$) was obtained from DAINATEC generator from Japan. Lyophilization was achieved in a Hetosicc Freeze dryer type CD-13.2. The preparation was carried out in a Nuaire larminar flow biological safety cabinet. The electrophoretic mobility studies were carried out using Whatman No.1 paper strips (1 inch wide) in veronal buffer, pH=8.6, μ=0.075M, at a potential 200 volts for 4 hours in 5^0C surroundings.[5,6] The paper were placed under gamma camera. The radiochemical purity was determined by selecting areas of interest regions by the computer. The animal experiments were conducted in adult rabbits.

Section of Nuclear Medicine, Department of Radiology, Siriraj Hospital Bangkok, Thailand

1. Preparation of *a* chloro-2',6'diisopropylacetanilide

31.7 ml of 2,6-diisopropylanilide was dissolved in 150 ml of acetone and cooled in ice-bath. 21 ml of chloroacetyl chloride was added dropwise to the amine solution and allowed to stand for one hour. The solution was then poured into 200 ml of 10% HCl. The precipitate was collected by using Buchner filter set and washed with 0.01% HCl. Recrystallization was performed by dissolving the precipitate with 500 ml of 99.9% ethanol and 200 ml of distilled water was slowly added then the *a* chloro-2',6'diisopropylacetanilide was collected. Recrystallization was done again by using the same method until the *a* chloro-2',6' diisopropylacetanilide was very pure.[7]

2. Preparation of 2,6-diisopropylacetanilide iminodiacetic acid (DISIDA)

10 g of iminodiacetic acid was dissolved in 80 ml of distilled water, 5 g of *a* chloro-2',6' diisopropylacetanilide was dissolved in 100 ml ethanol. Under 80°C reflux, the latter was slowly dropped from the separating funnel to the former. After 20 hours the reaction was complete, ethanol was removed by distillation at 45°C for 4 hours. The residue was acidified with 37% HCl. The precipitate was collected on sintered filter and washed with distilled water. The product was purified 3 times by recrystallization using the above method. Finally the precipitate was dissolved in 300 ml of ethanol and 150 ml of water and allowed to crystallize in the freezer. The product was collected and washed with cold ethanol, dried and stored.[8,9]

3. Preparation of DISIDA kits

1 g of DISIDA was suspended in 50 ml of distilled water for injection and dissolution was effected by the gradual addition of about 0.4 ml of 40% NaOH while stirring to a pH of 6 to 6.5. This solution was called solution A. 1 g of $SnCl_2.2H_2O$ was dissolved in 5 ml of concentrated HCl. This solution was stirred at least 30 min. and 15 ml of water for injection was added and called solution B. 0.5 ml of solution B was added to solution A. Then it was mixed well and readjusted pH to 6 with 0.1 ml of 40%NaOH. The solution was sterilized by passing through 0.22μm membrane filter and transfered 0.5 ml each to 7 ml presterilized serum vials. The content of each of the vials were lyophilized and closed with rubber closures. The process of closing the rubber was done in vacuum by using autometic stoppering arrangement. Finally, the vials with rubber closures were sealed with aluminium caps and stored at 0-5°C. Each kit contained 10 mg of DISIDA and 0.25 mg of $SnCl_2.2H_2O$.[10]

4. Lebelling DISIDA with ^{99m}Tc

2-4 ml of $Na^{99m}TcO_4$ (activity of 1 to 50 mCi) was added to DISIDA kit and mixed well. Let stand at least 5 min.

5. Quality control of ^{99m}Tc-DISIDA

Each lot of DISIDA kits has to be tested for radiochemical purity, stability, apyrogenicity, sterility and specific activity. The procedure will be explained as follows.

Assay The electrophoretic mobility studies were carried out using Whatman No.1 paper strips (1 inch wide) in veronal buffer pH 8.6, μ = 0.075M, at a potential gradient of 200 Volts for 4 hours, at 5°C atmosphere. The strips of paper were placed under gamma camera. Immages were recorded and data were stored on computer. Areas of interest were selected for ^{99m}Tc-DISIDA, ^{99m}Tc-Sn-colloid, free $^{99m}TcO_4$ and the whole paper strip regions as shown in Fig.1. The radiochemical purity was determined by dividing the activity at ^{99m}Tc-DISIDA area by the activity of the whole paper strip. It was found that more than 95% of the total activity was associated with ^{99m}Tc-DISIDA zone and less than 5% as free $^{99m}TcO_4$ plus ^{99m}Tc-Sn-colloid in the preparation.

Stability Shelf-life of the radiopharmaceutical is one year. The results showed that the DISIDA kit had excellent properties both in vitro and in vivo tests. Bench-life of the preparation was 6 hours.

Apyrogenicity 2 mCi in 1 ml of ^{99m}Tc-DISIDA was injected to three healthy adult rabbits. The results showed that our DISIDA kits met the requirement for the absence of pyrogen.[11]

Sterility The first and the last vials were sent to the Department of Microbiology for sterility test, the results were negative.

Specific activity Our kits could be mixed with 2 to 4 ml of 1-50 mCi of Na $^{99m}TcO_4$.

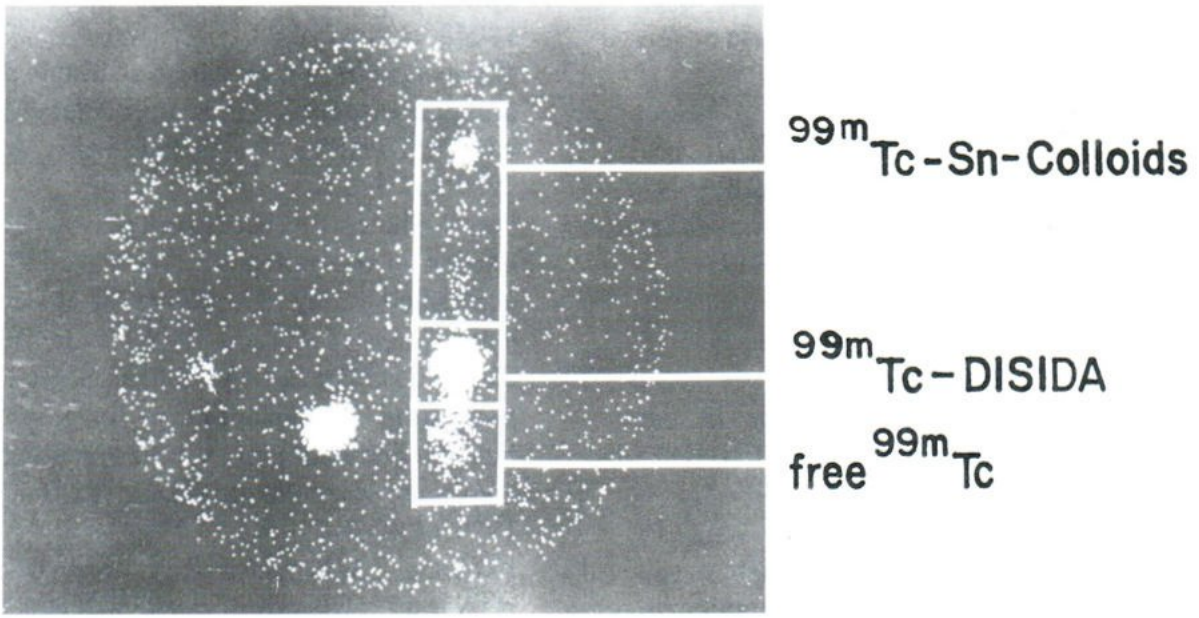

Fig. 1. Areas of interest were selected for ^{99m}Tc-DISIDA, ^{99m}Tc-Sn-colloid and free pertechnetate.

RESULTS AND DISCUSSION

a chloro-2',6'diisopropylacetanilide was synthesized from 2,6-diisopropylanilide and chloroacetylchloride. DISIDA (2',6'diisopropylacetanilide iminodiacetic acid) was synthesized from *a* chloro-2',6'diisopropylacetanilide and iminodiacetic acid. The DISIDA was made as DISIDA instant kit by addition of an appropriate amount of stannous chloride and stored in lyophilized form. DISIDA instant kit was used routinely instead of ^{131}I BSP. Radiographic immaging procedures such as oral cholecystography served a very useful purpose, but several of them are invasive and involve a certain degree of risk from the administered contrast media as well as discomfort to the patient. Cholescintigraphy have proved to be the most sensitive method available for documenting cystic duct patency or obstruction[12-17] and had become the diagnostic procedure of choice for acute cholecystitis.[12,18] In addition it has proved useful in postoperative patients because of its ability to evaluate ductal obstruction as well as detect the presence of cystic duct remnants and biliary leakage. Diagnosis of these organic causes of postcholecystectomy syndrome can result in relief of symptoms via appropriate therapy. By the same token, exclusion of these disorders can permit internist or surgeon to search elsewhere for the patient's cause of distress.[4]

Generally surgeons have been less enthusiastic about the role of nuclear imaging in clinical situations. This has been because(1) several nuclear imaging procedures have a limited diagnostic accuracy.(2) the scans generated often suffer from a lack of specificity and (3) the examinations have not been readily available and often had to be scheduled as special procedures. Despite these prior prejudices, their experiences with iminodiacetic (IDA) imaging of the biliary tract are changing their attitude.

REFERENCES

1. Chervu R, Nunn A, Loberg M. Radiopharmaceuticals for hepatobiliary imaging. Seminars in Nucl Med 1982;12:5-17.
2. Gliedman M, Wilk P. A surgeon's view of hepatobiliary scintigraphy. Seminars in Nucl Med 1982;12:2-4.
3. Rosenthall L. Cholescintigraphy in the presence of jaundice utilizing ^{99m}Tc-IDA. Seminars in Nucl Med 1982;12:53-63.
4. Weissmann H, Gliedman M, Wilk P, Sugarman L, Badia J, Guglielmo K, Freeman L. Evaluation of the postoperative patient with ^{99m}Tc-IDA cholescintigraphy. Seminars in Nucl Med 1982;12:27-52.
5. Noronha O, Sewatkar A, Ganatra R, Subramanian G. The transport, hepatobiliary distribution and clearance of ^{99m}Tc-Sn-Lidocaine iminodiacetic acid. Int J Nucl Med and Biol 1977;4:122-8.
6. Ruksawin N. Leukocytes labelling with ^{99m}Tc. Thesis, The University of Texas, M.D. Anderson Hospital and Tumor Institute, Houston, Texas, U.S.A. 1973.
7. Manual of radiopharmaceutical preparation. Division of nuclear medicine, Institute of medical and veterinary science, Adelaide, South Australia.
8. Loberg M, Cooper M, Harvey E, Cally P, Faith W. Development of new radiopharmaceuticals based on N-substitution of iminodiacetic acid. J Nucl Med 1976;17:633-8.
9. Callery P, Faith W, Loberg M, et al. Tissue distribution of ^{99m}Tc and ^{14}C labelled N-(2,6-dimethylphenylcarbamoyl-methyl) iminodiacetic acid. J Med Chem 1976;19:962.
10. Ruksawin N, Na Songkhla S, Pleehachinda R, Buranapong P, Suwanik R. Radiopharmaceutical for bone scanning. The Thai journal of radiology 1981;18:5-10.
11. U.S. Pharmacopeia XVIII, 18th revision, Mack publishing company, Easto PA. 18042,1970;856-87.
12. Weissmann H, Frank M, et al. Rapid and accurate diagnosis of acute cholecystitis with ^{99m}Tc-HIDA cholescintigraphy. AJR 1979;132:523-8.
13. Pare P, Shaffer EA, Rosenthall L. Nonvisualization of the gallbladder by ^{99m}Tc-HIDA cholescintigraphy as evidence of cholecystitis. Can Med Assoc J 1978;118:384-6.
14. Cheng TH, Davis MA, Seltzer SE, et al. Evaluation of hepatobiliary imaging by radionuclide scintigraphy, ultrasonography, and contrast cholangiography. Radiology 1979;133:761-7.
15. Ekelman EA, Cameron JL, Colman M, et al. A test for patency of cystic duct in acute cholecystitis. Ann Intern Med 1975;82:318-22.
16. Stadalnik RC, Matolo NM, Jansholt AL, et al. Technetium-99m pyridoxylideneglutamate (P.G.) cholescintigraphy. Radiology 1976;121:657-61.
17. Down RHL, Arnold J, Goldin A, et al. Comparison of accuracy of ^{99m}Tc- pyridoxylidene-glutamate scanning with oral cholecystography and ultrasonography in diagnosis of acute cholecystitis. Lancet 1979;-2:1094-7.
18. Weissmann H, Sugarman L, Frank M, et al. Serendipity in Technetium-99m dimethyl iminodiacetic acid cholescintigraphy. Radiology 1980;135:449-54.

ULTRASOUND OF FOCAL SPLENIC LESIONS IN PATIENTS WITH HUMAN IMMUNODEFICIENCY VIRUS

Pannee VISRUTARATNA, MD., Nitaya THONGSIBGAO, MD.

ABSTRACT

Abdominal ultrasonographic findings of 14 patients with human immunodeficiency virus (HIV) and focal lesions in the spleen were reviewed. There were solitary hypoechoic lesions in 2 patients and multiple hypoechoic lesions in 12 patients. The diagnoses were confirmed by hemoculture (6 patients), lymph node biopsy (5 patients), splenectomy (1 patient), bone marrow aspiration biopsy (1 patient), and response to therapy (1 patient). The causes of focal hypoechoic lesions in the spleen were tuberculosis (7 patients), salmonellosis (6 patients), and nocardiosis (1 patient). For HIV patients with focal hypoechoic lesions in the spleen, particularly in Northern Thailand, a diagnosis of tuberculosis, salmonellosis, or nocardiosis should be considered.

INTRODUCTION

Splenic abscess is an uncommon disease in general. In population-based autopsy studies the incidence of splenic abscess has been between 0.2 to 0.7 percent.[1] There are five distinct causes of splenic abscess: metastatic infection, contiguous infection, embolic noninfectious events causing ischemia and subsequent superinfection, trauma, and immunodeficiency.[1] As the number of patients with immunodeficiency, including that caused by cancer chemotherapy and acquired immunodeficiency syndrome has increased, the incidence of splenic abscess has also increased. The purpose of this study was to determine the causes of focal splenic lesions seen in ultrasonograms of patients with human immunodeficiency virus (HIV).

MATERIALS AND METHODS

Between 1992 and 1996, 14 patients with HIV and focal splenic lesions were examined by ultrasound at Chiang Mai University Hospital, 11 men and 3 women, aged between 18 to 38 years old. The diagnoses were confirmed by hemoculture (6 patients), lymph node biopsy (5 patients) , splenectomy (1 patient), bone marrow aspiration biopsy (1 patient), and response to therapy (1 patient). No focal splenic lesions were seen in follow-up ultrasonograms of 4 patients. The causes of the focal splenic lesions were tuberculosis (7 patients), salmonellosis (6 patients), and nocardiosis (1 patient).

RESULTS

CLINICAL HISTORIES. The most common clinical histories were fever (9 patients) and abdominal pain (7 patients). Others were neck mass (3 patients), cough (2 patients), and chest pain (1 patient). Physical examination revealed lymphadenopathy in 9 patients, and hepatomegaly in 4 patients.

Department of Radiology, Faculty of Medicine, Chiang Mai University, Chiang Mai 50200, Thailand.

ULTRASONOGRAPHIC FINDINGS. The ultrasonograms of the patients were reviewed for the length of the spleen, focal lesions, intra-abdominal lymphadenopathy, and ascites. A patient was considered to have splenomegaly when the length of spleen was more than 11 cm.[2] Splenomegaly was seen in only 3 patients, one with tuberculosis and two with salmonellosis. All focal splenic lesions were hypoechoic. The ultrasonographic findings are in Table 1.

In patients with tuberculosis the focal splenic lesions were smaller than 1 cm (Fig. 1), except for one patient who had a single 1.5 cm lesion. Intra-abdominal lymphadenopathy was seen in almost all patients. Enlarged lymph nodes were seen at the splenic hilum in one patient (Fig. 2). In another patient abscesses of the psoas muscles were seen (Fig. 3).

Salmonellosis was caused by *S. enteritidis* in 3 of our patients, *S. choleraesuis* in 2 patients, and an unknown species in 1 patient. Three patients had multiple focal splenic lesions smaller than 1 cm (Fig. 4). Another patient had a 1.5 cm splenic lesion. The two other patients had three splenic lesions, which were 2-4 cm (Fig. 5). Only one patient with salmonellosis had intra-abdominal lymphadenopathy.

The single patient with nocardiosis had multiple focal splenic lesions smaller than 1 cm (Fig. 6) and intra-abdominal lymphadenopathy.

Table 1. Causes of focal splenic lesions and ultrasonographic findings

Causes/Ultrasonographic findings	No. of patients
M. tuberculosis	7
Splenomegaly	1
Single focal splenic lesion	1
Two focal splenic lesions	1
Multiple focal splenic lesions	5
Intra-abdominal lymphadenopathy	6
Ascites	1
Abscesses of psoas muscles	1
Salmonella species	6
Splenomegaly	2
Single focal splenic lesion	1
Two focal splenic lesions	0
Three focal splenic lesions	2
Multiple focal splenic lesions	3
Intra-abdominal lymphadenopathy	1
Ascites	0
Nocardia species	1
Multiple focal splenic lesions	1
Intra-abdominal lymphadenopathy	1

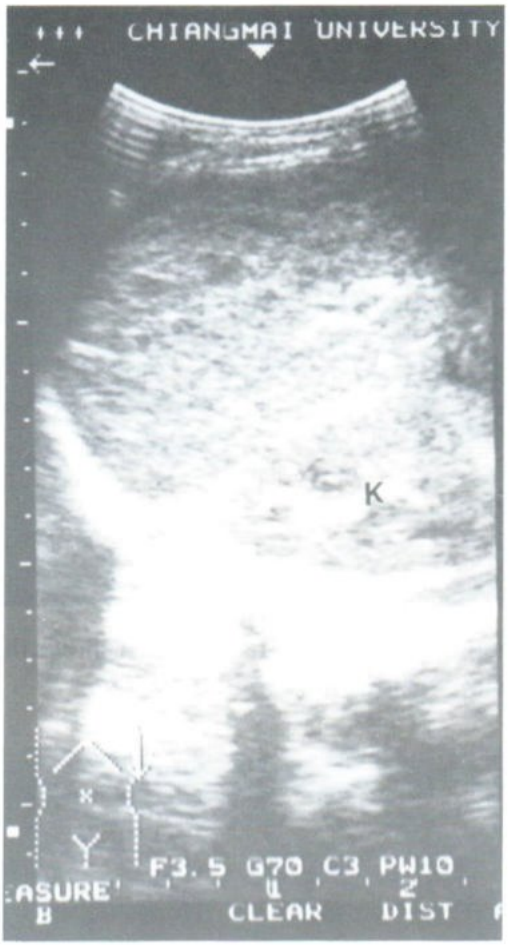

Fig.1 Tuberculosis. Sagittal ultrasonogram shows multiple hypoechoic lesions in the spleen (K = left kidney).

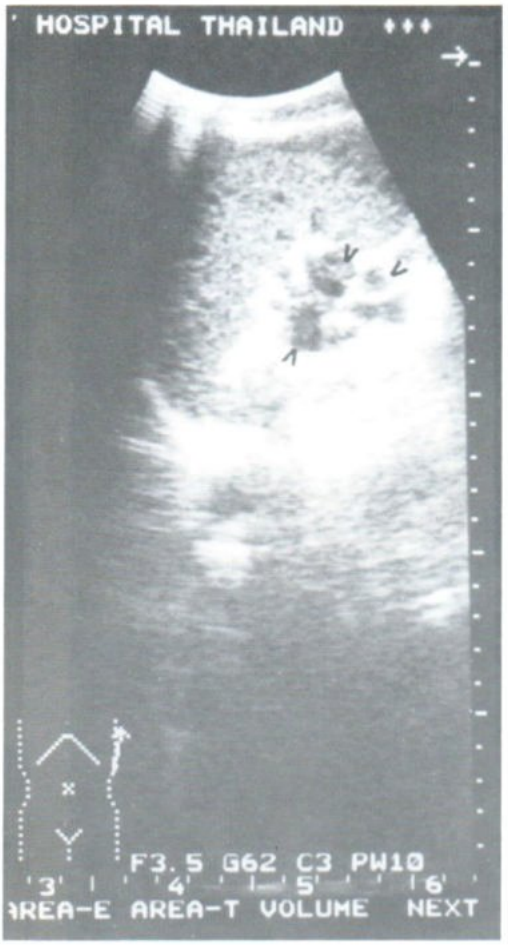

Fig.2 Tuberculosis. Sagittal ultrasonogram shows multiple hypoechoic lesions in the spleen. Note enlarged lymph nodes at the splenic hilum (arrows).

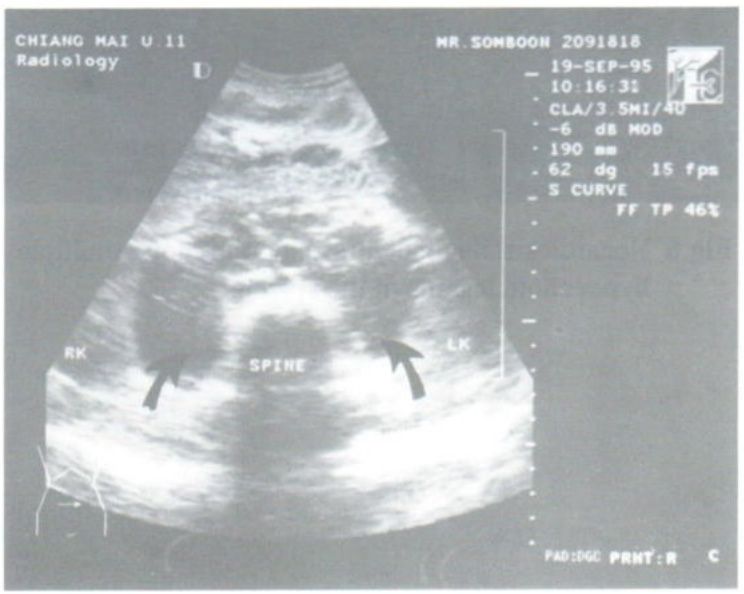

Fig.3 Tuberculosis. Transverse ultrasonogram shows bilateral psoas abscesses (arrows) and enlarged retroperitoneal lymph nodes (RK = right kidney, LK = left kidney).

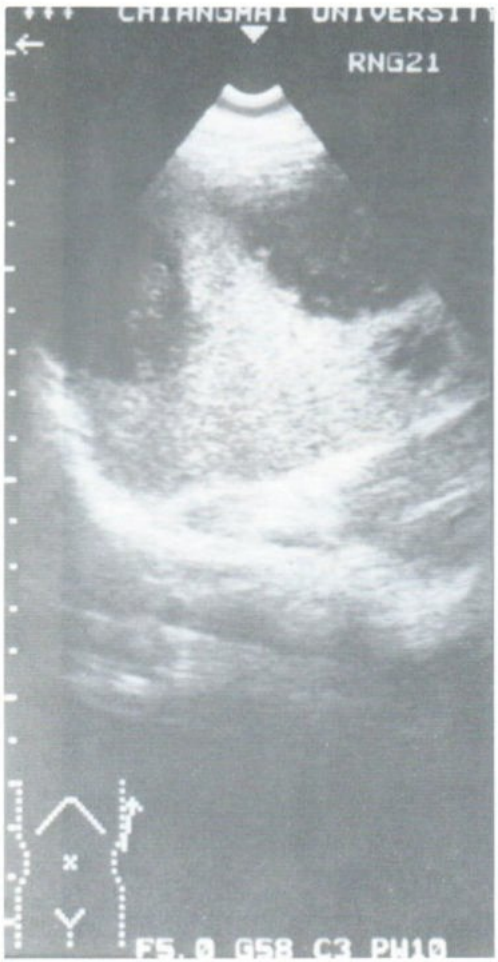

Fig.4 Salmonellosis. Sagittal ultrasonogram shows multiple hypoechoic lesions in the spleen.

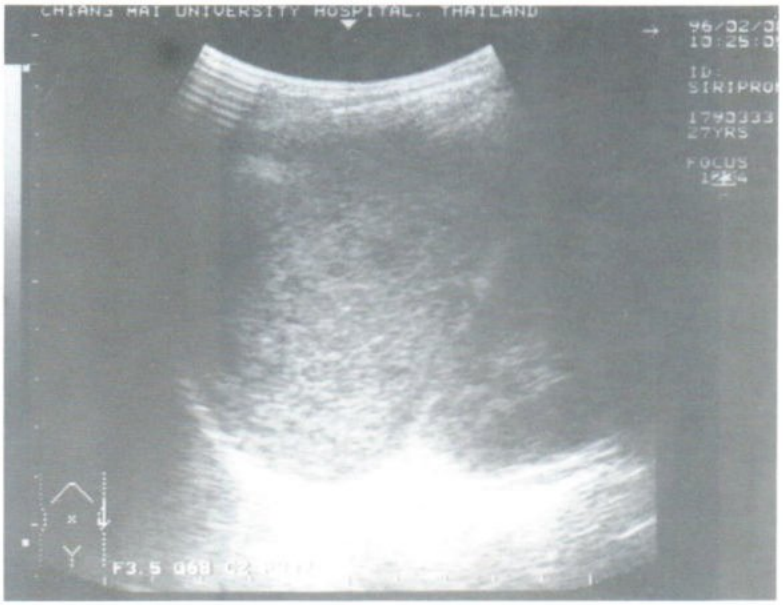

Fig.5 Salmonellosis. Sagittal ultrasonogram shows three hypoechoic lesions 2-4 cm in the spleen.

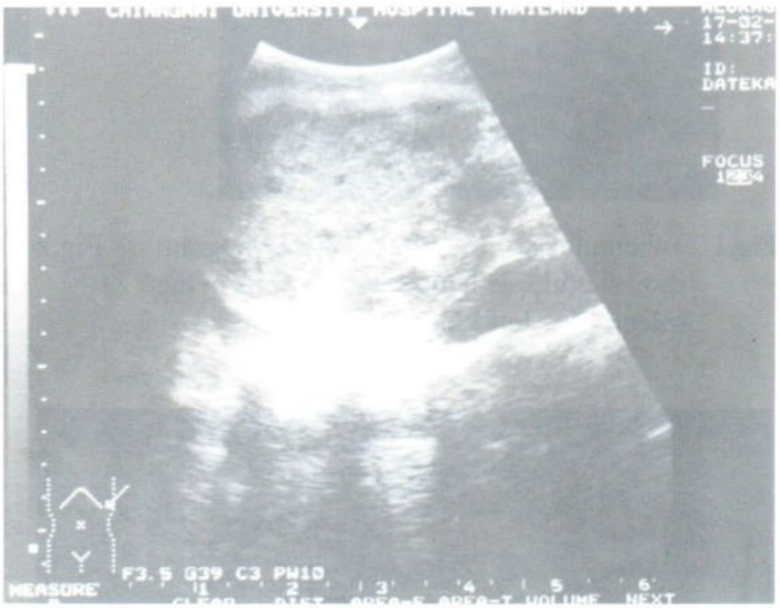

Fig.6 Nocardiosis. Sagittal ultrasonogram shows multiple hypoechoic lesions in the spleen.

DISCUSSION

Before the AIDS epidemic splenic abscess was an uncommon disease. The most frequently cultured organisms from splenic abscess were *Streptococci*, *Staphylococci*, and *Salmonellae*.[3] The most common symptoms described were fever and abdominal pain.

Since the spread of AIDS worldwide, there has been an increase of splenic abscess in AIDS patients.[4-8] The reasons may be severe depletion of lymphoid tissue, as has been seen in the histopathology of the spleen in AIDS[7, 9] and the common involvement of the spleen in systemic diseases.

The causes of focal splenic lesions in patients with HIV infection are infection and tumors. Hyperechoic splenic lesions have been reported in Kaposi sarcoma,[5] *Pneumocystic carinii* infection,[10] and *Mycobacterium avium-intracellulare* (MAI) infection.[11] Hypoechoic splenic lesions have also been reported in tuberculosis, MAI infection, fungal infection, lymphoma, and bacillary angiomatosis.[5,11,12]

In the abdomen tuberculosis can affect the gastrointestinal tract, peritoneum, lymph nodes, liver, spleen, or pancreas. Splenomegaly is the most common splenic involvement in tuberculosis.[13] Tuberculosis of the spleen usually occurs in the miliary form with nodules ranging from 0.5-2 mm in diameter, which cannot be detected on CT scans.[14] The macronodular form of splenic tuberculosis is extremely rare with multiple low-density masses on CT scans or hypoechoic masses on ultrasonograms.[15]

In a review of CT scans of 259 patients with HIV infection, low attenuation lesions in the spleen were found in 21% (55 patients).[4] The splenic lesions were almost always multiple. Three-fourths of the patients with splenic lesions smaller than 1 cm had tuberculosis. This is consistent with ultrasonographic findings in most of our tuberculosis patients, who had multiple hypoechoic splenic lesions smaller than 1 cm. Murray et al. also found multiple small hypoechoic splenic lesions in ultrasonograms of 6 AIDS patients with tuberculosis.[5] Focal hepatic or splenic lesions are rare manifestations of MAI infection.[6] Even though it is not possible to distinguish between this infection and *M. tuberculosis* infection without cultures, tuberculosis should be considered first in endemic areas such as Northern Thailand.

Our series consisted of only 14 patients, too small for statistical analysis. However, HIV patients with tuberculosis tend to have multiple small hypoechoic lesions in the spleen with enlarged intra-abdominal lymph nodes.

Salmonellal splenic abscess in HIV-infected patients has been reported.[16,17] One patient had two splenic abscesses caused by *S. enteritidis*.[16] Another patient had an 11 cm splenic abscess caused by *S. typhimurium*.[17] Our patients had salmonellal splenic abscesses of varying sizes and numbers.

Nocardiosis is an uncommon opportunistic infection in HIV patients. *Nocardia* can cause lung disease and abscesses in various organs.[18] In our study we found only one nocardiosis patient with multiple hypoechoic splenic lesions and multiple enlarged intra-abdominal lymph nodes.

CONCLUSION

The incidence of opportunistic infections and tumors in HIV patients varies geographically. In Northern Thailand, for HIV patients with focal hypoechoic lesions in the spleen, a diagnosis of tuberculosis, salmonellosis, or nocardiosis should also be considered.

REFERENCES

1. Nelken N, Ignatius J, Skinner M, Christensen N. Changing clinical spectrum of splenic abscess: a multicenter study and review of the literature. Am J Surg 1987;-154:27-34.
2. Taylor KJW, Aronson D. Spleen. In: Goldberg BB, ed. Textbook of abdominal ultrasound. Baltimore: Williams & Wilkins, 1993;202-220.
3. Chun CH, Raff MJ, Contreras L, et al. Splenic abscess. Medicine 1980;59(1): -50-65.
4. Radin R. HIV infection: analysis in 259 consecutive patients with abnormal abdominal CT findings. Radiology 1995;-197:712-722.
5. Murray JG, Patel MD, Lee S, Sandhu JS, Feldstein VA. Microabscesses of the liver and spleen in AIDS: detection with 5-MHz sonography. Radiology 1995;197:723-727.
6. Radin DR. Intraabdominal *Mycobacterium tuberculosis* vs *Mycobacterium avium-intracellulare* infections in patients with AIDS: distinction based on CT findings. AJR 1991;156:487-491.
7. Klatt EC, Meyer PR. Pathology of the spleen in the acquired immunodeficiency syndrome. Arch Pathol Lab Med 1987;-111:1050-1053.
8. Mathew A, Raviglione MC, Niranjan U, Sabatini MT, Distenfeld A. Splenectomy in patients with AIDS. Am J Hematol 1989;-32:184-189.
9. Welch K, Finkbeiner W, Alpers CE, et al. Autopsy findings in the acquired immune deficiency syndrome. JAMA 1984;252:-1152-1159.
10. Radin DR, Baker EL, Klatt EC, et al. Visceral and nodal calcification in patients with AIDS-related *Pneumocystic carinii* infection. AJR 1990;154:27-31.
11. Smith FJ, Mathieson JR, Cooperberg PL. Abdominal abnormalities in AIDS: detection at US in a large population. Radiology 1994;192:691-695.
12. Moore EH, Russell LA, Klein JS, et al. Bacillary angiomatosis in patients with AIDS: multiorgan imaging findings. Radiology 1995;197:67-72.
13. Lundstedt C, Nyman R, Brismar J, Hugosson C, Kagevi I. Imaging of tuberculosis II. Abdominal manifestations in 112 patients. Acta Radiol 1996;37:489-495.
14. Sheen-Chen SM, Chou FF, Wan YL, Eng HL. Tuberculosis presenting as a solitary splenic tumour. Tuber Lung Dis 1995;76:80-83.
15. Kapoor R, Jain AK, Chaturved U, Saha MM. Ultrasound detection of tuberculomas of the spleen. Clin Radiol 1991;43:128-129.
16. Torres JR, Gotuzzo E, Isturiz R, et al. Salmonellal splenic abscess in the antibiotic era: a Latin American perspective. Clin Infect Dis 1994;19:871-875.
17. Van der Laan RT, Verbeeten B, Smits NJ, Lubbers MJ. Computed tomography in the diagnosis and treatment of solitary splenic abscess. J Comput Assist Tomogr 1989;-13(1):71-74.
18. Javaly K, Horowitz HW, Wormser GP. Nocardiosis in patients with human immunodeficiency virus infection: report of 2 cases and review of the literature. Medicine 1992;71(3):128-138.

A CASE OF SIMULTANEOUS HEPATIC, SMALL INTESTINAL, AND ADRENAL CAVERNOUS HEMANGIOMAS

Pannee VISRUTARATNA, MD., Wattanawan AUEPITAKSAKUL, MD.

ABSTRACT

We report a case of multiple cavernous hemangiomas of the liver, small intestine, and left adrenal gland. A 29-year-old woman was found to have multiple hemangiomas of the small intestine during an exploratory laparotomy for acute abdominal pain. After surgery, abdominal CT scans showed multiple hemangiomas in the liver, small intestine, and left adrenal gland. A barium study showed multiple polypoid filling defects in the duodenum, jejunum and ileum, which were hemangiomas.

INTRODUCTION

Hemangiomas of the gastrointestinal tract are rare; only about 200 cases have been reported in the literature.[1] Many hemangiomas of the bowel are associated with vascular malformations in other regions. We report a patient who had multiple hemangiomas of the liver, small intestine, and left adrenal gland.

CASE REPORT

A 29-year-old woman had had abdominal pain for 2 days with nausea and vomiting. She did not have a fever. She had been diagnosed as having hemangiomas of the right foot and conjunctiva when she was 7 years old. On physical examination tenderness of the right lower abdomen was noted. She underwent an exploratory laparotomy because acute appendicitis was suspected, but it was not found to be the case. However, multiple hemangiomas were seen scattered throughout the jejunum and ileum. An appendectomy was performed. Afterwards a plain abdominal radiograph taken before surgery was reviewed. Multiple calcifications were seen in the upper abdomen and in the pelvic cavity (Fig. 1). Precontrast CT scans showed multiple hypodense masses with multiple calcifications in the liver (Fig. 2). Postcontrast CT scans showed nodular enhancement at the periphery of the masses with fill-in on delayed scan (Fig. 3). There were multiple calcifications in the left adrenal gland (Fig. 4). Multiple enhanced intramural masses with calcifications were seen in the terminal ileum (Fig. 5). A barium study showed a few polypoid filling defects in the duodenum (Fig. 6) and multiple polypoid filling defects in the jejunum and terminal ileum (Fig. 7). The patient received symptomatic therapy.

DISCUSSION

Benign neoplasms of the small intestine are uncommon. In a review of 1721 patients with these, Wilson et al.[2] found 212 patients with hemangioma. The common locations were jejunum and ileum. Preoperative diagnosis of this disease has always been extremely difficult.[3]

There are four types of gastrointestinal hemangiomas: (i) multiple phlebectasia; (ii)

Department of Radiology, Faculty of Medicine, Chiang Mai University, Chiang Mai 50200, Thailand.

cavernous hemangioma, either diffuse infiltrating or circumscribed polypoid; (iii) simple capillary hemangioma; and (iv) angiomatosis.[4] Cavernous hemangioma is the most common type. The hemangiomas in our patient contained calcifications, which were phleboliths, so they were the cavernous type. Hemangiomas of the small bowel usually occur with intestinal bleeding that may be chronic or acute. Other clinical manifestations include intussusception, obstruction , and perforation.[1] Our patient had acute abdominal pain.

Imaging findings of intestinal cavernous hemangioma have been described. Multiple phleboliths have been seen in plain abdominal radiographs.[4,5] In barium studies multiple polypoid filling defects have been seen.[3,6] In a CT scan of a patient with cavernous hemangiomas of the small bowel multiple calcifications in the thickened wall of the intestine, were reported.[3] The CT findings were similar to those of our patient.

There are many hemangioma syndromes such as Rendu-Osler-Weber, Sturge-Weber-Dimitri, and Von Hippel-Lindau.[7] Our patient may have had Rendu-Osler-Weber syndrome (hereditary hemorrhagic telangiectasia), which is an autosomal dominant condition that may occur in childhood, but does so usually after puberty. In this syndrome discrete, bright red, spider-like macropapules appear on the face; tongue; lips; nasal, oral, and conjunctival membranes; the palmar aspect of the fingers; the nail beds; liver; lung; spleen; pancreas; brain; and mucosal surfaces.[8]

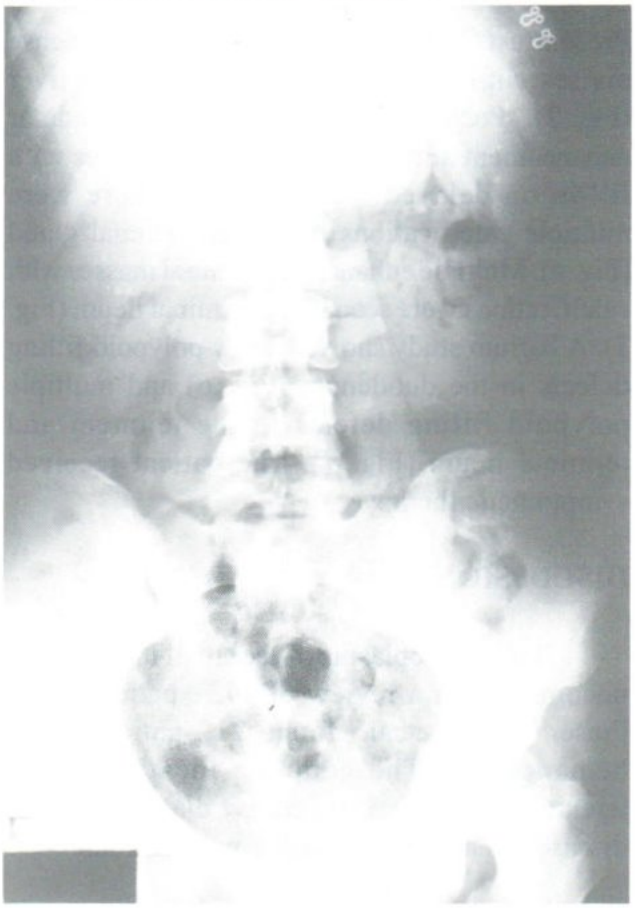

Fig.1 A plain abdominal radiograph shows multiple calcifications in the upper abdomen and pelvic cavity.

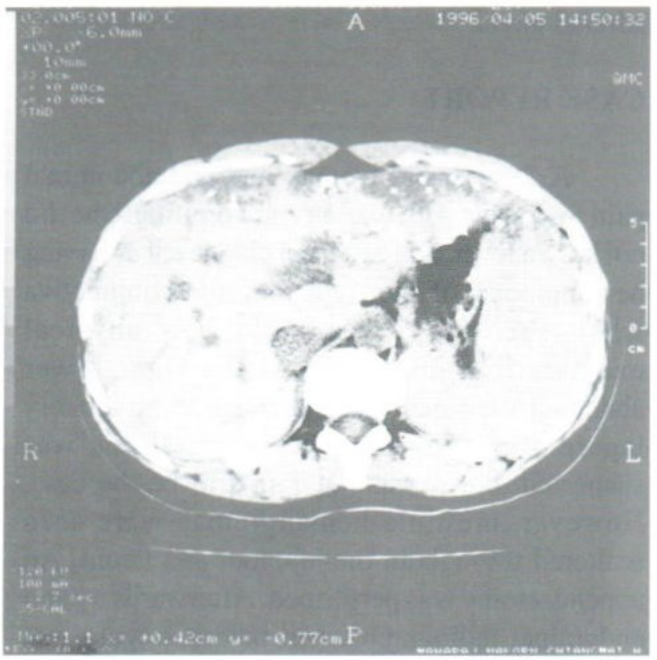

Fig.2 Precontrast CT scan shows multiple hypodense masses in the liver with calcifications.

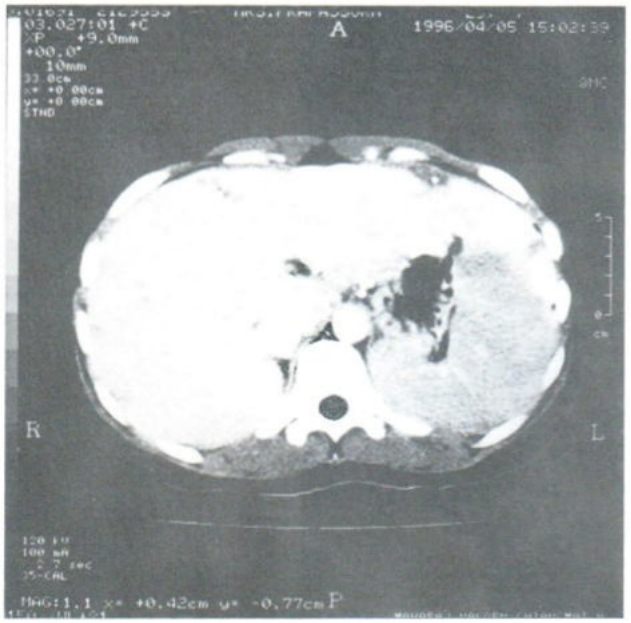

Fig.3 Delayed CT scan (10 minutes after contrast infusion) shows intense enhancement of multiple masses in the liver with multiple calcifications.

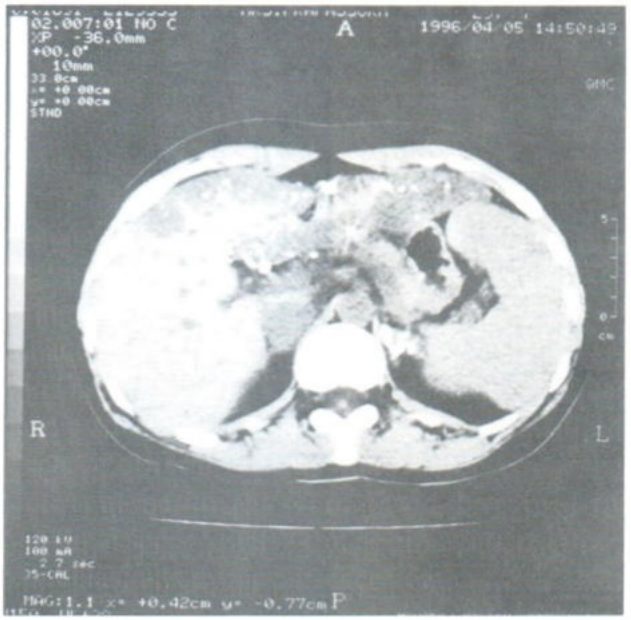

Fig.4 Precontrast CT scan shows multiple calcifications in the left adrenal region and multiple hypodense masses in the liver with calcifications.

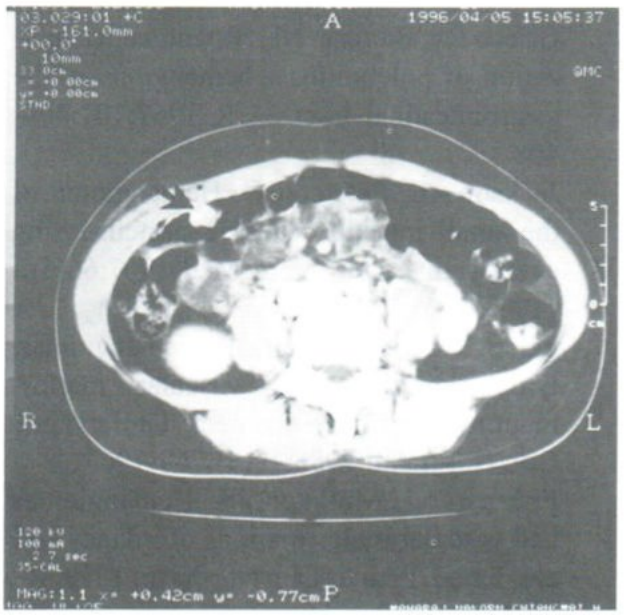

Fig.5 Postcontrast CT scan shows focal thickening of the ileal wall with calcifications (arrow).

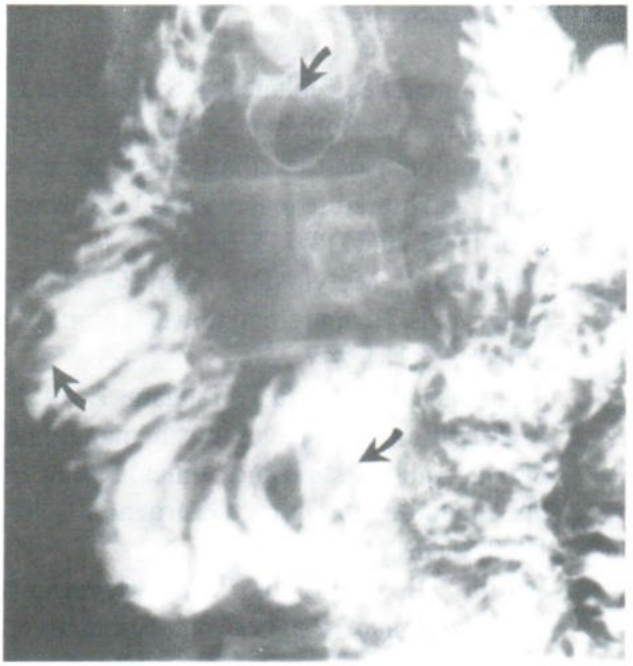

Fig.6 Barium study shows a few polypoid filling defects in the duodenum (arrows).

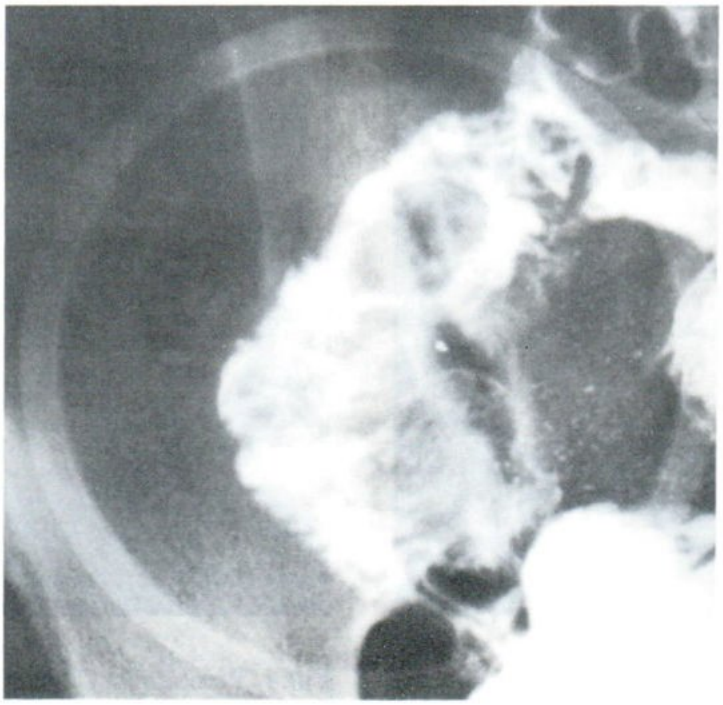

Fig.7 Barium study shows multiple polypoid filling defects in the ileum.

REFERENCES

1. Ramanujam PS, Venkatesh KS, Bettinger L, Hayashi JT, Rothman MC, Fietz MJ. Hemangioma of the small intestine: case report and literature review. Am J Gastroenterol 1995;90(11):2063-2064.
2. Wilson JM, Melvin DB, Gray G, Thorbjarnarson B. Benign small bowel tumor. Ann Surg 1975;181:247-250.
3. Akamatsu T, Matsuda Y, Tsugane E, et al. A case of multiple cavernous hemangioma of the small intestine and clinical review of the Japanese literature. Gastroenterol Jpn 1990;25:494-498.
4. Marine R, Lattomus WW. Cavernous hemangioma of the gastrointestinal tract: report of a case and review. Radiology 1958;70:860-863.
5. Grieco Rv, Bartose NF. Roentgen visualization of phleboliths in hemangioma of the gastrointestinal tract. AJR 1967;101:406-408.
6. Jackson AE, Peterson C. Hemangioma of the small intestine causing protein-losing enteropathy. Ann Intern Med 1967;66(6):-1190-1196.
7. Stal S, Hamilton S, Spira M. Hemangiomas, lymphangiomas, and vascular malformations of the head and neck. Otolaryngol Clin North Am 1986;19(4):769-796.
8. Fishman SJ, Mulliken JB. Hemangiomas and vascular malformations of infancy and childhood. Pediatr Clin North Am 1993;40-(6):1177-1200.

COMPUTED TOMOGRAPHIC IMAGING OF PEDIATRIC ORBITS

Kanokporn ORANRATANACHAI, Noppaklao MANOWATANA, Malai MUTTARAK, Pannee VISRUTARATNA, Wantana PRAPAKORN

ABSTRACT

From January 1995 to December 1996, computed tomographic imaging of the orbits was performed on 48 pediatric patients at the Department of Radiology, Faculty of Medicine, Chiang Mai University. Pathological and/or clinical proofs of diagnoses were successfully obtained from only 35 of these patients, in whom ocular (n=21) and orbital (n=14) diseases were found. These ocular diseases included retinoblastoma (n=14) and non-tumoral retinal detachment (n=3); the remainder were persistent hypertrophic primary vitreous, congenital glaucoma, intraocular foreign body, and posttraumatic lens aspiration. The orbital diseases included acute myeloblastic leukemia (n=3), preseptal cellulitis (n=3), neurofibroma (n=2); the remainder were neuroblastoma, primitive neuroectodermal tumor, rhabdomyosarcoma, capillary hemangioma, orbital cellulitis, and optic neuritis. The computed tomographic findings of these patients are reviewed and discussed.

INTRODUCTION

Imaging is particularly important and useful in the very young child when clinical evaluation of visual functions is difficult and may not be precise. Computed tomography (CT) represents an important form of imaging for the evaluation of the pediatric eye and orbit, since orbital fat provides excellent natural contrast for the demonstration of soft tissue structures.[1] In addition, bony details and calcification are also well demonstrated by CT.[2] The axial and coronal sectional imagings provided by CT are well suited for the depiction of the complex anatomic relationships of orbital structures.

MATERIALS AND METHODS

From January 1995 to December 1996, CT of the orbits were performed on 48 pediatric patients in the Department of Radiology, Chiang Mai University Hospital. Thirty-five patients who had had pathological and/or clinical diagnoses of orbital abnormalities were retrospectively studied. In all cases, the plain CT scans were performed on a GE Sytec 3000i scanner with the X-ray beam at 0 or -10 degree from the orbitomeatal line with 5 mm slice thickness. Postcontrast axial scans were obtained in 32 cases. The 5 mm thick coronal scans were performed after enhanced axial scans in 15 cases.

The cases were divided into two groups, those with ocular and those with orbital diseases, according to the location of the lesions on CT scans. Ocular disease was defined as lesions which originated within the eye globe, orbital disease as lesions arising in the extraocular orbital compartment.

Department of Radiology, Faculty of Medicine, Chiang Mai University, Chiang Mai 50200 Thailand

RESULTS

There were 17 boys and 18 girls, ranging from 2 months to 14 years of age. The CT scans demonstrated ocular diseases in 21 and orbital diseases in 14 (Table 1).

The ocular diseases (Table 2) included retinoblastoma (n=14) and non-tumoral retinal detachment (RD) (n=3); the remainder were persistent hypertrophic primary vitreous (PHPV), congenital glaucoma, intraocular foreign body (FB) and posttraumatic lens aspiration.

The orbital diseases included 8 orbital tumors (Table 3); the remainder (Table 4) were preseptal cellulitis (n=3), orbital cellulitis, optic neuritis, and capillary hemangioma.

TABLE 1: Location of disease in CT scan

DISEAES	No. of patients
I. OCULAR DISEASES	21
A. Congenital malformation:	
Congenital glaucoma	1
PHPV	1
B. Vitreoretinal disorder:	
Retinal detachment	3
C. Tumor:	
Retinoblastoma	14
D. Trauma:	
Intraocular foreign body	1
Posttraumatic lens aspiration	1
II.. ORBITAL DISEASE	14
A. Infection:	
Preseptal cellulitis	3
Orbital cellulitis	1
B. Inflammation:	
Optic neuritis	1
C. Vascular lesion:	
Capillary hemangioma	1
D. Tumor:	
Acute myeloblastic leukemia	3
Neurofibroma	2
Neuroblastoma	1
Primative neuroectodermal tumor	1
Rhabdomyosarcoma	1

TABLE 2: Clinical and CT findings of ocular diseases

patient & age	sex	presenting symptoms	site	globe: S,N,L	No. of masses	margin	calci-fication	enhance-ment	extraocular extension	diagnosis
1. 1 y	F	leukokoria	RE	N	single	good	+	+	none	retinoblastoma
2. 3 y	F	leukokoria	RE	N	single	good	+	+	none	retinoblastoma
3. 2 m	F	leukokoria	RE	N	single	good	+	+	none	retinoblastoma
4. 2 m	M	leukokoria	BE	N,L	multiple	good	+	+	none	retinoblastoma
5. 2 y	F	leukokoria	LE	N	single	good	+	+	none	retinoblastoma
6. 14 m	F	leukokoria	BE	L,L	multiple	good	+	+	none	retinoblastoma
7. 2 y	F	leukokoria	LE	N	single	good	+	+	none	retinoblastoma
8. 9 y	F	blindness	LE	N	multiple	poor	+	+	optic nerve	retinoblastoma
9. 8 y	F	proptosis	RE	L	single	poor	+	+	optic nerve & soft tissue	retinoblastoma
10. 1 y	M	leukokoria	LE	L	single	good	+	+	optic nerve	retinoblastoma
11. 2 y	M	leukokoria	RE	S	single	poor	+	+	leptomeningeal invasion	retinoblastoma
12. 3 m	F	leukokoria	RE	N	singlr	good	+	+	none	retinoblastoma
13. 1 y	F	leukokoria	LE	N	multiple	good	+	+	lacrimal gland	retinoblastoma
14. 1 y	F	leukokoria	BE	N	multiple	good	+	+	none	recurrent retinoblastoma
15. 7 y	F	leukokoria	LE	S	single	-	-	+	none	PHPV
16. 4 y	F	leukokoria	RE	N	no mass	-	-	-	-	RD
17. 8 y	M	leukokoria	RE	N	no mass	-	-	-	-	RD
18. 5 y	M	leukokoria	RE	N	no mass	-	-	-	-	RD
19. 4 m	M	cataract	LE	L	no mass	-	-	-	-	congenital glaucoma
20. 14 y	M	trauma	LE	N	FB	good	metal	-	none	intraocular FB
21. 2 y	M	trauma	LE	N	no mass	-	-	-	-	posttraumatic lens aspiration

RE = right eye, LE =left eye, BE = both eye

S = small, N = normal, L = large

TABLE 3: CT findings of orbital tumors

	No. of Patients	Proptosis	Bone Change	Location	Well-defined Margin	Infiltration		Attenuation			Enhancement	
						Muscle	Nerve	Hyper-dense	Iso-dense	Hypo-dense	Homo-geneous	Hetero-geneous
Acute myeloblastic leukemia	3	3	2	Extraconal 1 Extra-and intra-conal 1 Lacrimal gland 1	2	1	1	3	0	0	3	0
Neurofibroma	2	1	0	Extraconal 1 Extra-and intra-conal 1	1	0	0	1	1	0	0	2
Neurofibroma	1	1	1	Extraconal 1	1	0	0	1	0	0	1	0
Primitive neuroectodermal tumor	1	1	0	Extra-and intra-conal 1	1	1	1	1	0	0	1	0
Rhabdomyosarcoma	1	1	0	Extra- and intra-conal 1	1	1	0	1	0	0	1	0

TABLE 4: CT findings of non-tumoral orbital lesions.

DISEASES	No. of patients	CT findings
Preseptal cellulitis	3	Swelling and enhancement of preseptal soft tissue,
Orbital cellulitis	1	Proptosis and swelling of left periorbital soft tissue. superomedial extraconal mass and enlarged left medial rectus and superior rectus muscles, opacified left maxillary and ethmoid sinuses.
Optic neuritis	1	Uniformly enlarged, enhanced left optic nerve.
Capillary hemangioma	1	Hyperdense enhanced extraconal lesion.

DISCUSSION

The spectrum of ocular and orbital pathology in the pediatric age group is quite different from that seen in adults.[1,3]

Retinoblastoma is the most common primary intraocular malignant tumor of childhood.[2,4-7] There were 14 cases of this tumor with pathologically proven retinoblastoma, which is the most common ocular disease (14/21 = 66%). This was the only ocular tumor in this study. These affected 10 girls and 4 boys, ranging from 2 months to 9 years of age. Most of the patients (12) were younger than 4 years of age. The most frequent presenting symptom was leukokoria (n=12). Three cases had bilateral retinoblastoma (Fig.1). In all cases, the CT findings showed iso- to hyperdense intraocular enhanced mass(es) with calcification. Almost all of the tumors were well defined. Multifocal lesions were seen in 5 patients, including three with bilateral retinoblastoma. The affected globes were either normal in size (n=10) or enlarged (n=5). Only one small globe appeared in our study. Recurrent retinoblastoma in a postenucleated eye was seen in one case of bilateral retinoblastoma. Of the cases with extraocular invasion (n=5), three had extension of the tumor along the optic nerve (Fig.2) and retrobulbar soft tissue, one had leptomeningeal involvement, and the remainder had lacrimal gland involvement. Clinically it is frequently difficult to differentiate retinoblastoma from benign diseases causing leukokoria such as PHPV, Coat's disease and toxocara endophthalmitis.[3,6-8] CT is essential for the radiologic diagnosis of retinoblastoma, primarily because it is most sensitive to calcification, an important feature distinguishing retinoblastoma from other entities.[7] The presence of intraocular calcification in children under 3 years of age is highly suggestive of retinoblastoma.[5-7] Retinoblastoma is seen on CT as an intraocular mass lesion which is calcified in about 95% of cases and located posterior to the lens. There is usually mild or moderate enhancement of the tumor which helps to separate the tumor from accompanying subretinal effusion. Bilateral retinoblastoma occasionally may be associated with a pineal neuroectodermal tumor, a so-called trilateral retinoblastoma.[3,7] Three of our patients had bilateral retinoblastoma without evidence of pineal tumor. CT readily reveals the size of the intraocular lesion and the important role of CT is the delineation of the retro-orbital extent of the tumor and determining if the optic nerve is involved or if there is intracranial extension[4]. This information is of prognostic value, as patients with tumors that have spread beyond the confines of the globe have a life expectancy of only a few months.[4] The most common route of extraocular extension is along the optic nerve; there can be extension into the subarachnoid space.

PHPV is the second most common cause of leukokoria, but we had only one case (Fig.3). Theoretically, PHPV results from failure of a portion of the embryonic intraocular vascular system to involute. CT findings of PHPV are microphthalmia, diffuse high attenuation appearance of the vitreous with intense enhancement of a thin, triangular or S-shape band in the vitreous. The enhanced band consists of remnants of the hyaloid vascular system. Other reported findings have been a small optic nerve and vitreous fluid-fluid levels of differing attenuation resulting from the recurrent hemorrhage in the subhyaloid or subretinal space.[8] PHPV can be differentiated from retinoblastoma by the presence of microphthalmia and absence of calcification within the globe.[1,7,8]

CT is important in the diagnosis of intraocular foreign bodies.[1,2] A metallic foreign body as small as 5 mm in diameter was detected in one of our cases by CT with a slice thickness of 5 mm. By this means, it is also possible to accurately determine the location of a radiopaque foreign body in relation to the globe.

Abnormalities that occur in the infected orbit were classified according to the involved structures and compartments, i.e. the preseptal soft tissues, and the intraconal, extraconal and subperiosteal compartments.[2] In our study, preseptal cellulitis was the most common manifestation of an orbital infection (Fig.4). Anatomically, the orbital septum serves as a barrier to the extension of disease into the orbital proper. Therefore, an important function of CT in this condition is to detect extension of disease into the orbit proper and to evaluate the paranasal sinuses.[1] Orbital cellulitis usually involves both the preseptal tissues as well as extraconal compartment of orbital structures, as seen in one of our cases (Fig.5). Acute inflammation of the orbit is frequently secondary to extension from the ethmoid sinusitis. Both inflammatory edema and cellulitis were demonstrated with CT as increased attenuation of orbital fat and enlargement of the extraocular muscles.[1,9] A medial extraconal soft-tissue mass that caused proptosis and lateral displacement of the globe and optic nerve was easily recognized on CT.

There were 8 pathologically proven orbital tumors in our studies (Table 3). Almost all of these patients had proptosis. The most of the tumors had extraconal hyperdense mass with homogeneous enhancement and well-defined margin. Bone destruction was seen in two cases of acute myeloblastic leukemia (Fig.6) and in one case of neuroblastoma (Fig.7), all of which were aggressive secondary tumors of the orbit. Acute myeloblastic leukemia was the most common orbital tumor in our study. However, rhabdomyosarcoma of the orbit, which is the most common orbital malignancy in children, was found in only one of our cases (Fig.8). There were only 5 different histological types of tumors in our study with the number of cases ranging from 1 to 3; therefore these data cannot be considered representative of the complete CT spectrum. Although CT scans do not permit the specific feature or accurately diagnose orbital tumors, CT scans do detect them and show extension, particularly in the retrobulbar space, in patients with proptosis.[10,11] The tumor masses can be located and identified according to their relation to the muscular cone. Bone destruction is often present with aggressive lesions.

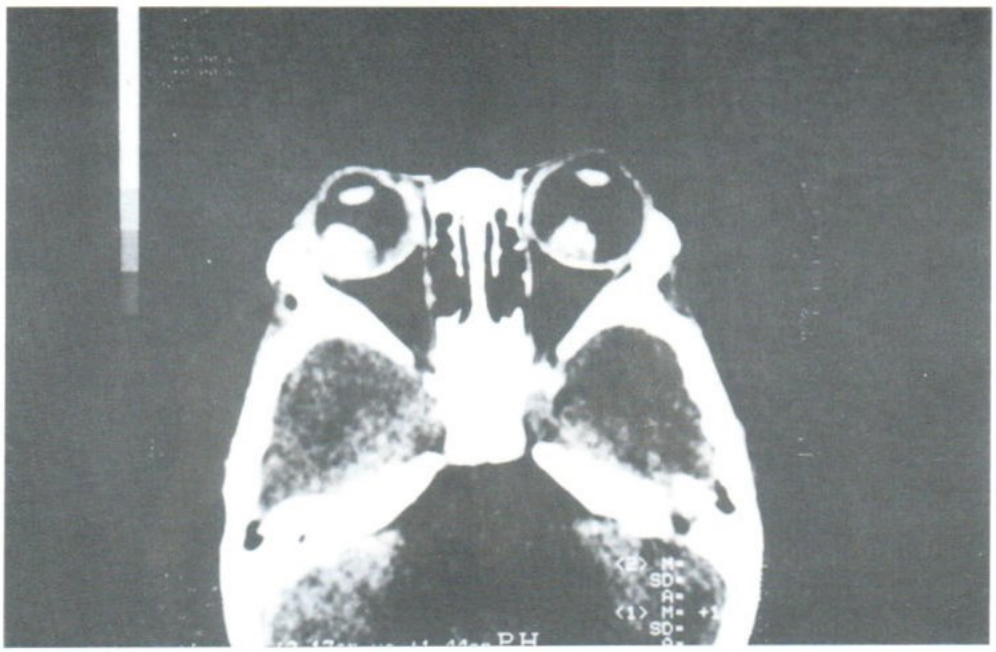

Fig.1 Bilateral Retinoblastoma: CT scan demonstrates bilateral intraocular masses. A portion of both masses is densely calcified.

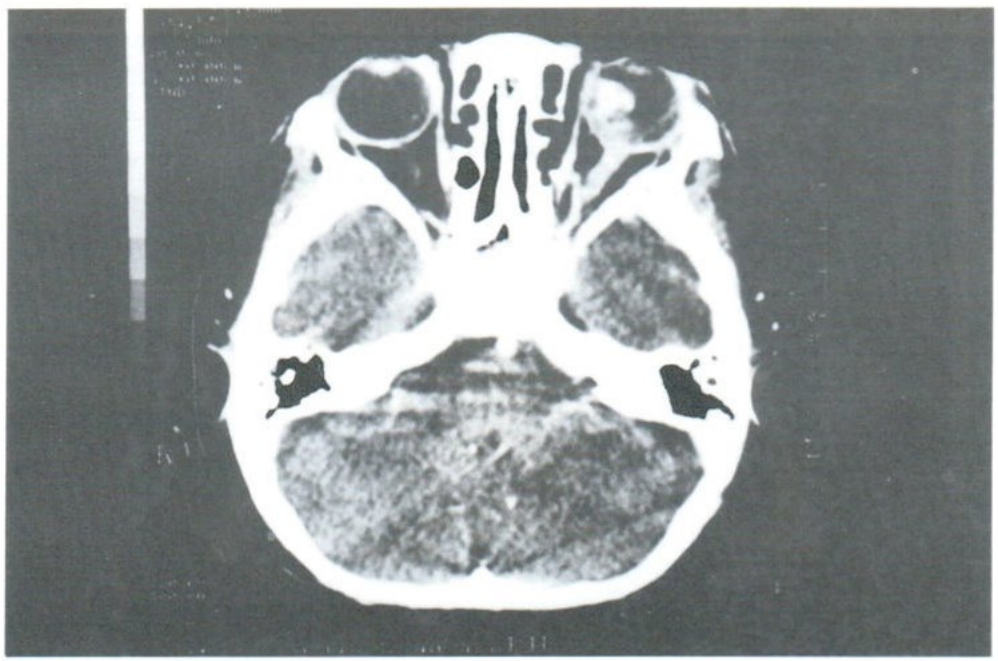

Fig.2 Retinoblastoma of left eye involves optic nerve.

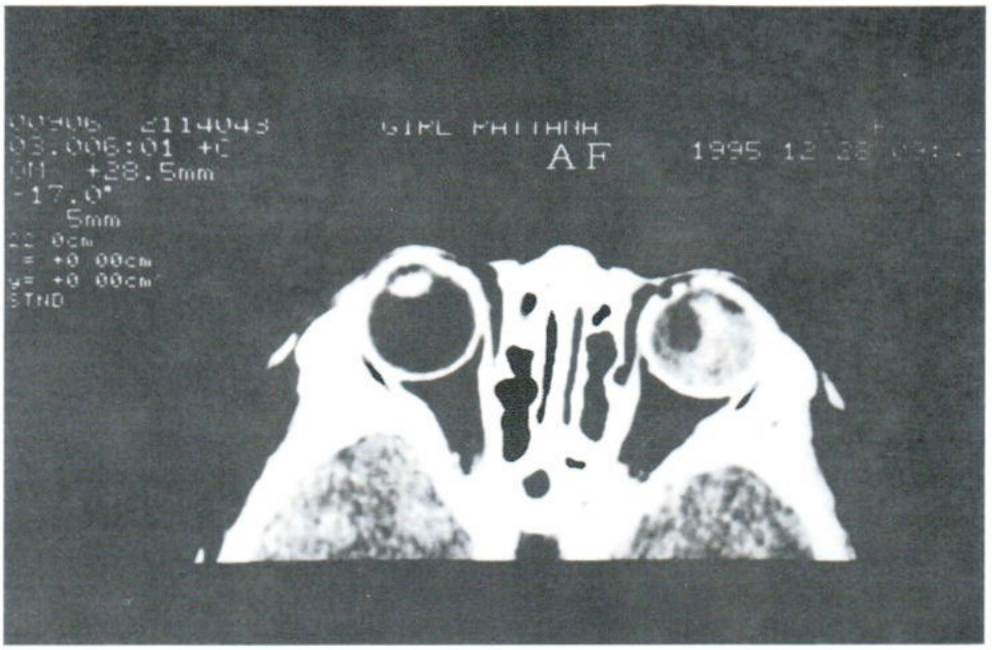

Fig.3 PHPV: There is enhanced retrolental S-shaped mass that represents the hyperplastic primary vitreous of left eye. The accompanying retinal detachment is seen as nonenhanced hyperattenuating area.

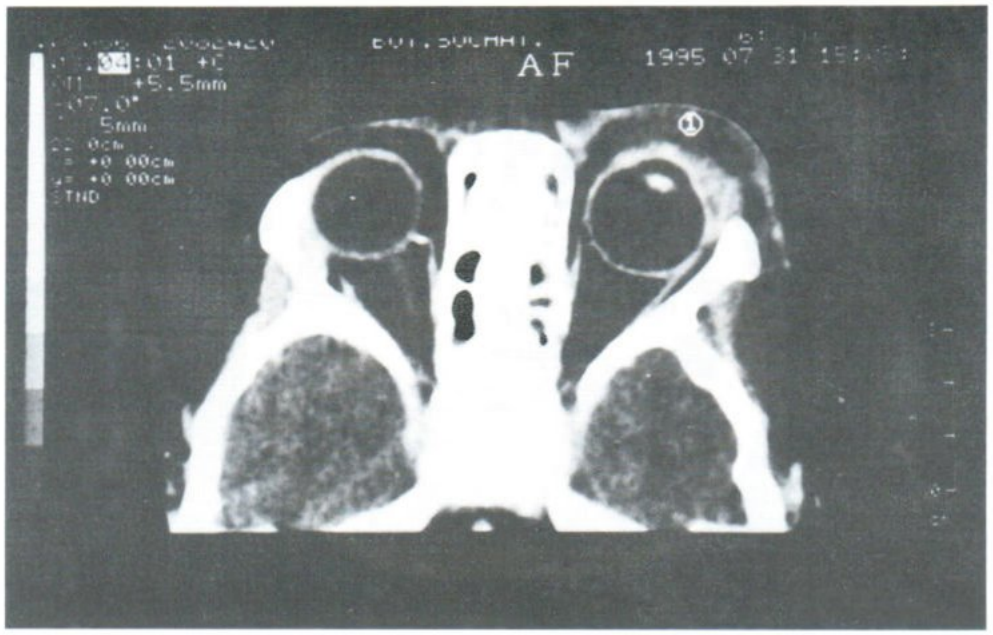

Fig.4 Preseptal Cellulitis: Axial CT scan shows diffuse soft tissue swelling involving the lid and conjunctiva anterior to the orbital septum.

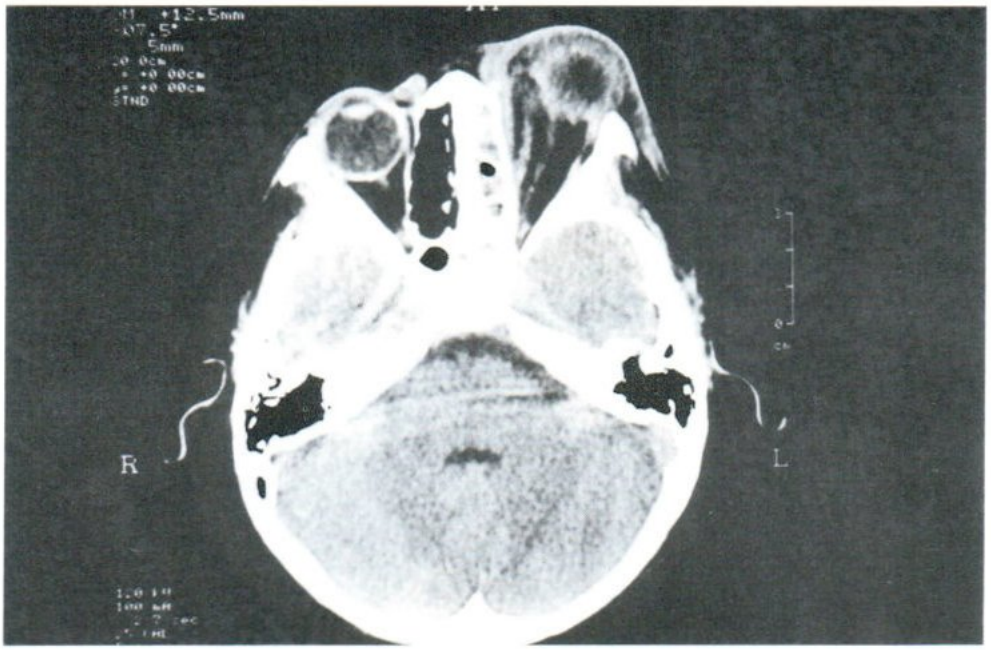

Fig.5 Orbital Cellulitis: Axial CT scan shows inflammatory edema of periorbital soft tissue and medial extraconal compartment of left orbit secondary to ethmoid sinusitis.

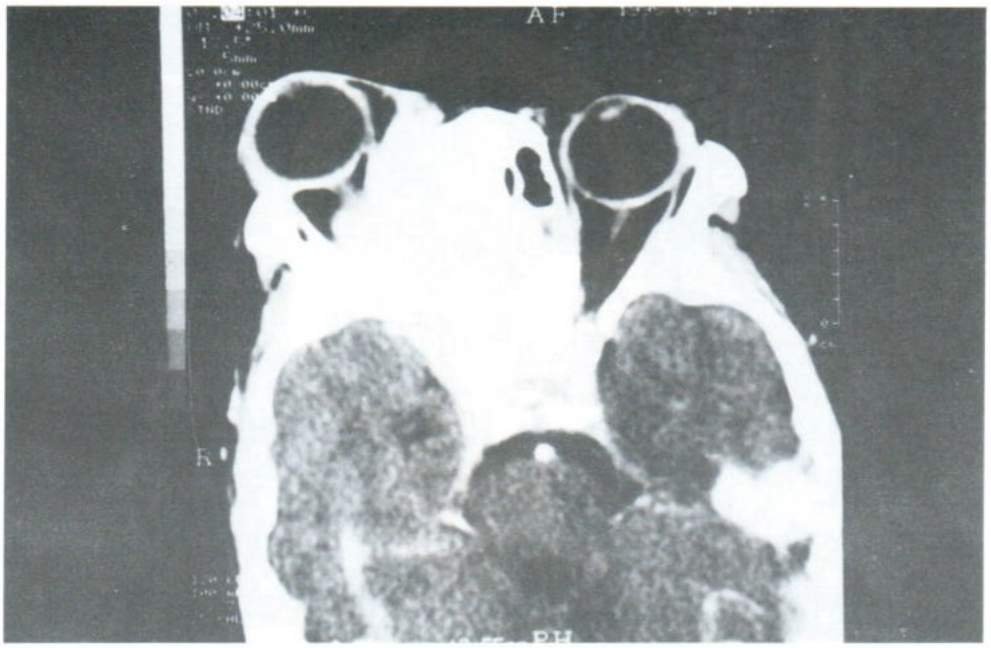

Fig.6 Acute Myeloblastic Leukemia: CT scan of 8-year-old girl shows large, enhanced, infiltrative mass involving paranasal sinuses with bone destruction and extension into both extra- and intraconal spaces of right orbit.

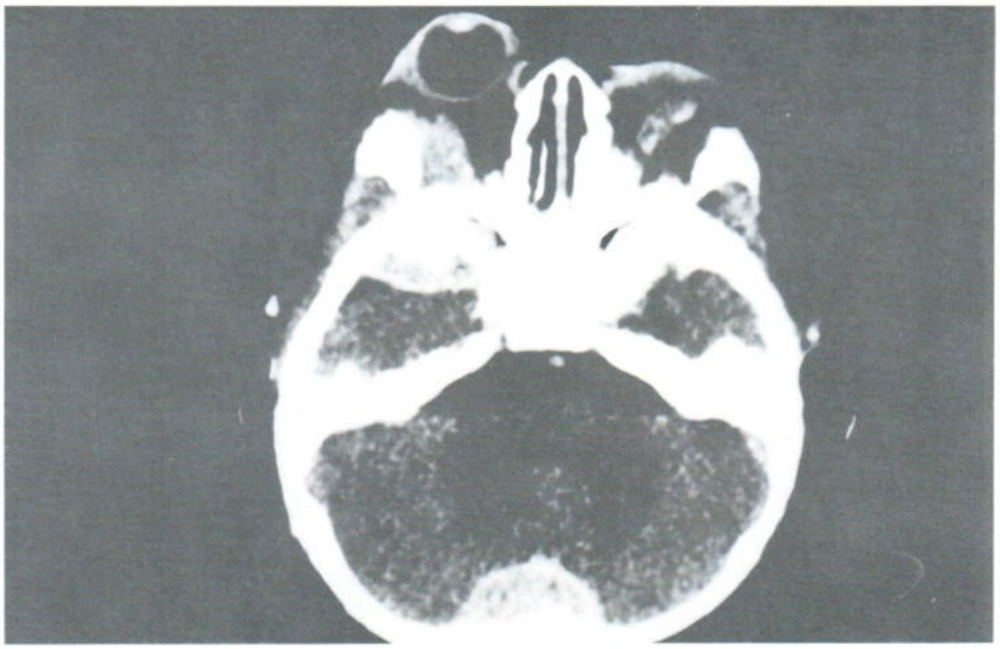

Fig.7 Neuroblastoma: CT scan of 3-year-old boy shows bone involvement from metastatic neuroblastoma with extraconal extension.

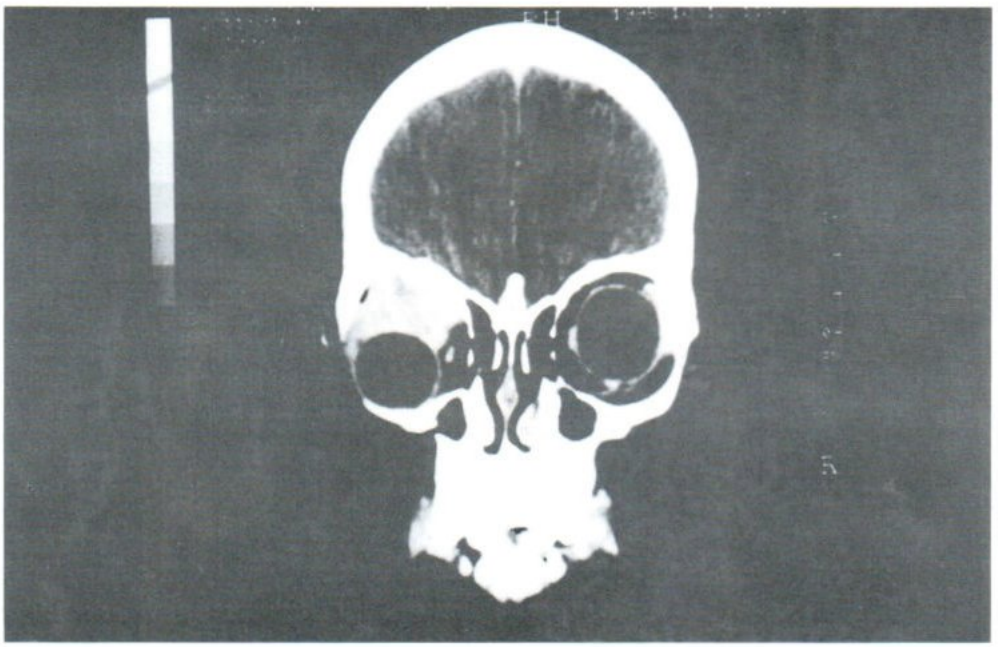

Fig.8 Rhabdomyosarcoma: Coronal CT scan shows homogeneous enhanced left orbital mass.

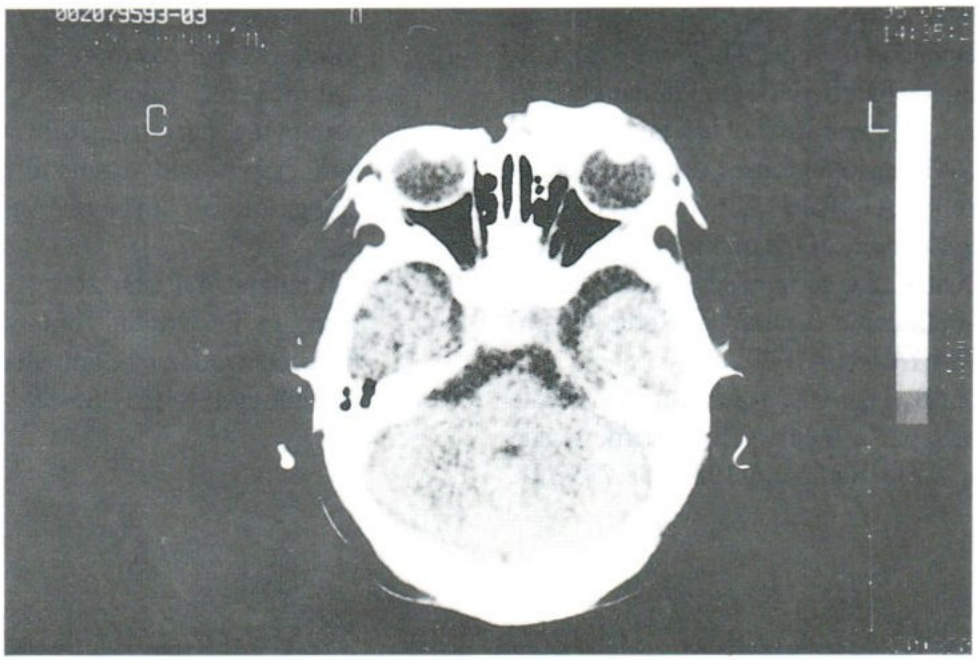

Fig.9 Capillary Hemangioma: CT scan of 2-month-old boy shows lobulated, markedly enhanced extraconal mass.

CONCLUSION

We reviewed the CT of pediatric orbits in 35 patients; 21 had ocular diseases and 14 had orbital diseases. Retinoblastoma was the most common ocular disease and the only ocular tumor in our study. In the orbital group, orbital tumor was found to be the most common lesion.

We found that CT is the optimal imaging for demonstration and delineation of lesions in pediatric orbits. Bony detail and calcification show up very well on CT. Particularly in retinoblastoma CT is considered to be the imaging of choice in children under 3-4 years of age who have leukokoria.

REFERENCES

1. Wells RG, Sty JR, Gonnering RS: Imaging of the pediatric eye and orbit. RadioGraphics 1989;9:1023-1043.
2. Bilaniuk LT, Atlas SW, Zimmerman RA: The orbit. In: Lee SW, Rao K C.V.G., Zimmerman RA, eds. Cranial MRI and CT, 3rd ed.,1992;119-191.
3. Hopper KD, Sherman JL, Boal DK, Eggli KD: CT and MR imaging of pediatric orbit. RadioGraphics 1992;12:485-503.
4. Danziger A, Price HI: CT Findings in Retinoblastoma. AJR 1979;133:783-785.
5. Mafee MF, Schatz CJ: The orbit. In: Som PM, Bergeron RT, eds. Head and Neck Im aging, 2nd ed. St. Louis, Mosby, 1991;693-827.
6. Mafee MF, Goldberg MF, Greenwald MJ, et al: Retinoblastoma and simulating lesions: Role of CT and MR imaging. Radiol Clin North Am 1987; 25:667-682.

7. Provenzale JM, Weber AL, Klintworth GK, McLendon RE: Radiologic-Pathologic Correlation: Bilateral Retinoblastoma with Coexistent Pinealoblastoma (Trilateral Retinoblastoma). AJNR 1995;16:157-165.
8. Smirniotopoulos JG, Bargallo N, Mafee MF: Differential diagnosis of leukokoria: Radiologic-Pathologic correlation. Radio-Graphics 1994;14:1059-1079.
9. Towbin R, Han BK, Kaufman RA, Burke M: Postseptal cellulitis: CT in diagnosis and management. Radiology 1986;158:735-737.
10. Mafee MF, Putterman A, Valvassori GF, Campos M, Capek V: Orbital space-occupying lesions: Role of computed tomography and magnetic resonance imaging. Radiol Clin North Am 1987;25:529-559.
11. Lallemand DP, Brasch RC, Char DH, Norman D: Orbital Tumors in Children: Characterization by Computed Tomography. Radiology 1984;151:85-88.

PITUITARY BRIGHT SPOT : INCIDENCE IN ROUTINE BRAIN MRI STUDYING IN THAI PEOPLE

O. CHAWALPARIT, W. UOOWATANASOMBUT, S.JITBANCHUEN, P. CHARNCHAOWANISH, A. TOSAKUL, S. SUTHIPONGCHAI, P. JITNUSON

ABSTRACT

The brain MRI of 215 patients referred to our department without signs and symptoms relating to pituitary gland were studied. In each case, two to three images of the mid-sagittal region from routine brain protocol of the sagittal $T_{1\text{-wi}}$ were selected to determine the posterior bright spot of the pituitary glands. The age distribution of the patients which had been studied, were as followed : 0 - 12 years ; 73, 12 - 20 years ; 17, and more than 20 years ; 155 respectively. The incidence of the posterior bright spot, we found were 39 in 73 of the 0 - 12 years age group, 15 in 17 of the 12 - 20 years age group and 122 in 155 of the group aged more than 20 years. No significant differences in the detection rates of the posterior bright spot in different age groups ($x^2 = 0.05$). The total detection rate of the bright spot for the total study of 215 patients is 82 %

Key word : Posterior bright spot, Pituitary gland, MR Imaging.

Magnetic resonance imagings (MRI) of the pituitary gland is now the optimal technique for imaging this region. MRI has opened the new era for studying pituitary lesion as well as for studying of its function. The posterior lobe or neural lobe has been localized by MRI as the "bright spot" on $T_{1\text{-weighted}}$ image. However, it is not detected in some healthy patients. In this paper, we studied the detection rate of the "bright spot" in normal Thai patients by routine MRI protocol for brain and the significance of age distribution for the detection rate.

MATERIALS AND METHODS

The retrospective study of MRI brains of 215 Thai patients in our department was done. All were undergone routine MRI for other clinical indications that were not from pituitary lesion and no history of diabetes insipidus or other pituitary hormonal dysfunction. The two to three images in mid-sagittal region of brains from sagittal TSE-$T_{1\text{-wi}}$ were studied. Images were acquired with a standard head coil, 256 x 256 matrix, 23 cm. field of view, 6 mm. thickness, TR = 450 - 550 msec. and TE = 12 - 15 msec. with 2 excitations. The rates of identification of posterior high signal intensity or "bright spot" of the pituitary gland were statistically calculated using the chi-Square (X^2-test) to test the relationship of the detection rate and age group and the total detection rate.

Department of Radiology, Siriraj Hospital, Faculty of Medicine, Mahidol University, Thailand.

RESULTS

The 215 patients were devided into three groups by age : 0 - 12, 12 - 20, and more than 20 years old. The detection rates of the posterior bright spot in each age group are demonstrated in table I. The total detection rate is 82 %. There is no relationship between detection rate and age group ($p = 0.05$).

DISCUSSION

Mark et al[7] first reported the high signal intensity or bright spot in the posterior part of the sella turcica. They considered it to represent a "fat pad". Shortly thereafter, Fujisawa et al[3,4] in 1986 proposed and provided evidence from $T_{2\text{-wi}}$ and chemical shift experiments that the signal from the bright spot arose not from fat but from water protons in the neural lobe. They also postulated that the source of the bright spot should be related with the amount of neurosecretory granules of the hypothalamohypophyseal axis. They found the bright spot in all of their normal adults. However, other reported some detection rates of from 60 - 90 % in healthy person[2]. The detection rate can be increased by using multiplanar imagings, contiguous sections and strict anteroposterior orientation of the readout gradient. The detection rate of our series was studied from the routine cranial MRI and agreeable with other previous reports. We also found that no significant difference for the detection rates in various age groups. We believe that if careful imaging is done, the bright spot should be found in all patients regardless of the age group.

Patients with diabetes insipidus were found to have absent bright spot in the posterior lobe or arrested bright spot in the infundibulum or median eminence.[1,3,5,6] In our unreported 8 cases with suspected central DI, no posterior bright spot was found in all cases. However, we won't conclude that the abscence bright spot in routine cranial MRI means the disease. But if the patient has the history of central DI, the abscence of bright spot should be considered significant and careful imaging of the pituitary gland is recommended.

Table I : Detection rate of bright spot by age.

Aged (years old)	Number of patients	Number of bright spot (%)
0 - 12	73	39 (53.4 %)
12 - 20	17	15 (88.2 %)
> 20	155	122 (78.7 %)
Total	215	176 (82 %)

REFERENCES

1. Colombo N., Berry I., Kucharezyk J., et al. Posterior pituitary gland : appearance on MR images in normal and pathologic states. Radiology 1987 ; 165 : 481 - 485.
2. Elster AD. Modern imaging of the pituitary. Radiology 1993 ; 187 : 1 - 14.
3. Fujisawa I., Kikuchi K., Nishimura K., et al. Transection of the pituitary stalk : development of an ectopic posterior lobe assessed with MR imaging. Radiology 1987 ; 165 : 487 - 489.
4. Fujisawa I., Asato R., Kawata M., et al. Hyperintense signal of the posterior pituitary on T1- weighted MR images : an experimental study. J. comput Assist Tomogr 1989 ; 13 : 371 - 377.
5. Gammal TE., Brooks BS., Hoffman WH. MR imaging of the ectopic bright signal of posterior pituitary regeneration. AJNR 1989 ; 10 : 323 - 328.
6. Gudinchet F., Brunelle F., Barth MO., et al. MR imaging of the posterior hypophysis in children. AJNR 1989 ; 10 : 511 - 514.
7. Mark L, Peck P, Daniels D, et al. The pituitary fossa : a correlative anatomic and MR study. Radiology 1984 ; 153 : 453 - 457.

Process beautiful images without a drop of liquid in sight.

DryView Imager

It's no mirage. Our Imation™ DryView™ laser imager, with its revolutionary new dry processing technology, really does eliminate the hassles and costs of messy, toxic chemicals. It also travels well, because it doesn't depend on plumbing. And it costs a lot less than the competition. All this and the DryView imager produces images sharp as a cactus needle. No wonder we're a world leader in medical laser imaging. And it's only from Imation, formerly a part of 3M. Contact us at info@imation.com or see us at www.imation.com.

We're thinking what you're thinking.

IMATION
Borne of 3M Innovation

Imation (Thailand) Limited, 99/349, 9th Floor Na-Nakorn Building, Chengwatana Road, Donmuang, Bangkok 10210. Ph: (662) 576 0067-9 Fax: (662) 576 0065.

South Asia

Singapore	Malaysia	Philippines	Pakistan	Mumbai, India	Bangalore, India	Delhi, India
(65) 383 7676	(03) 703 7576	(632) 812 6981	(9221) 584 0176	(9122) 837 7053	(9180) 552 0407	(9111) 622 0234

MID ESOPHAGEAL PULSION DIVERTICULUM RESULTING FROM SPONTANEOUS INTRAMURAL ESOPHAGEAL HEMATOMA

SUCHADA HOONPONGSIMANONT,M.D.
SUWANNA PHOOMGLIN,Cert. in Med.Radiol.
MUTTANA CHUNTANA,Cert. in Med.Radiol.

ABSTRACT

Esophageal diverticula have 2 types which reflect the pathological causes and locations. Traction diverticulum is resulted from chronic granulomatous adhesion and usually at mid esophagus. Pulsion type is associated with motility disorder and located in the lower esophagus. We describe a large mid esophageal pulsion diverticulum resulting from an intramural esophageal hematoma. Barium swallow reveals normal esophagogastric junction and no motility disorder. We consider intramural hematoma is another associated condition of pulsion diverticulum.

Key words: esophageal diverticulum,spontaneous intramural esophageal hematoma

CASE REPORT

A 62 year-old male who was a professional singer with a history of four-day severe cough and odynophagia,was admitted on August 19,1994. Esophagoscopy and computed tomography (CT) showed spontaneous intramural esophageal hematoma (SIEH) (fig 1). His symptoms were relieved within 5 days by conservative treatment consisting of antibiotics and total parenteral nutrition. Three months later, he complained hoarseness when singing in high notes. He had no further swallowing problem until nine months after SIEH episode when he developed dysphagia for a couple of days. Esophagoscopy found a large pulsion diverticulum,confirmed by CT and barium swallow (fig 2). The site of diverticulum corresponded with the location of previous SIEH. The rest of the esophagus and esophagogastric junction appear normal.

DEPARTMENT OF RADIOLOGY LERDSIN GENERAL HOSPITAL BANGRAK, BANGKOK 10500 THAILAND
TELEPHONE: (662) 235-0330,-7 EXT 2112 FAX: (662) 235-6909

Address reprint requests to:
SUCHADA HOONPONGSIMANONT,M.D.
RADIOLOGY DEPARTMENT LERDSIN GENERAL HOSPITAL SILOM ROAD, BANG-RAK BANGKOK 10500, THAILAND
TELEPHONE: (662) 235-0330,-7 EXT 2112FAX: (662) 235-6909 E-mail: dahoon@health.moph.go.th

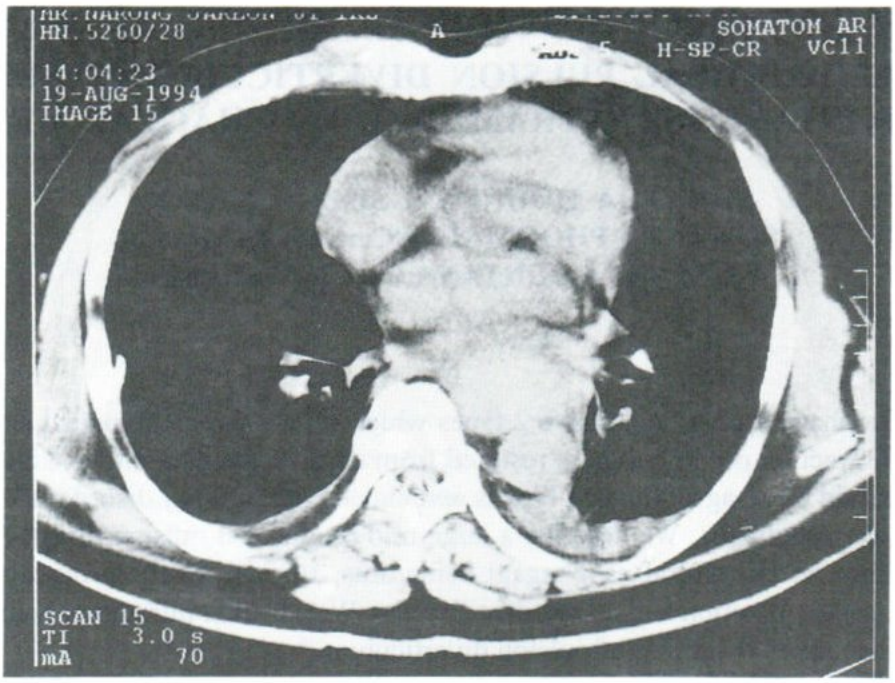

Fig. 1A. CT scan on the first day of admission showed a large intramural esophageal hematoma at mid esophagus and bilateral pleural effusion.

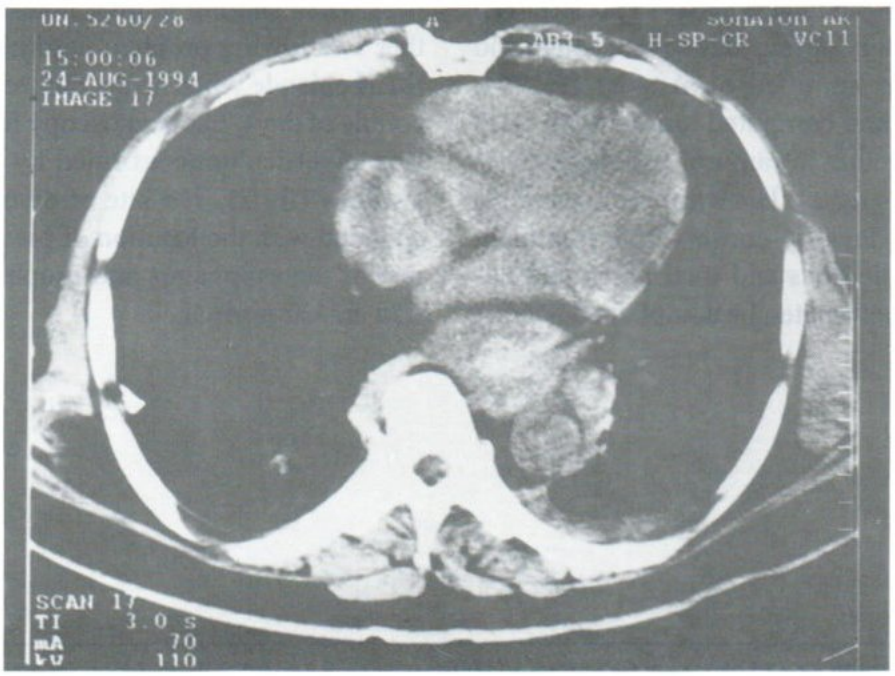

Fig. 1B. There is marked reduction of hematoma on the fifth day of admission and the symptom has much improved.

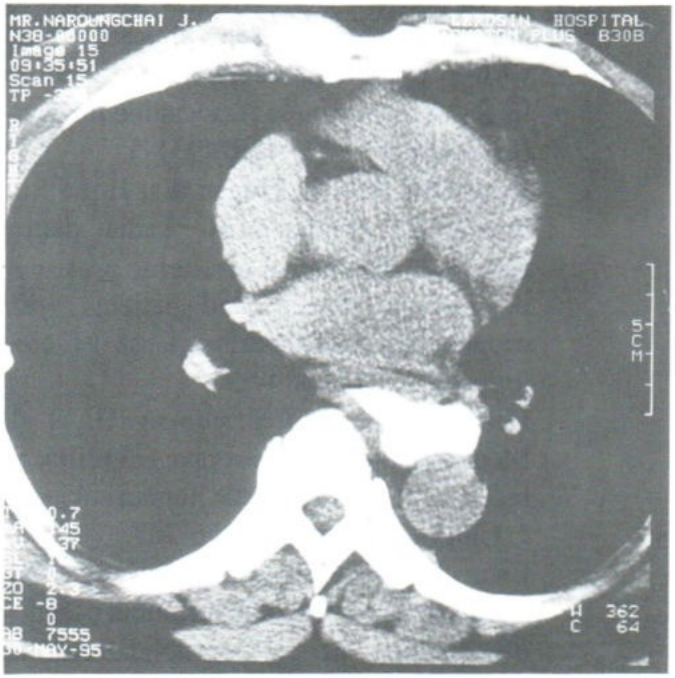

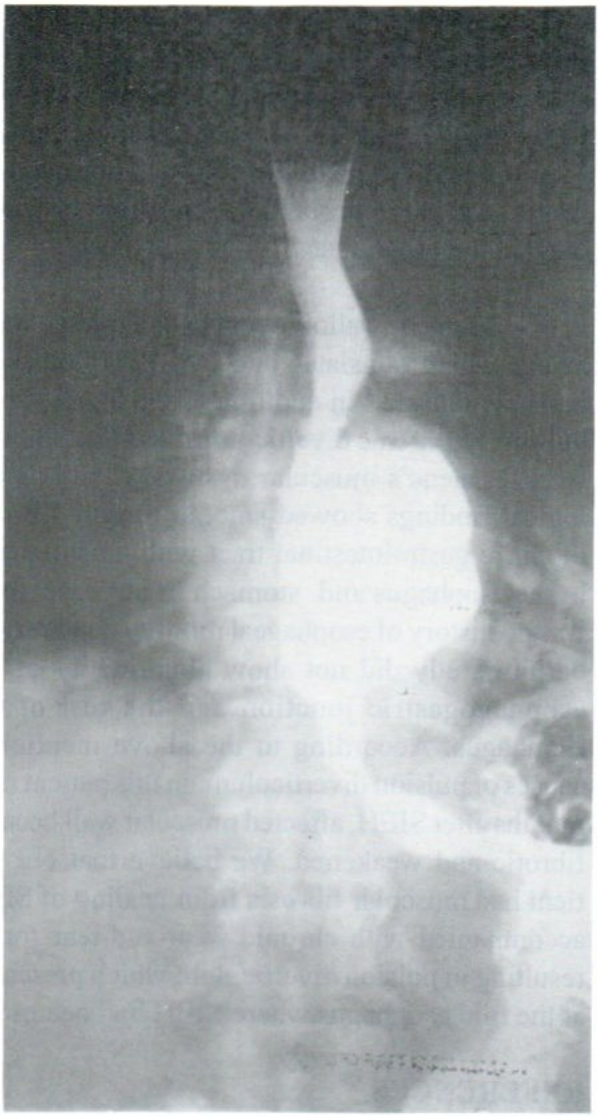

Fig. 2. A large pulsion diverticulm occurred at mid esophagus where the previous SIEH was found.

DISCUSSION

Pulsion esophageal diverticulum is actually more commonly found than traction type. The commonest site is at lower esophagus. It is however commonly believed that traction diverticulum occurs frequently and is found at mid esophagus.[1] Most esophageal diverticula are asymptomatic.[1,2] Dysphagia, chest pain and reflux symptoms are usually related to the underlying motor disorder. Apart from that, dysphagia may be caused by diverticulum of larger size or its complications.[1] Regurgitation also occurs when diverticulum reaches a large size.[2] Causes of pulsion diverticulum include esophageal motility disorder, mechanical obstruction and chronic wear-and-tear forces.[1] Therefore evidence of motility disorder or obstructive lesion is usually found with pulsion diverticulum especially at lower esophagus. However, Penagini[3] reported pulsion diverticulum associated with achalasia at mid esophagus and Suzuki[4] described a traction epiphrenic diverticu-

lum associated with a giant esophageal leiomyoma. Stewart[1] believes that chronic wear-and-tear forces appear to account for most pulsion esophageal diverticula. During each normal peristaltic sequence, substantial radial pressure forces exist in the esophagus.[5]

Human swallow about once a minute while awake which translates into 2 to 3 million swallows per decade.[6] In addition to the 3 categories, pulsion epiphrenic diverticulum has been reported with Duchene's muscular dystrophy[7] and pathological findings showed smooth muscle fibrosis of entire gastrointestinal tract with most marked in the esophagus and stomach.In our case, there was no history of esophageal motility disorder and barium study did not show abnormality of the esophagogastric junction and the rest of the esophagus. According to the above mentioned causes of pulsion diverticulum, in this patient nine months after SIEH, affected muscular wall became fibrotic and weakened. We believe that our patient had muscular fibrosis from healing of SIEH accompanied with chronic wear-and-tear forces resulting in pulsion diverticulum which presented at the mid esophagus where SIEH had occurred.

REFERENCES

1. Stewart ET, Dodds WJ. Radiology of the esophagus. In: Freeny PC, Stevenson GW, eds. Margulis and Burhenne's alimentary tract radiology. St.Louis: Mosby, 1994: 214-216.
2. Bremner CG. Other conditions. In: Bouchier IAD, Allan RN, Hodgson HJF, Keighley MRB, eds. Gastroenterology clinical science and practice. London: WB Saunders, 1993:168.
3. Penagini R, Bianchi PA. Primary achalasia associated with a midthoracic esophageal diverticulum. J Clin Gastroenterology 1990;12(3):365-7.
4. Suzuki I, Oho K, Ariizumi K, Nakayama S, Tamura K, Serizawa H. A case report of giant esophageal leiomyoma associated with an epiphrenic esophageal diverticulum. J of the Japanese Association for Thoracic Surgery 1994;42(6):931-5.
5. Dodds WJ, Stef JJ, Hogan WJ, Hoke SE, Stewart ET, Arndorfer RC. Radial distribution of esophageal peristaltic pressure in normal subjects and patients with esophageal diverticulum. Gastroenterology 1975;69(3):584-590.
6. Dent J, Dodds WJ, Friedman RH, et al. Mechanism of gastroesophageal reflux in recumbent asymptomatic human subjects. J. Clin Invest 1980;65:256-267.
7. Leon SH, Schuffler MD, Kettler M, Rohrmann CA. Chronic intestinal pseudoobstruction as a complication of Duchenne's muscular dystrophy. Gastroenterology 1986;90(2):455-9.

PULMONARY CRYPTOCOCCOSIS IN AIDS PATIENTS : RADIOGRAPHIC APPEARANCES AND SOME CLINICAL ASPECTS

Praparnrat VEERAPAND, M.D. [1], Ponglada SUPANNACHART, M.D. [2], Pairote FUANGTONG, M.D. [2], Sutharat TUNGSAKULVATTANA, M.D. [2]

ABSTRACT

PURPOSES : To study radiographic appearances and some clinical aspects of pulmonary cryptococcosis in AIDS patients.

MATERIALS AND METHODS : Medical records and chest radiographs were retrospectively reviewed during October 1990 to February 1996

RESULTS ; Pulmonary cryptococcosis were diagnosed in 22 patients with AIDS (21 men, 1 woman ; age range 22-64 years). Fever, cough, headache and dyspnea were the main presenting symptoms. The most common radiographic appearance was diffusely mixed interstitial infiltration, predominantly fine or intermediate pattern (12/22). Bilateral coarse interstitial infiltration were noted in 2 patients, localized infiltration in 6 patients, unilateral pleural effusion with questionable infiltration in 1 patient and mediastinal adenopathy alone in 1 patient. Associated minimal pleural effusion and cavities were found as associated lesions in 5 and 2 patients respectively. Seventeen patients had concurrent cryptococcal meningitis with or without cryptococcal infection of other organs and 2 patients had cryptococcemia. Four cases could be diagnosed as pulmonary cryptococcosis prior to cryptococcal meningitis. Of the 18 patients receiving antifungal drugs, 13 patients improved and 5 patients died. The remaining 4 patients who had no specific treatment were all dead.

Pulmonary cryptococcosis should be the considered diagnosis more frequently in AIDS patients. In the presence of cryptococcal meningitis with abnormal chest radiograph, the earlier it was diagnosed, the better will be the treatment outcome.

Cryptococcal neoformans infection at the present time has been an important problem accompanying world-wide spread of the HIV virus. It is the fourth most common systemic opportunistic infection in patients with AIDS in USA[1] whereas it is the second most common in Thailand following tuberculosis.[2] The organisms usually infect meninges and brain but many other organs could also be involved particularly the lung.[3] The prevalence of pulmonary cryptococcosis is expected to increase. Hence the purposes of this study are to describe radiographic appearance of pulmonary cryptococcosis in comparison with others and to describe some aspects of clinical manifestations.

[1] Department of Radiology, Bamrasnaradura hospital, Nonthaburee
[2] Department of Radiology, Central Chest hospital, Nonthaburee

MATERIALS AND METHODS

Medical records and chest radiographs of patients with AIDS and pulmonary cryptococcosis diagnosed during October 1990 to February 1996 in Bamrasnaradura Hospital were retrospectively reviewed. The pulmonary cryptococcosis was definitely diagnosed by the presence of organism in histopathologic specimen (from either biopsy or necropsy material) or probably diagnosed by the presence of organism on stain and/or culture of bronchial secretion or fluid with correlated chest radiograph. We excluded patient who has other coexisting pathogen in the lung.

Chest radiographs were independently analysed by 4 radiologists from Bamrasnaradura Hospital and Central Chest Hospital. The following were recorded: presence or absence of infiltration, any ground-glass appearance, cavity, pleural effusion and lymphadenopathy. Types of infiltration were classified as predominantly alveolar or interstitial pattern which was also divided to be fine or intermediate or coarse interstitial pattern. If there was any different radiographic interpretation the consensus would be needed for final opinion.

RESULTS

There were 22 AIDS patients with documented pulmonary cryptococcosis. Twenty-one patients were men and 1 was woman with ages ranging from 22 to 64 years. Twelve patients were heterosexual, 2 were homosexual and intravenous drug users, 2 were bisexual and 6 had no documented risk factor. Most of the patients presented with fever, cough and headache.(Table.1) Four patients had lung crepitation and only 5 patients had obvious neck stiffness on physical examination. The duration of symptoms varied from 1 week in 5 patients, around 1 month in 11 patients and 2-4 months in 6 patients.

Eight patients met criteria of definite diagnosis for pulmonary cryptococcosis and the remaining 14 patients met criteria of probable diagnosis.

Diffuse infiltration in both lungs, predominantly interstitial pattern were presented in 14 patients, localized infiltration in 6 patients (Fig.1) and mediastinal adenopathy without infiltration was seen in only 1 patient (Fig.2). One patient had mild to moderate degree of Rt. pleural effusion with equivocal infiltration or crowded interstitial markings in Rt lung. (Table 2) Of the 14 patients with diffuse infiltration ; 7 were fine pattern (Fig.3), 2 were coarse pattern (Fig. 4) and 5 were intermediate pattern. Ground- glass patterns were described in 4 of 14 patients with diffuse infiltration. (Fig. 5) Most of diffuse infiltration pattern involved the mid or the lower lung zones more than the upper zone.

Table 1. Summaries of symptoms and signs of 22 AIDS patients with pulmonary cryptococcosis

fever	17
cough	12
headache	9
dyspnea	5
gastrointestinal symptoms (diarrhea,nausea,vomitting,melena)	3
chest pain	1
adenopathy	6
lung crepitations	4
neck stiffness	5
skin nodules	1

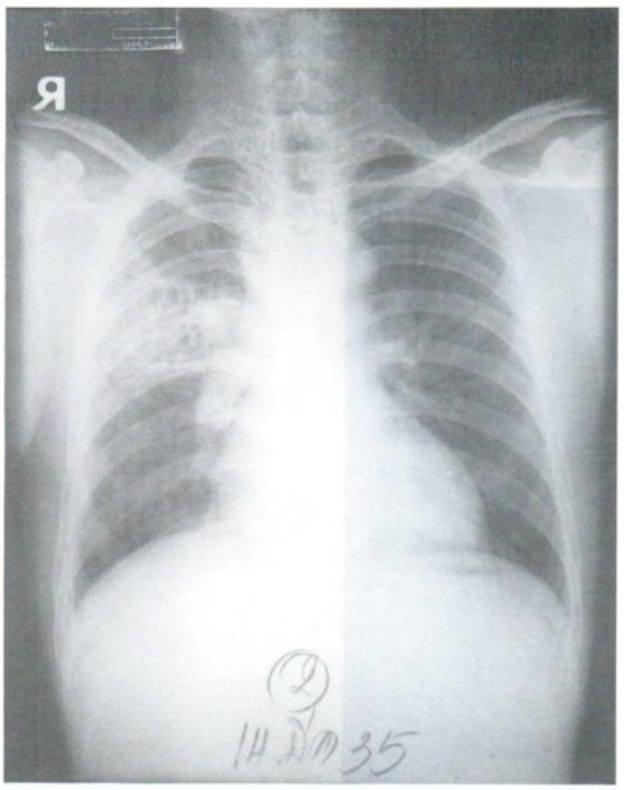

Fig. 1 Localized infiltration are present in Rt. upper lobe.

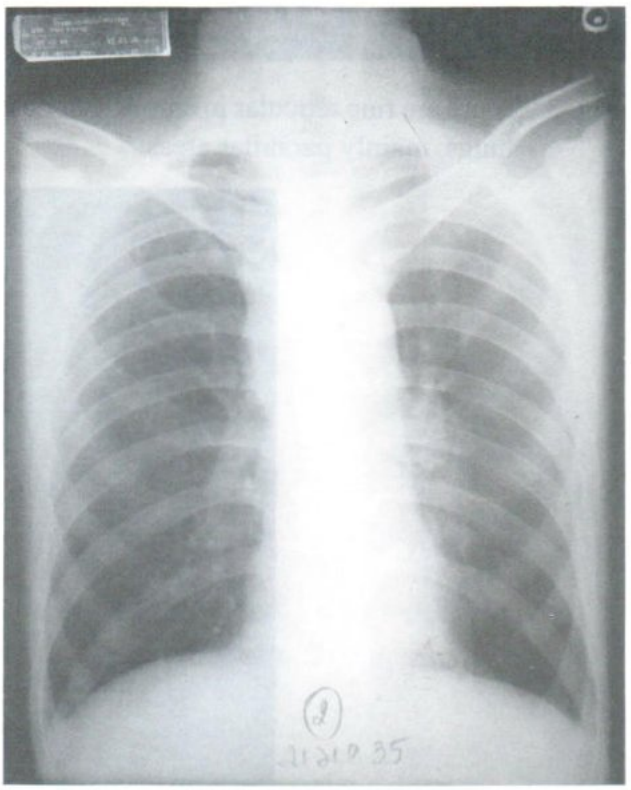

Fig. 2 There is superior mediastinal lymphade -nopathy without pulmonary infiltration.

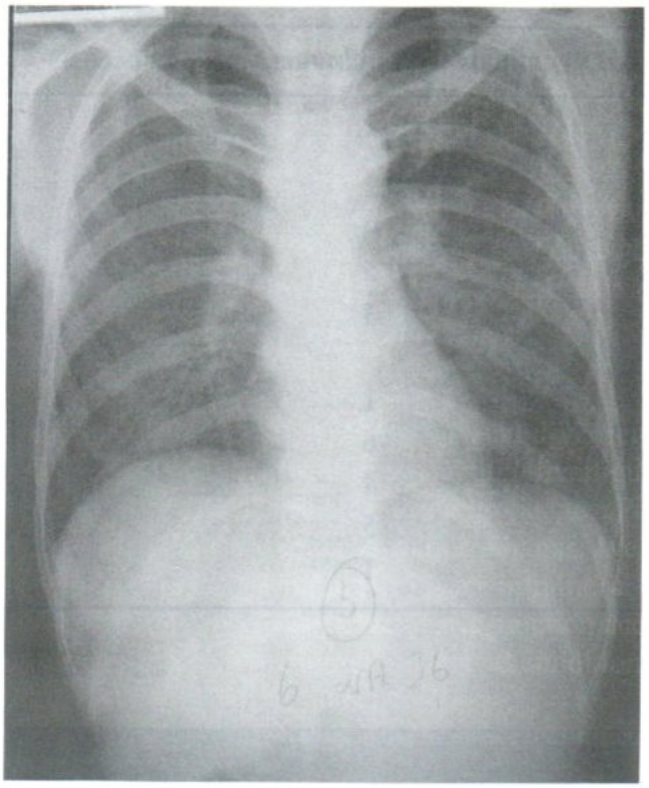

Fig. 3 There are fine reticular infiltration in both lungs, mainly parahilar areas.

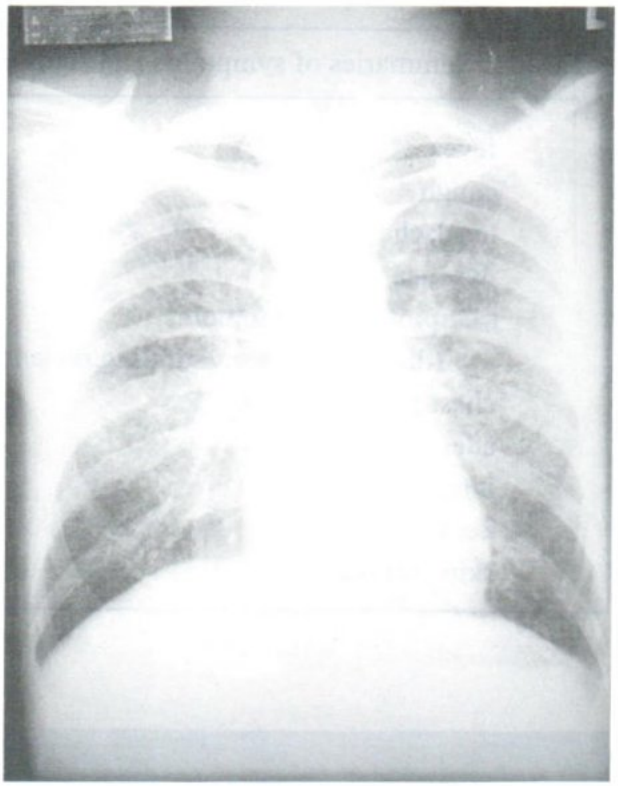

Fig. 4 Chest radiograph shows coarse reticular infiltration in both lungs.

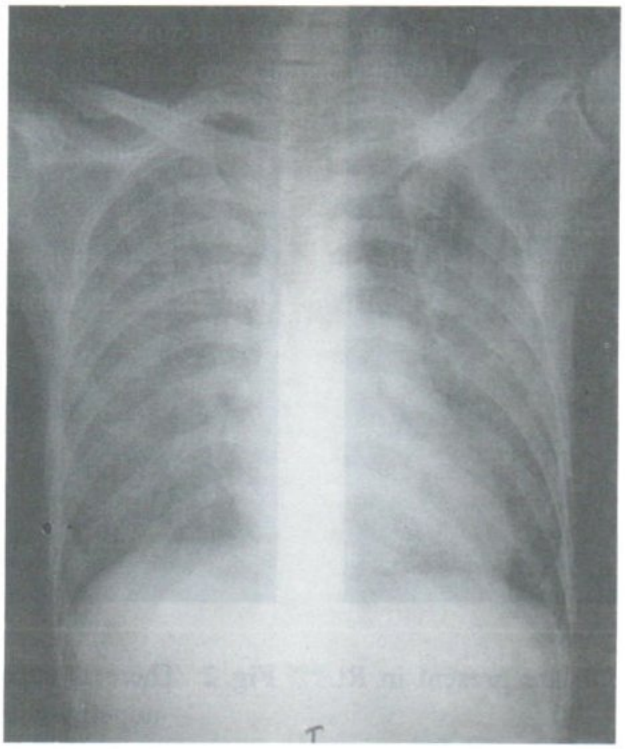

Fig. 5. Diffuse pulmonary infiltration with ground-glass appearance.

Associated abnormalities were minimal pleural effusion and cavity, presenting in 5 and 2 patients respectively.

There were 19 patients having documented concurrent extrapulmonary cryptococcal infection. Seventeen of these patients had cryptococcal meningitis with or without cryptococcal septicemia, lymphadenitis, hepatitis, urinary tract infection and skin infection. (Table. 3) Lumbar puncture was not performed in two patients who had only documented cryptococcemia. In the remaining 3 patients extrapulmonary tissue was not sampled for evidence of cryptococcal infection. Four patients were diagnosed pulmonary cryptococcosis prior to meningitis.

Of the 18 patients receiving antifungal drugs, 12 patients improved, 1 patient initially improved but had been lost to follow-up and 5 patients died. All 4 patients who had not received antifungal treatment were dead.

Table 2. Summaries of radiographic appearances of pulmonary cryptococcosis

Diffuse infiltrates, predominantly interstitial pattern	14
- fine pattern (7)	
- intermediate pattern (5)	
- coarse pattern (2)	
Localized mixed infiltrates	6
Unilateral pleural effusion with equivocal infiltrate	1
mediastinal adenopathy alone	1
associated lesion	
pleural effusion	5
cavity	2

Table. 3 Presence of extrapulmonary cryptococcal infection

	No. of cases
meningitis	8
meningitis + septicemia	4
meningitis + septicemia + lymphadenitis	2
meningitis + septicemia + hepatitis	1
meningitis + septicemia + nephritis + skin infection	1
meningitis + lymphadenitis	1
septicemia	2
no document	3

DISCUSSION

Cryptococcus neoformans is a nonmycelial budding yeast found in a variety of environmental sites but most abundant in pigeon and chicken excreta. Lung is the portal of entry and in the normal host the organism could be irradicated by host defense mechanism, mainly cell mediated immunity (CMI).[1] In the immunocompromised host such as AIDS or immunosuppressed patients due to corticosteroid therapy, malignancy or immunosuppressive drugs, C. neoformans can significantly proliferate in the lungs and disseminate to other organs.[4]

Radiographic appearance of pulmonary cryptoccosis is found to be related to immunological competency.[5] In the study of Khoury et al revealed that immunocompetent hosts tended to have a single or multiple nodules but immunocompromised hosts demonstrated a wider varity of radiographic abnormalities including single or multiple nodules that progressed to confluence and/or cavitation, segmental consolidation, bilateral bronchopneumonia or a mixed pattern. Single or multiple nodules were the most common lesion followed by consolidation lesion. Adenopathy, cavitation and pleural effusion were limited to the immunocompromised hosts. However radiographic features of HIV-seronegative immuno -compromised patients are quite different from HIV infected patients. Several series and this study had found no large pulmonary nodule in AIDS patients with pulmonary cryptococcosis and interstittal infiltration had more frequently been reported, ranging from 57% to 80 %.[6-13] So far, to our knowledge only one series of Chechani et al found large nodule (> 2 cm.) or circumscribed infiltration in 3 of 12 patients.[11] These figures may indicate more severity of immunosuppression in patients with AIDS and may reflect the inability to localize an infectious process to form large granulomatous nodules.

Two available series had described the patterns of interstitial infiltration which are more or less different from our series. Most of the patients in our series with diffuse interstitial infiltration had fine or intermediate patterns (12 in 14 patients) resembling pneumocystis carinii pneumonia and lesions in 4 of 12 patients could be described as ground-glass appearance. The coarse nodular infiltration were found in only 2 patients. In contrast, infiltration found in Miller et al series were predominantly nodular or coarse infiltration patterns and resembled advanced miliary TB in two patients.[6] Friedman et al also found predominantly coarse interstitial pattern in 9 of 14 patients and miliary nodules in one patient.[8] We postulate that the immunity in most of our AIDS patients may be more severely suppressed than those of the other two series causing less ability to form

such a coarse nodular infiltration. However our study is a retrospective form so the complete data of lymphocytic count could not be obtained and the number of patients in our study and other studies are too small to be statistically significant. Furthermore, the study of Friedman et al did not exclude cases with pulmonary copathogen, so comparison cannot be clearly made.

Cavities were associated lesion uncommonly found. Five series reported no obvious cavity[6-9,12] while 3 series found a small number of cavities ; 2 in 17 patients,[10] 2 in 12 patients,[11] 1 in 3 patients respectively.[13] Our study found cavities in only 2 of 22 patients. Since in severely immuno -compromised HIV- positive patients there is poor immune response to form granuloma and central necrosis, so cavities are less frequent.

Intrathoracic adenopathy was quite uncommon in our study being observed in only 1 out of 22 patients. The presence of adenopathy in each series varied from ; 3 in 7 patients,[6] 4 in 5 patients,[7] 3 in 17 patients[10] and 1 in 10 patients.[12] These series had excluded all cases with pulmomary copathogen.

There are series of Chechani , Friedman and Mayohas which reported negative chest films; 3 in 12 patients, 2 in 14 patients and 1 in 17 patients respectively, suggesting endobronchial lesion or early infection. No negative chest film was noted in our study.

Even though signs and symptoms of pulmonary cryptococcosis were nonspecific such as fever, cough and headache we noted that most of the patients had concurrent extrapulmonary cryptococcal infection particulary meningitis similar to that of the others.[6,8,10,11,13] Although the study of Wasser et al had focused on primary pulmonary cryptococcosis, soon after, all patients did develop cryptococcal meningitis.[7] These confirm that the nature of pulmonary cryptococcosis in immuno-compromised host is a disseminated disease and pulmonary cryptococcosis alone may be unusual.

Occasionally, pulmonary cryptococcosis could be an initial presentation of cryptococcal infection or diagnosed prior to the diagnosis of cryptococcal meningitis as depicted by our study (4 in 20 patients), Wasser et al (5 in 20 patients),[7] Kovacs et al (3 in 27 patients),[14] Zuger et al (4 in 26 patients)[15] and Chuck et al (4 in 106 patients).[16] Recent reports had suggested that more than half of the patients have primary cryptococcal pneumonia.[9,17]

The treatment outcome was quite good as there were 12 from 16 patients improved following antifungal drug administration, whereas 4 patients who did not receive any specific treatment died. So, precised and early diagnosis is very important in order to decrease mortality rate.

In conclusion, pulmonary cryptococcosis in AIDS patients is becoming a more frequent opportunistic infection and usually has concurrent extrapulmonary cryptococcosis, particularly meningitis. Occasionally it is the initial presentation. Clinical features are nonspecific such as fever, cough and headache. Radiographic appearances were mostly diffusely mixed infiltration, predominantly fine or intermediate interstitial pattern, resembling pneumocystis carinii pneumonia. Localized infiltration are less frequent. Small pleural effusion, mediastinal adenopathy and cavities are evident in some cases. Pulmonary cryptococcosis should be considered in AIDS patients than ever before and the sooner the diagnosis is made the better therapeutic outcome can be expected.

REFERENCES

1. Murray JF, Mills J. Pulmonary infectious complications of human immunodeficiency virus infection. Am Rev Respir Dis 1990;141:1582 -98

2. Prasest P, Peerapatanapokin V, Tharmphornpilas P, et al. Opportunistic infection and AIDS related conditions among AIDS/ARC cases in Thailand. Thai AIDS Journal 1993;5:181-7
3. Grant IH, Armstrong D. Fungal infections in AIDS. Cryptococcosis. Infect Dis Clin North Am 1988;2:457-64
4. Fraser RG, Pare JAP. Diagnosis of disease of the chest. Philadelphia Saunders, 1989: 975-85
5. Khoury MB, Godwin JD, Ravin CE, Gallis HA, Halvorsen RA, Putman CE. Thoracic cryptococcosis : immunologic competence and radiologic appearance. AJR 1984; 141:893-6
6. Miller WT Jr, Edelman JM, Miller WT. Cryptococcal pulmonary infection in patients with AIDS : radiographic appearance. Radiology 1990;175:725-8
7. Wasser L , Talavera W. Pulmonary cryptococcosis in AIDS. Chest 1987;92:692-5
8. Friedman EP, Miller RF, Severn A, Williams IG, Shaw PJ. Cryptococcal pneumonia in patients with the acquired immunodeficiency syndrome. Clin Radiol 1995;50:756 -60
9. Batungwanayo J, Taelman H, Bogaerts J. Pulmonary cryptococcosis associate with HIV-1 infection in Rwanda:a retrospective study of 37 cases. AIDS 1994;8:1271-6
10. Meyohas MC, Roux P, Bollens D, et al. Pulmonary cryptococcosis localized and disseminated infections in 24 patients with AIDS. Clin Infect Dis 1995;21:625-33
11. Chechani V, Kamholz SL. Pulmonary manifestation of disseminated cryptococcosis in patients with AIDS. Chest 1990;98:1060-6
12. Sider L, Wescott MA. Pulmonary manifestation of cryptococcosis in patients with AIDS : CT features. J thoracic imaging 1994;9:78-84
13. Martos A, Mascoro J, Santin M, et al. Pulmonary cryptococcosis in AIDS. Enfermedades infection y Microbiologia clinica 1992;10:607-10
14. Kovacs JA, Kovacs AA, Polis M , et al. Cryptococcosis in the acquired immunodeficiency syndrome. Ann Intern Med 1985;103:533-8
15. Zuger A, Louie E, Holzman RS, Simberkoff MS, Rahal JJ. Cryptococcal disease in patients with acquired immunodeficiency syndrome. Ann Intern Med 1986;104:234-40
16. Chuck SL, Sande MA. Infections with cryptococcal neoformans in acquired immunodeficiency syndromes. New Eng J Med 1989;12 :794-9
17. Clerk RA, Greer DL, Valainis GT, et al. Cryptococcal neoformans pulmonary infection in HIV-1- infected patients. J acquir immune Defic Syndr 1990;3:480-4

MR IMAGING OF PERIPHERAL NERVE SHEATH TUMORS OF THE EXTREMITIES

Sirikan WONGSRISOONTORN MD[1], Pimjai SIRIWONGPAIRAT MD[1]
Suphaneewan JAOVISIDTH MD[1]

ABSTRACT

Two patients with peripheral nerve sheath tumors (PNST) of the extremities were presented, emphasizing on magnetic resonance (MR) imaging findings. In both cases, T2-weighted images showed inhomogeneously hypersignal intensity and contrast enhanced studies revealed intense enhancement predominantly at periphery. An oval shape or tapering of longitudinal end of the mass suggest its extension along longitudinally oriented structure such as neurovascular bundle.

Keywords : Nervous system; neoplasm Nerves; peripheral, MR

INTRODUCTION

PNST most frequently results from proliferation of neural supporting tissues and the two most common entities of PNST are neurofibroma and neurilemoma (schwannoma).[1] PNST can be found as a solitary lesion or as a part of clinical presentation of neurocutaneous syndrome e.g. neurofibromatosis.

Diagnosis of PNST while having many features suggestive of such syndrome is not difficult. But for a solitary PNST in the extremity, the diagnosis may be problematic. We reported 2 cases of PNST of the extremity emphasizing on their MR characteristics.

CASE REPORTS:

Case 1:

An eighty-seven-years-old female patient presented with a palpable, gradually enlarging mass in her right arm for 1 year with paresthesia along the course of ulnar nerve. Physical examination revealed a hard mass locating in posterior aspect of right arm. Plain film showed soft tissue mass corresponding to the palpable lesion without calcification or ossification. MR imaging revealed a 2.7x 2.7x 4.5 cm-size mass lesion, having well-defined margin with tapering of its inferior aspect, within the triceps muscle of the right arm (Fig. 1 a). On T1-weighted images, the mass showed slightly inhomogeneously isosignal with surrounding muscle (Fig. 1 b). On T2-weighted images, the mass exhibited inhomogeneously hypersignal; composing of peripheral hypersignal area with central mixed hyper- & hyposignal intensities (Fig. 1 c). After gadolinium administration; thick, irregular, intense enhancement of the mass was observed peripherally in fat suppressed T1-weighted images (Fig. 1 d). The ulnar nerve could not be well separated from the mass. No muscle atrophy, bone involvement, internal calcification, or signal void was detected. Surgery was

Department of Radiology, Ramathibodi Hospital, Faculty of Medicine, Mahidol University, Rama 6 Street, Bangkok 10400, Thailand.

performed and revealed a 3-cm mass with necrosis, with questionable its location within the ulnar nerve. Pathologic examination disclosed an oval-shape mass in the center of ulnar nerve trunk, with middle part of the nerve trunk blended into the deep part of the mass. Histologic diagnosis was schwannoma with focal hemorrhagic infarction.

Case 2:

A 42-year-old male patient presented with pain and ill-defined nodular mass in his right forearm for 8 months. He had no fever and there was no change in size of the mass as compared to the first detection. Ultrasonography disclosed a hypoechoic well-defined solid mass. MR imaging was performed later, and revealed a 2.0x 1.3x 1.2 cm-size well-defined oval-shape mass in right forearm, showing homogeneously slightly hypersignal intensity on T1-weighted images, inhomogeneously hypersignal intensity on T2-weighted images particularly at periphery (Fig 2), and inhomogeneously intense enhancement more at periphery after intravenous gadolinium administration. No associated muscle atrophy, bony involvement, internal calcification, cyst formation or signal void was detected. Excisional biopsy was performed and the section revealed a schwannoma.

al. MR imaging of extracranial nerve sheath tumors. J Comput Assist Tomogr 1992; 16: 448-453

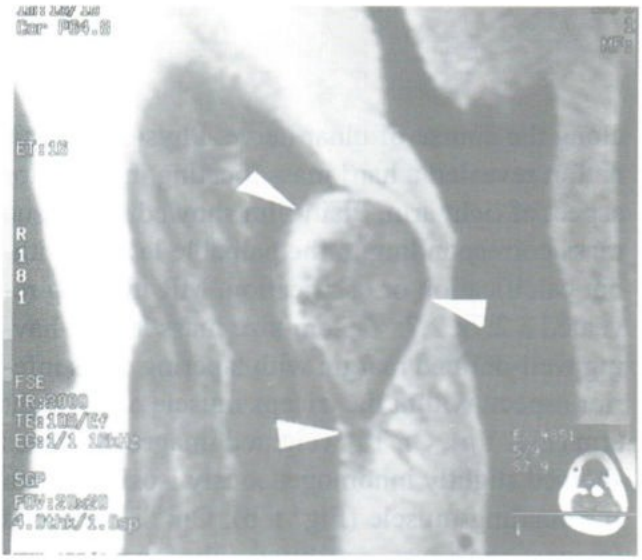

Figure 1 a-d. Case 1.

Fig. 1 A : T2-weighted sagittal MR image shows inhomogeneously hypersignal teardrop-shape mass (arrowheads). Inferior tapering of the mass indicates extension along longitudinally oriented structures.

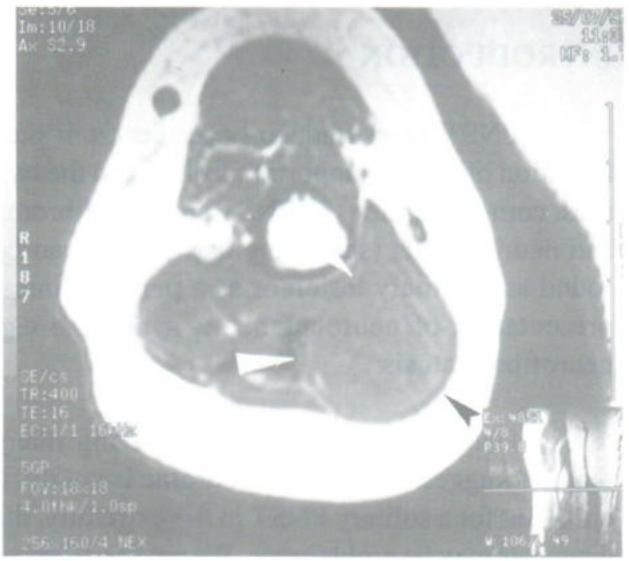

Fig. 1 B : T1-weighted axial MR image reveals the mass to be slightly inhomogeneously isosignal to surrounding muscles (arrowheads).

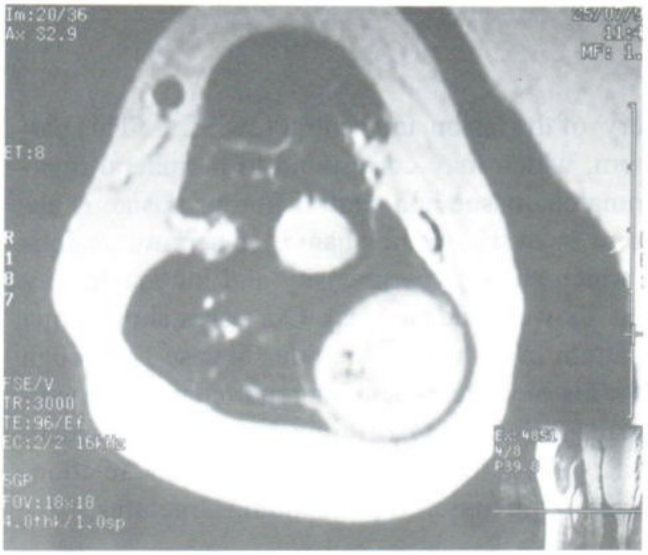

Fig. 1 C : T2-weighted axial MR image discloses peripheral hypersignal area whereas the central area shows mainly hyposignal intensity.

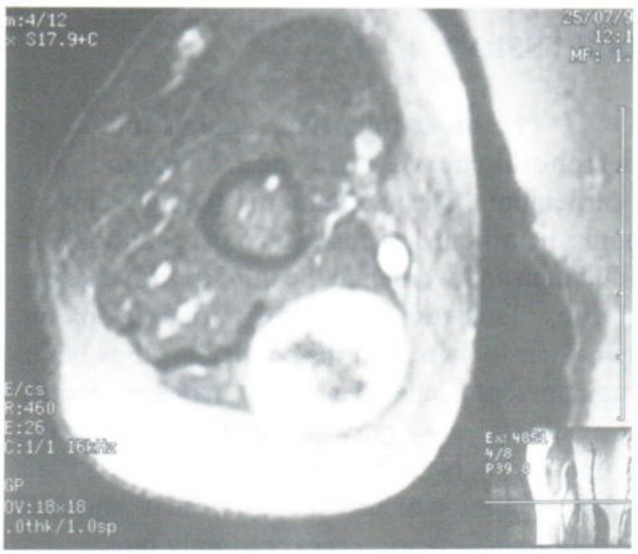

Fig. 1 D : Gadolinium enhanced fat-suppressed T1-weighted axial MR image exhibits thick, irregular peripheral enhancement.

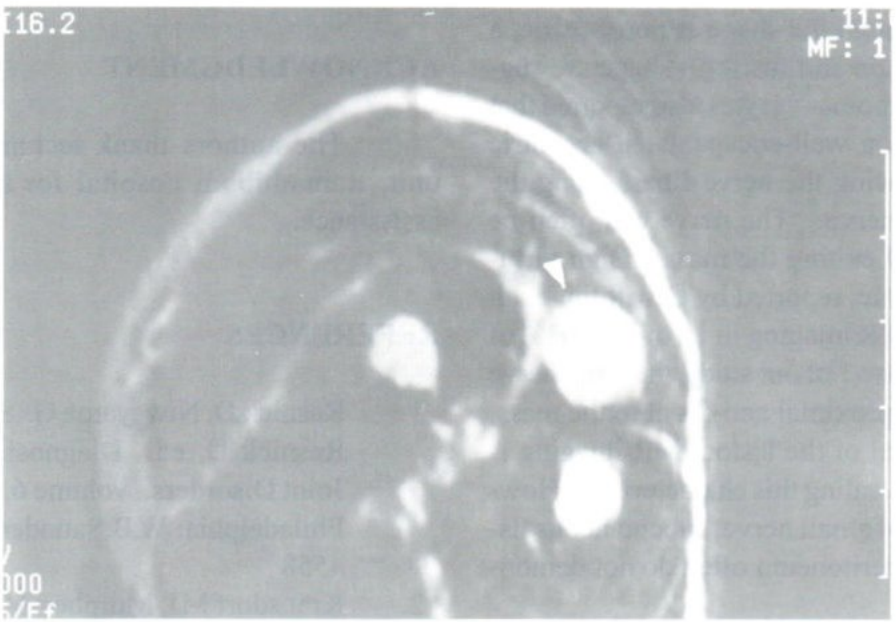

Figure 2 . Case 2.

Fig. 2 : T2-weighted axial MR image reveals the mass to have inhomogenously hypersignal on T2-weighted image predominantly at periphery (arrowhead).

DISCUSSION

The most important benign tumors of peripheral nerves are neurofibroma and neurilemoma. The neurilemoma (benign schwannoma, neurinoma) is observed most commonly in adult men and women in the third to fifth decades of life.[1] This tumor typically arises from the spinal nerve roots, and the cervical, sympathetic, vagus, peroneal, and ulnar nerves. It predominantly is a solitary, slow growing, and non-aggressive neoplasm.[1-3] Neurilemomas are benign in their behavior; tumor recurrence is unusual, and malignant transformation is exceedingly rare.[4]

There are only a few reports concerning MR imaging findings of PNST, especially of the extremities.[5,6] The size of PNST are variable and there is no clue of diagnosis. Data from 2 series,[7,8] comprising 22 benign and 8 malignant peripheral nerve sheath tumors, also showed great variability in size. Although the shape is nonspecific, a well-defined margin and fusiform shape are suggestive of neurilemoma.[6,9] It was also reported that neurilemoma has a well-encapsulated eccentric nature and displacing the nerve fibers along the long axis of the nerve.[9] The nerve can often be seen entering and exiting the mass, a sign virtually pathognomonic, reported by Cerofolini et al. to be present on MR imaging in 16 of 17 (94%) of their cases.[10] In case 1 of our study, the ulnar nerve can be identified proximal and distal to the mass, but not at the level of the lesion. MR imaging is of great help in revealing this characteristic. However, the lesions of small nerve, subcutaneous tissue and the retroperitoneum often do not demonstrate this finding.[3]

Regarding the internal signal intensity (SI), most of PNST reveal relatively low SI on T1-weighted MR images and high SI on T2-weighted images.[11] On T2-weighted images and on T1-weighted images following intravenous administration of gadolinium, a target pattern may be identified,[1,6] consisting of increased SI at the periphery of the lesion and central low SI.[1,12] This pattern, which may correspond to peripheral myxomatous tissue and central fibrous tissue, is absent in cystic, hemorrhagic, or necrotic lesions (which show hyperintensity and inhomogeneity on T2-weighted images). Our cases show target pattern in both, more obvious in case 1 although the histologic examination reported internal hemorrhagic infarction. MR imaging also allows identification of the nerve trunk of origin and relationship of the tumor to surrounding structures.[1]

In conclusion, MR characteristics of peripherally increased SI on T2-weighted images and on T1-weighted images after contrast injection, an oval shape or tapering longitudinal end of the lesion, and demonstration of nerve entering and exiting the mass should suggest the diagnosis of PNST.

ACKNOWLEDGMENT

The authors thank technicians of MRI unit, Ramathibodi hospital for their technical assisstance.

REFERENCES

1. Resnick D, Niwayama G. Soft tissues. In: Resnick D, ed. Diagnosis of Bone and Joint Disorders. Volume 6. Third edition. Philadelphia: W.B.Saunders, 1995: 4549-4558
2. Kransdorf MJ, Murphey MD. Neurogenic tumors. In: Kransdorf MJ, Murphey MD, eds. Imaging of Soft Tissue Tumors. Philadelphia: W.B.Saunders, 1997: 235-254
3. Sundaram M, Sharafuddin MJA. MR imaging of benign soft tissue masses. Magn Reson Imaging Clin N Am 1995; 3: 620-621

4. Carstens H, Schrodt G. Malignant transformation of a benign encapsulated neurilemoma. Am J Clin Pathol 1969;51:144-146
5. Murphey MD, Smith WS, Temple HT. Imaging of malignant peripheral nerve sheath tumors. Radiology 1996;201 (P): 359-360
6. Smith WS, Murphey MD, Temple HT. Imaging of benign peripheral nerve sheath tumors with pathologic correlation. Radiology 1996;201 (P): 360
7. Levine E, Huntrakoon M, Wetzel LH. Malignant nerve-sheath neoplasms in neurofibromas: Distinction from benign tumors by using imaging techniques. AJR Am J Roentgenol 1987;149:1059-1063
8. Stull MA, Moser RP Jr, Kransdorf MJ, et al: Magnetic resonance appearance of peripheral nerve sheath tumors. Skeletal Radiol 1991;20:9-13
9. Suh J-S, Abenoza P, Galloway HR, Everson LI, Griffiths HJ. Peripheral (extracranial) nerve tumors: Correlation of MR imaging and histologic findings. Radiology 1992;183:341-346
10. Cerofolini E, Landi A, DeSantis G, et al: MR of benign peripheral nerve sheath tumors. J Comput Assist Tomogr 1991;15: 593-597
11. Burk DL, Brunberg JA, Kanal E, et al. Spinal and paraspinal neurofibromatosis: Surface coil MR imaging at 1.5 T. Radiology 1987;162:797-801
12. Varma DGK, Moulopoulos A, Sara AS, et al. MR imaging of extracranial nerve sheath tumors. J Comput Assist Tomogr 1992;16:448-453

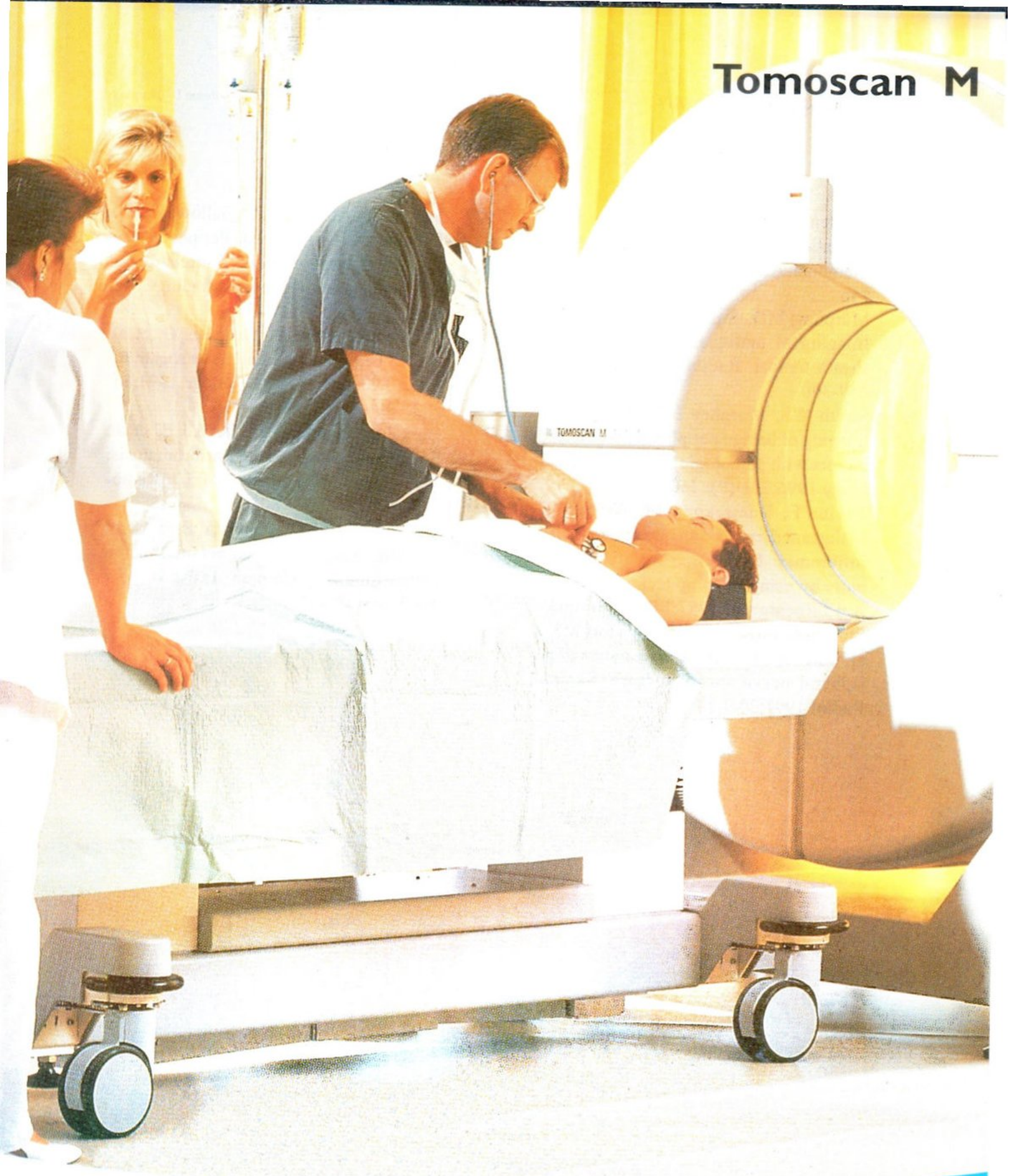

FOR MORE INFORMATION PLEASE CONTACT

PHILIPS MEDICAL SYSTEMS

- TEL. 745-4090 Ext. 3332
- FAX. 398-0792

Philips Electronics (Thailand) Ltd.
209/2 Sanpavuth Road, Prakanong, Bangkok 10260

PHILIPS

Let's make things better.

MRI IN A CASE OF HERPES ZOSTER OPHTHALMICUS

Patchrin PEKANAN , Suphaneewan JAOVISIDTH, Thitiporn RANGSITPOL

ABSTRACT

A case report of herpes zoster ophthalmicus was demonstrated by MRI study in a 61 year-old female patient. There was an abnormal enhancement of the intraorbital structures of left eye, the tissue in left eye was mildly thickened . The increased enhancement of left trigeminal nerve was noted.

INTRODUCTION

The most commonly reported complication of herpes zoster is postherpetic neuralgia.[1] Ocular involvement is shown in 20%-71% of cases of herpes zoster ophthalmicus[2] and includes: keratoconjunctivitis,[3] ocular motor palsies,[4] acute retinal necrosis,[5] acute phthisis bulbi,[6] optic neuritis,[7] and central retinal artery occlusion.[8] MR is proved to be useful for identifying the wide array of inflammatory and ischemic complications associated with herpes zoster ophthalmicus. Serial MR may document both the regression and progression of various aspect of this unusual disorder.[9]

CASE REPORT

A 61-year-old man came to the eye clinic because of decreasing vision to hand movement of his left eye for 20 days. Scar and ptosis of the left eyelid was found. Slit-lamp examination of left eye revealed ciliary injection, generalized bedewing with stromal edema and pigmented keratic precipitates of the cornea. There was hyphema about 1.6 mm in height in the left anterior chamber. There was impaired downward and medial movement of the left eye. The left pupil was semidilated and did not react to light, whereas the right pupil showed positive reverse relative afferent pupillary defect. Slit-lamp examination of the right eye was unremarkable. ESR was 68 mm/ hour. Complete blood count and blood chemistry was within normal limit. Anti- HIV titer was nonreactive.

MRI of the orbits was performed. It showed abnormal enhancement in left orbit: along left optic nerve (Fig.1) , in the mildly enlarged extraocular muscles of left orbit (Fig.1,2), of the intraorbital fat (Fig.1,2), of the mildly thickened sclera of left eyeball (Fig.3), at the cranial nerve V (Fig. 4) (cisternal and intracavernous portion) and the 1st division of the cranial nerve V. The pre-septal soft tissue was slightly thickened and enhanced (Fig.5). The left ethmoid sinus was mildly inflammed (Fig.5).

Department of Radiology, Ramathibodi Hospital , Rama 6th street, Bangkok 10400, Thailand

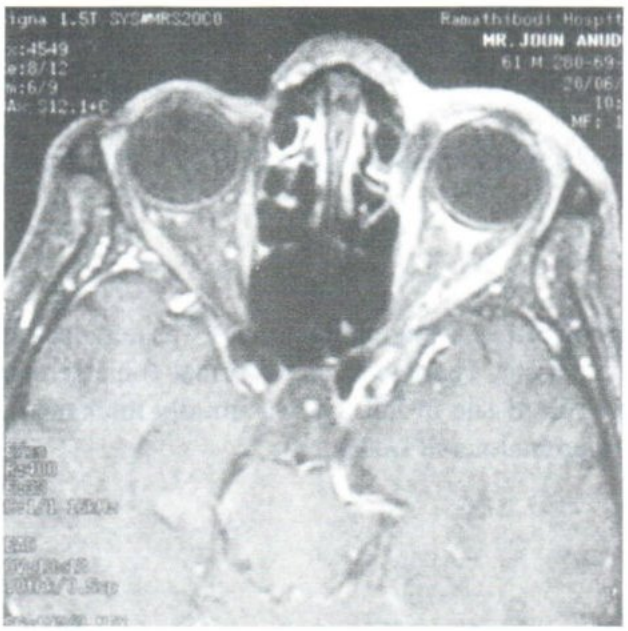

Fig. 1. I.V. enhanced axial MRI of the orbits showed abnormally increased enhancement of the intraorbital fat, subcutaneous fat plane over left eye.

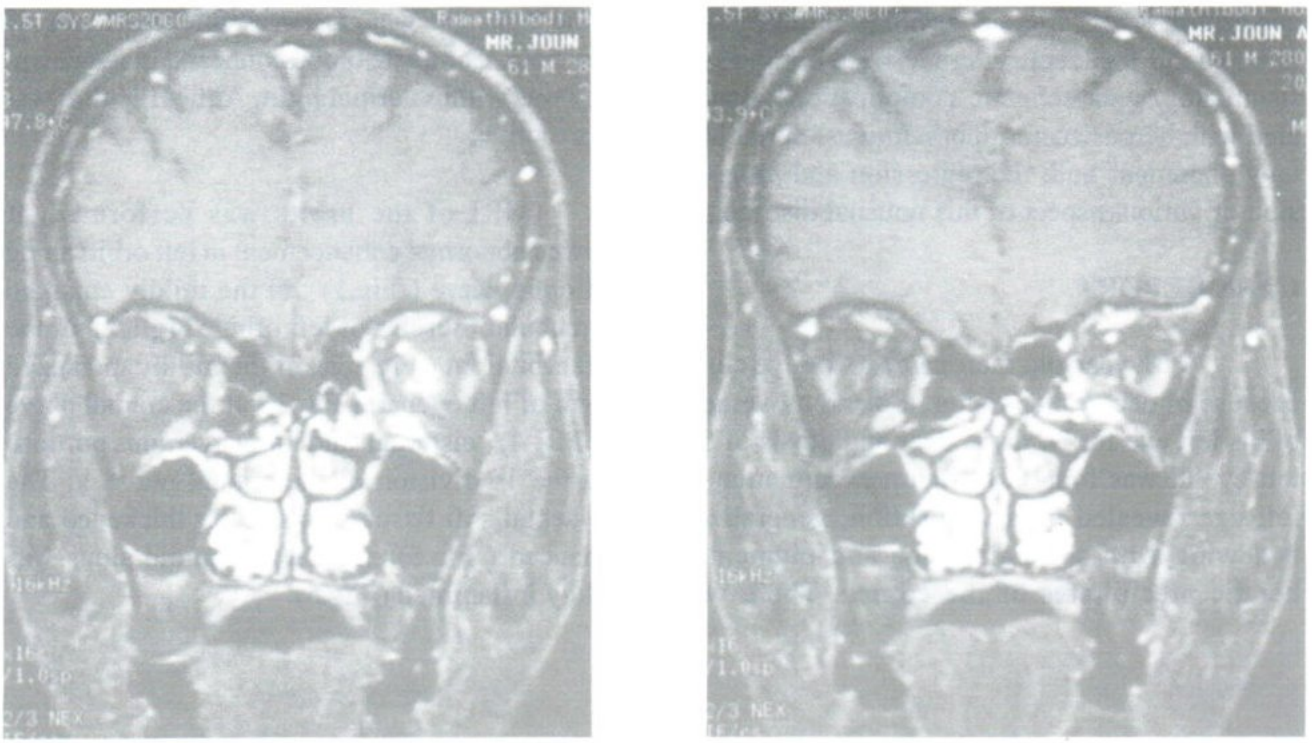

Fig. 2. I.V. enhanced coronal MRI of the orbis showed abnormally increased enhancement of the mildly enlarged extraocular muscles of left orbit.

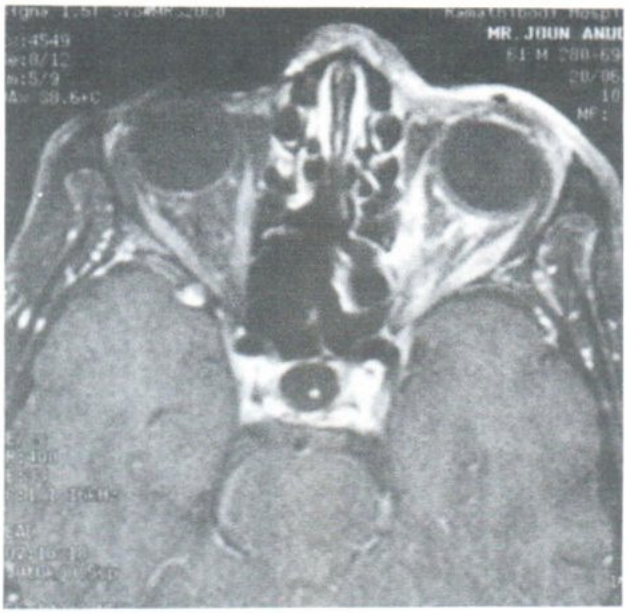

Fig. 3. I.V. enhanced axial MRI of the orbits showed abnormally increased enhancement of the mildly thickened sclera of left orbit.

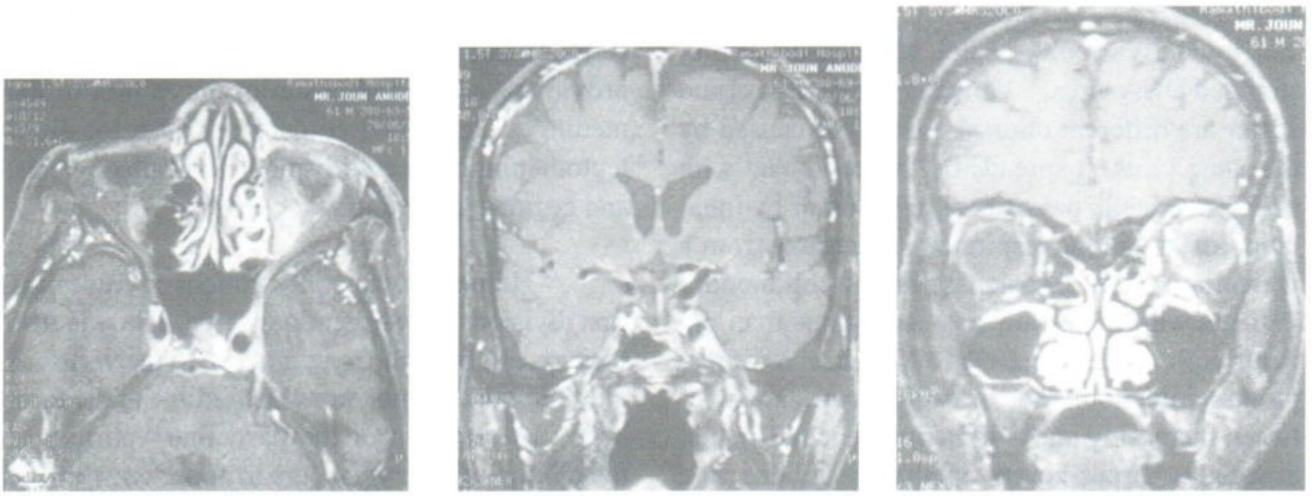

Fig. 4. I.V. enhanced axial and coronal MRI of the orbits showed abnormally increased enhancement of the cisternal, intracavernous portions of the trigeminal nerve and the V1 branch of left side.

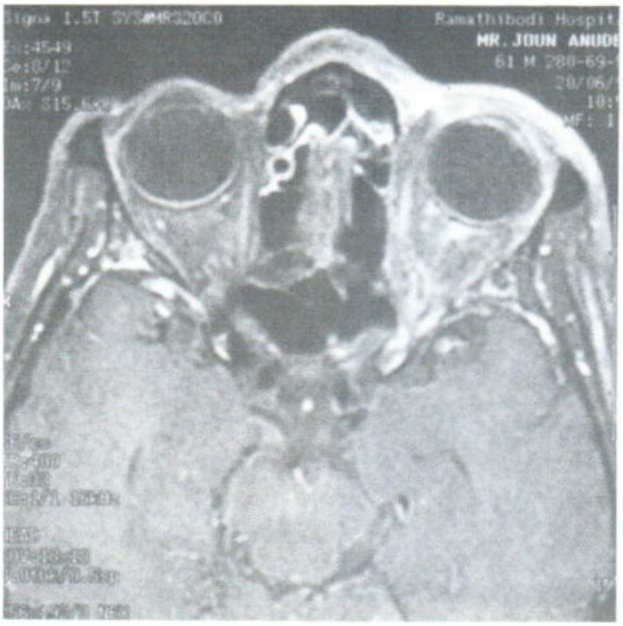

Fig. 5. I.V. enhanced axial MRI of the orbits showed abnormally increased enhancement of the preseptal soft tissue, subcuta neous fat over left eye and nose, besides enhancement of the intraorbital fat.

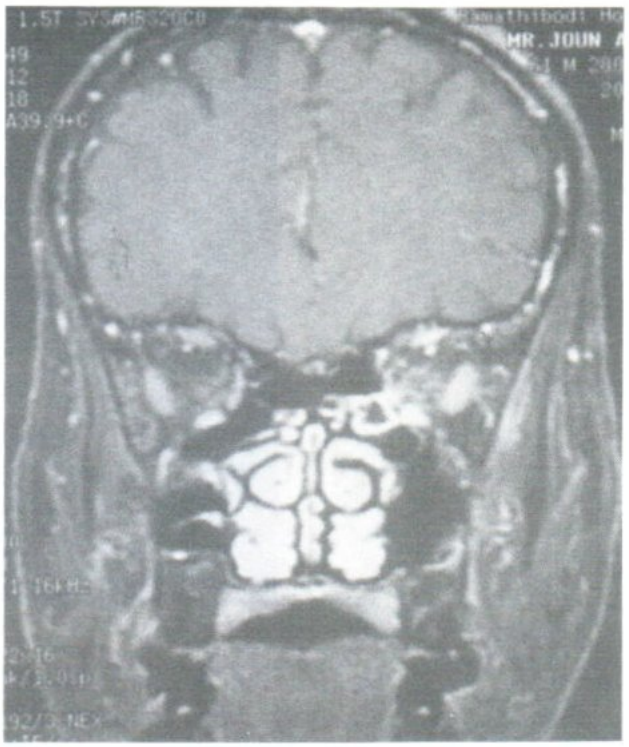

Fig. 6. I.V. enhanced coronal MRI of the orbits showed mild ethmoidal sinusitis.

DISCUSSION

The varicella-zoster virus is a double-stranded DNA virus.[10] Varicella (chickenpox) and zoster are different clinical conditions caused by the same virus. It spreads by direct contact with either a varicella or zoster skin lesion or by inhalation of infectious respiratory secretions from a varicella patient.[11] Zoster is rare in childhood.[12] Patients with zoster are less contagious than patients with varicella because of the absence of respiratory infection. There is a direct correlation between increasing age and the incidence of zoster, especially herpes zoster ophthalmicus, due to a decline in cell-mediated immunity.[13] Factors that increased risk of zoster include previous history of cancer, anticancer therapy, bone marrow transplantation, surgery and trauma.[14]

A prodrome of fever, malaise, headache, and dysesthesia herald the neuralgia component that precedes and eventuates in the cutaneous lesions of zoster. Spread of ganglionic infection proximally along the posterior nerve root to the meninges and spinal cord results in a localized leptomeningitis, cerebrospinal fluid pleocytosis, and segmental myelitis.

Herpes zoster ophthalmicus involves the first division of the trigeminal nerve. The skin rash may extend from the nose and eye to the vertex of the skull but does not cross the midline of the forehead. Involvement of the nasociliary portion of the ophthalmic nerve occurs in about one third of patients with herpes zoster ophthalmicus and is significantly correlated with the development of ocular complications.[2,11] The development of ocular complications, is not related to age, sex, or the severity of the skin rash. Overall, ocular involvement occurs in about 50% of patients with herpes zoster ophthalmicus. Zoster affects the second and third division of the trigeminal nerve less fre-

quently and rarely in contiguity with the first division.

The multiple and diffuse ocular complications of herpes zoster ophthalmicus are related to multiple mechanisms including presumed viral spread, nerve damage, ischemic vasculitis and an inflammatory granulomatous reaction.The complications may present acute, chronic, or relapsing.[14] Lid vesicles of zoster evolve with pitting, pigmentation,and scarring of the eyelids along the lid retraction, damage to lash roots and damage to meibomian glands. Ischemic vasculitis may lead to lid ulcers or necrosis. Orbital complications include proptosis, ptosis, chemosis, and ocular motor palsies resulting from local spread of infection within the orbit and /or brain stem or as a result of ischemic vasculitis. Conjunctival inflammation with hyperemia, petechial hemorrhage, follicular reaction, and occasionally conjunctival vesicles or membranous conjunctivitis is seen in the early stages of the disease. Inflammation of the episclera or sclera is frequently delayed for several months.

The corneal complications are frequent, resulting from a combination of factors including presumed replicating virus, limbal vasculitis, abnormal tear film, hyperesthesia and neurotropic damage, corneal exposure, and the host inflammatory and vascular response to injury.[15] Punctate epithelial keratitis and pseudodendrites develop within a few days of disease onset due to viral replication in the corneal epithelium. Later corneal complications are associated with presumed viral infection, vasculitis, immunologic mechanisms, or host inflammatory reactions. These include anterior stromal infiltrates, sclerokeratitis, keratouveitis, endotheleitis, serpiginous ulceration, and disciform keratitis. Corneal sensation is often diminished and when it persists, it leads to neurotropic keratitis. Exposure keratitis from cicatricial lid changes or the development of trichiasis may add additional insult to the cornea. Prolonged chronic disease results in corneal edema or an interstitial keratitis accompanied by vascularization , crystalline lipid deposits, stromal scarring, thinning, and even perforation

Uveitis is the most frequent finding heralding intraocular involvement. It results from presumed viral replication, ischemic vasculitis, or from lymphocytic infiltration of iris, stroma, or intraocular nerves.The disease may settle into a chronic or relapsing keratouveitis. Posterior subcapsular cataracts are seen in chronic disease from uveitis and/ or steroid use.

The vasculitis of herpes zoster may manifest in the retina and optic nerve with central retinal vein occlusion, central retinal artery occlusion, retinal vasculitis, or with ischemic optic neuropathy. Acute retinal necrosis could occur.

In herpes zoster ophthalmicus, the lesions are centered in the trigeminal ganglion but also extend into the brain-stem, orbital tissues, meninges, vessels of the brain, and ocular tissue.[16] The ocular damage presumably results from a combination of factors including viral invasion, vasculitis, and direct inflammation with involvement of posterior ciliary nerve and vessels and with a prominent ischemic necrosis.[17] With chronicity of the disease, a granulomatous reaction with epithelioid and giant cells develops within the cornea ,ciliary body, choroid, and retina in some patients. Virus had been identified at some stage in all tissues and is clearly the inciting agent in ocular disease. The end stage of inflammation is a granulomatous reaction in some tissues; the nerves develop thickening of the sheaths, fibrosis, and disappearance of ganglion cells.

MR orbital images[9] of Herpes Zoster infection include uveal-scleral thickening of the globe, ill-defined soft tissue throughout the pre- and postseptal soft tissues, and the rectus muscle and tendon enlargement. The optic nerve sheath complex showed abnormal peripheral enhancement, particularly prominent about the nerve head, with slight enhancement within the nerve head it-

self. The ophthalmic histopathologic examination showed periaxial infarction of the optic nerve and chronic inflammation in the uveal tract and vitreous and also the retinal perivasculitis in that case report of Lexa et al.

REFERENCE

1. Ragozzino MW, Melton LI III, Kurland LT Chu CP, Perry HO. Population-based study of herpes zoster and its sequalae. Medicine 1982; 61: 310-316
2. Bucci FA, Salvia PV, Mauriello JA. Herpes zoster ophthalmicus. Am Fam Physician 1987; 35:121-128
3. Harding SP, Lipton JR, Wells JC. Natural history of herpes zoster ophthalmicus: predictors of post-herpetic neuralgia and ocular involvement. Br J Ophthalmol 1987; 71:353-358
4. Carmody RF. Herpes zoster ophthalmicus complicated by ophthalmoplegia and exophthalmos. Arch Ophthalmol 1937;18: 707-711
5. Forster DJ, Dugel PU, Frangieh GT, Liggett PE, Rao NA. Rapidly progressive outer retinal necrosis in the acquired immunodeficiency syndrome. Am J Ophthalmol 1990;110:341-348
6. Amanat LA, Cant JS, Green FD. Acute phthisis bulbi and external ophthalmoplegia in herpes zoster ophthalmicus. Ann Ophthalmol 1985; 17:46-51
7. Winward KE, Hamed LM, Glaser JS. The spectrum of optic nerve disease in human immunodeficiency virus infection. Am J Ophthalmol 1989;107:373-380
8. Scharf Y, Kraus E, Zonis S. Optic neuropathy and central retinal artery occlusion in a case of herpes zoster ophthalmicus. Ann Ophthalmol 1987;19:77-78
9. Lexa FJ, Galetta SL, Yousem DM, Farber M, Oberholtzer,et al. Herpes Zoster ophthalmicus with orbital pseudotumor syndrome complicated by optic nerve infarction and cerebral granulomatous angiitis: MR-pathologic correlation. AJNR 1993;14:185-190
10. Barnes DW, Whitley RJ.CNS diseases associated with varicella zoster virus and herpes simplex virus infection: pathogenesis and current therapy. Neurol Clin 1986;4: 265-283
11. Liesegang TJ. Diagnosis and therapy of Herpes Zoster ophthalmicus. Ophthalmology 1991;98:1216-1229
12. Brunell PA, Kotchmar GS Jr. Zoster in infancy: failure to maintain virus latency following intrauterine infection. J Pediatr 1981;98:71-3
13. Miller AE. Selective decline in cellular immune response to varicella-zoster in the elderly. Neurology 1980;30:582-7
14. Cobo M, Foulks GN, Liesegang T,et al. Observations on the natural history of herpes zoster ophthalmicus. Curr Eye Res 1987;6:195-9
15. Liesegang TJ. Corneal complications from herpes zoster ophthalmicus. Ophthalmology 1985; 92: 316-24
16. Hedges TR III, albert DM. The progression of the ocular abnormalities of herpes zoster: histopathologic observations in nine cases. Ophthalmology 1982;89:165-77
17. Naumann G, Gass JDM.,Font RL. Histopathology of herpes zoster ophthalmicus. Am J Ophthalmol 1968; 65: 533-4

TRANSCATHETER GLUE EMBOLIZATION IN A CASE OF POST-TRAUMATIC PSEUDOANEURYSM AND AV FISTULA OF THE RENAL ARTERY

Jiemjit TAPANEEYAKORN M.D., Chamaree CHUAPETCHARASOPON M.D.
Sirintara PONGPECH M.D., Chatchai THANUDUMRONG M.D.

ABSTRACT

Transcatheter glue embolization in a case of a large post stabwound pseudoaneurysm and AV fistula of left renal artery was presented.The patient was 18-year-old man who had left flank pain and hematuria. The process of treatment was simple , cheap, effective and safe. The kidney and its function could be preserved.

INTRODUCTION

The reported incidence of pseudoaneurysm and AV fistula was considered rare, it occurred only about 0.01%-6.25%.[1] The main encountered causes are iatrogenic, usually following needle biopsy or percutaneous catheterization[1] and other traumatic events .The incidence of renal artery aneurysms is 0.01%-1%[2] and it accounts for 22% of all visceral aneurysms.[3]

Usually renal artery aneurysms are treated surgically.[3] Various percutaneous embolization techniques have also been performed with success.[4] Therapeutic embolization of the renal artery has been used to control bleeding, devascularize tumors, close AV fistula, obliterate aneurysms, control hypertension and infarct kidneys in an end-stage renal disease.

We report the treatment of a case of renal artery pseudoaneurysm and AV fistula, using the transcatheter glue embolization.

CASE REPORT

An 18-year-old Thai male had a stab wound injury at left flank for 1 week with left flank pain and hematuria . No excretion was observed from left kidney at IVP (Fig.1) and the contrast medium was seen only at the cortical part of left kidney and an enhanced tubular structure in the central part of left kidney from the images of the first CT scan (Fig.2). Retrograde pyelography showed an old blood clot at left ureteric orifice and left ureteric obstruction at mid ureter. Doppler ultrasonography and arterial phase ultrafast CT scan of the kidneys showed an AV fistula with a large false aneurysm, about 4 cm in diameter of the intrarenal branch of left renal artery (Fig.3-5). Left renal angiography confirmed this diagnosis (Fig.6).

The left renal fistula and aneurysm was embolized using a total of 1 cc.of glue (Histoacryl) with good success. The first 0.5 cc of glue was injected through a 3-F microcatheter which was introduced via the original 5-F Cobra catheter, while the tip of the catheter was placed in the feeding artery and the tip of the microcatheter was placed in the aneurysm. After the first embolization and the microcatheter was removed, the fistula was still seen whereas the aneurysm was smaller. Then, the second 0.5 cc of glue was

Department of Radiology, Ramathibodi Hospital , Rama 6 street, Bangkok 10400, Thailand.

injected via the same Cobra catheter, while the tip of the catheter was placed in the left renal artery, just proximal to the fistula.

Selective left renal angiography with a new Cobra catheter after the second embolization showed the disappearance of the aneurysm and fistula. Minimal nephrogram at the lateral aspect of the middle pole kidney was lost due to ischemia which was an accepted finding (Fig.7).

Follow up CT scan 2 weeks later showed only small renal infarction but the renal function and the creatinine level was normal (Fig.8). The hematuria also disappeared after the embolization.

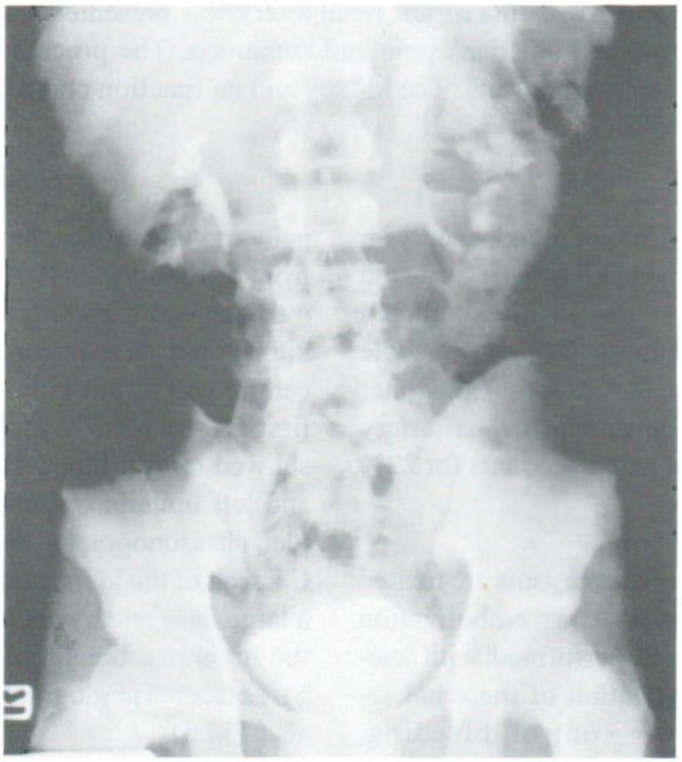

Fig. 1. No excretory function was seen from left kidney with an IVP study.

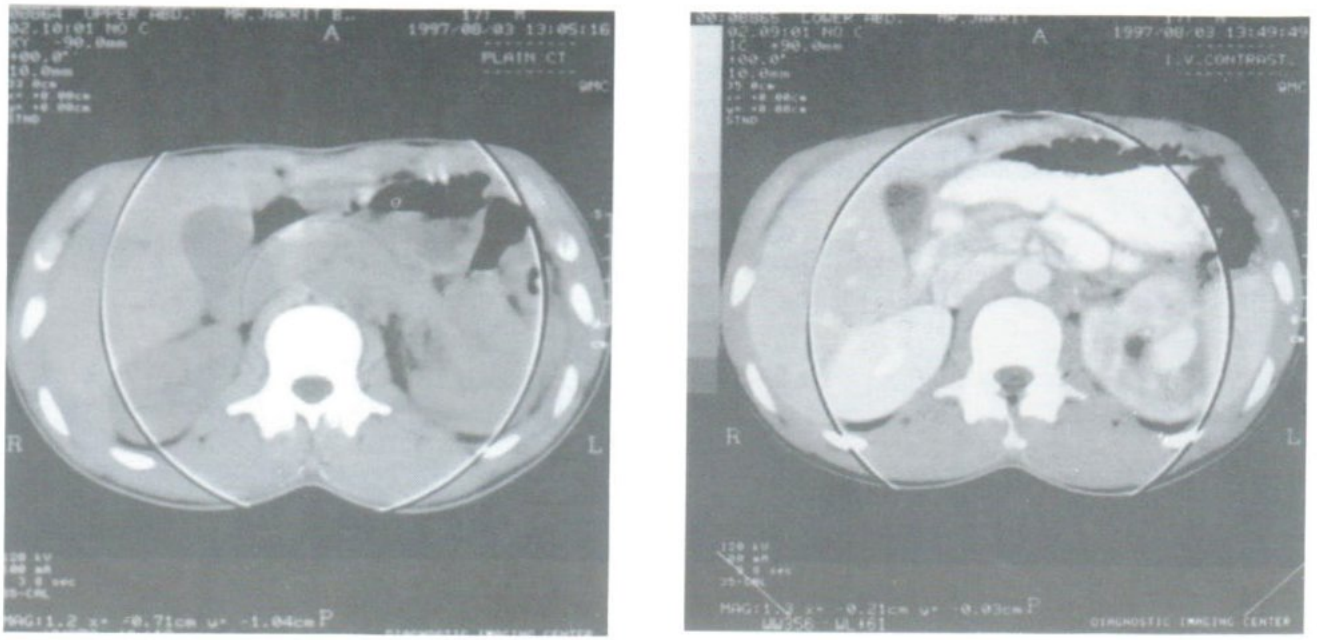

Fig. 2. AT CT scan, the excreted contrast medium was seen only at the cortical part of left kidney. An enhanced tubular structure was noted in the central part of left kidney.

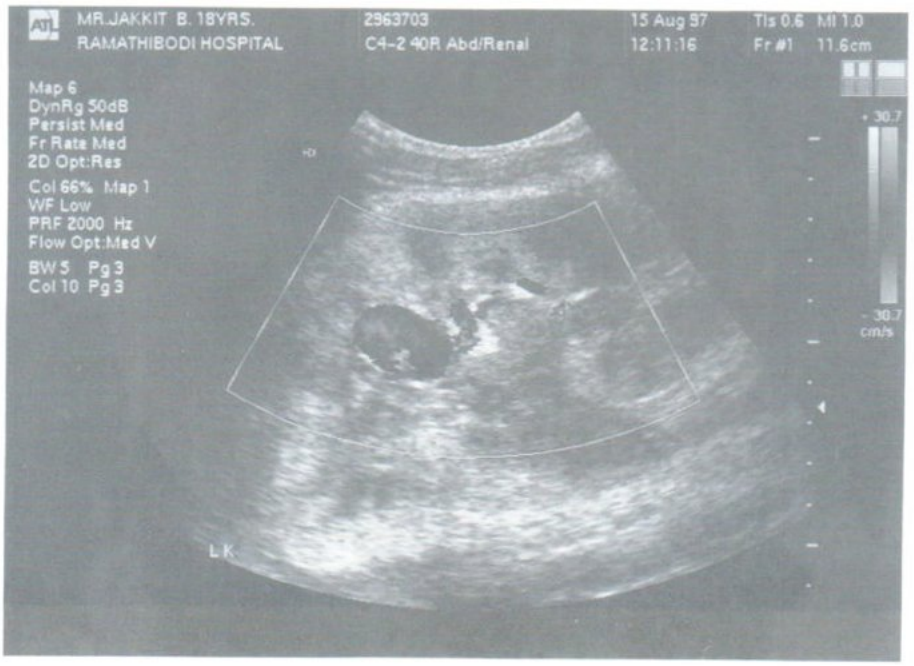

Fig. 3. Doppler ultrasonography showed an AV fistula and large intrarenal pseudoaneurysm.

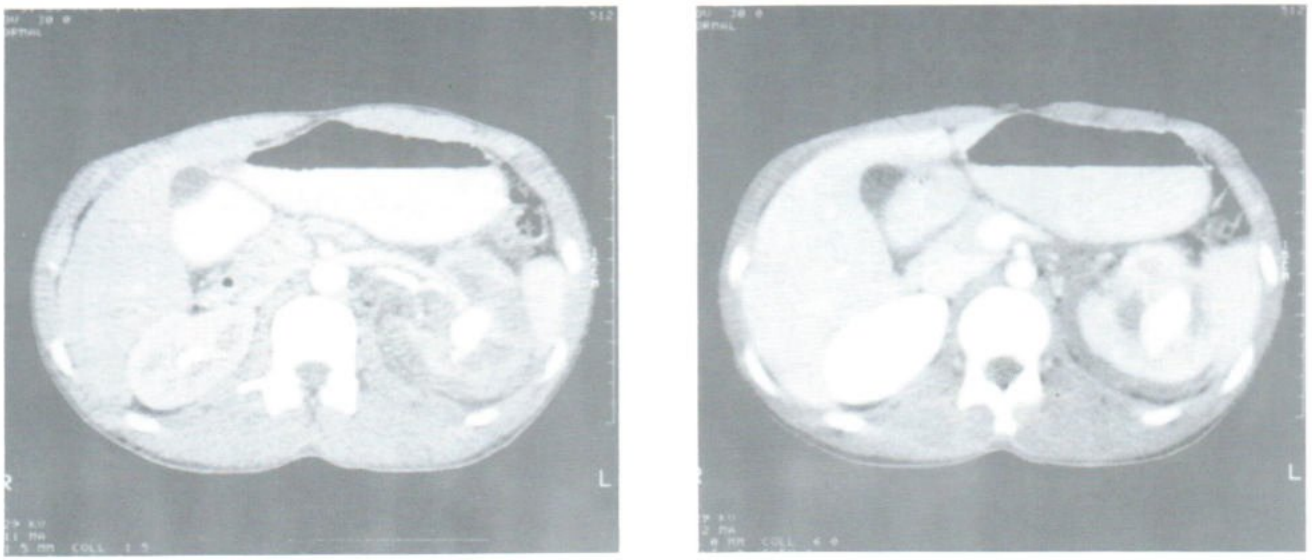

Fig. 4,5. Early and late arterial phase ultrafast CT scan of the kidney showed a large pseudoaneurysm with an early draining vein, representing an AV fistula.

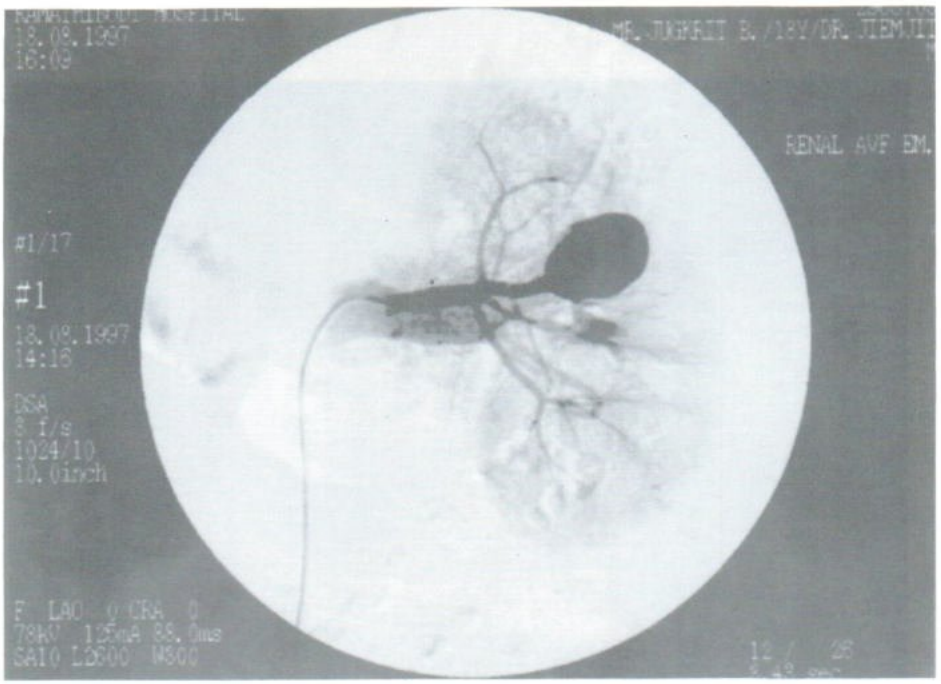

Fig. 6. Renal angiogram showed an early draining vein, representing AV fistula. Some turbulent flow within the large pseudoaneurysm was observed.

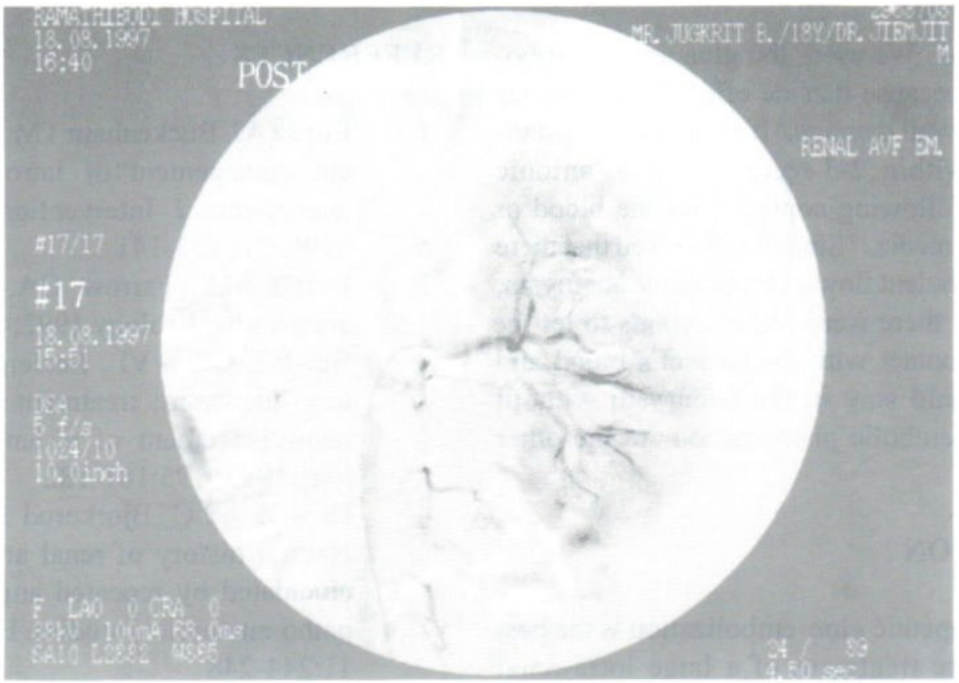

Fig. 7. Left renl angiogram immediately post embolization showed disappearance of the pseudoaneurysm and the fistula and ischemia of middle pole of left kidney.

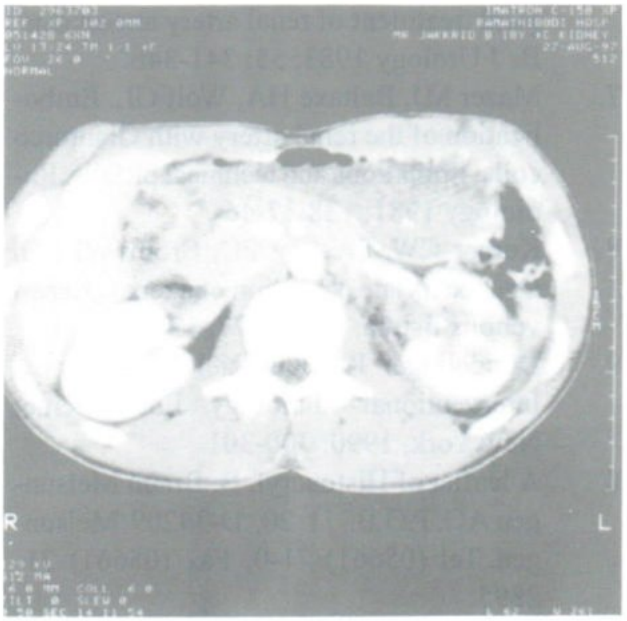

Fig. 8. Follow up CT scan two weeks later showed the disappearance of both fistula and the pseudoaneurysm; good excretory function of left kidney was observed.

DISCUSSION

The indications for the treatment of the renal artery aneurysms include pain, hypertension, hematuria,large aneurysm and pregnancy.[5] Aneurysms that are greater than 1 centimeter in diameter (calcified or not) should be treated surgically.[6,7] The involved urologist had the opinion that surgical treatment could not save the involved kidney in our case.

The Gianturco steel coils with or without gelfoam, has become particularly popular and effective in occluding the main renal artery.[2] The pseudoaneurysm in this case was too large to use the coils, because more than five coils were probably needed and its cost would be about 12,500 Bahts. One cc. of the glue costs only 492 Bahts.

The active principle of the glue is Enbucrilate which is known as a tissue adhesive agent and is classified as an investigational device by the United states food and drug

administration. We used the glue as a thrombogenic agent because its side effect is thrombosis and vascular wall damage.[9] It polymerizes instantaneously (within 2-3 seconds) by an anionic mechanism following contact with the blood or other ionized media.[10] Since we observed that there was some turbulent flow of blood in the aneurysm, it meant that there were some seconds to let the glue make contact with the patient's blood and polymerize and stay in the aneurysm without causing any embolic phenomenon to the other vessels.

CONCLUSION

Therapeutic glue embolization is the best option for the treatment of a large intra-renal pseudoaneurysm and AV fistula, to preserve renal parenchyma and the renal function.[8] High quality digital subtraction arteriography (DSA) with a rapid frame rate and multiple oblique projections is desirable prior to any attempts to embolization. The size of the parent vessel, and the communication between the parent artery and the aneurysmal sac must be accurately defined before the treatment.

ACKNOWLEDGMENTS

We would like to extend our thanks to Rames Watcharasin M.D., and Vithya Varavithya M.D. for scanning images, Bussanee Wibulpolprasert M.D. for doppler examination and Krisada Ratana-Olarn M.D., the urologist in charge.

REFERENCES

1. Lopez AJ, Buckenham TM. The radiological management of iatrogenic pseudoaneurysms. J Interventional Radiology 1996; 11: 133-141
2. Bulbul MA, Farrow GA. Renal artery aneurysms. Urology 1992;40:124-126
3. Bui BT, Oliva VL, Leclere G. Renal artery aneurysm: treatment with percutaneous placement of a stent graft. Radiology 1995; 195:181-182
4. Henriksson C, Bjorkerud S, Nilson AE. Natural history of renal artery aneurysm elucidated by repeated angiography and patho-anatomical studies. Eur Urol 1985; 11:244-248
5. Glass PM. Aneurysms of the renal artery: a study of 20 cases. J Urology 1967; 98: 285-292
6. Ortenberg J, Norick AC, Stretten RA. Surgical treatment of renal artery aneurysms. Br J Urology 1983; 55: 341-346
7. Mazer MJ, Baltaxe HA, Wolf GL. Embolization of the renal artery with Gianturco coils: limitations and technical pitfalls. Radiology 1981; 138:37-46
8. Kerber CW, Freency PC, Cromwell LD. Cyanoacrylate occlusion of a renal arteriovenous fistula. AJR 1977; 128: 663
9. Dondelinger RF, Kurdziel JC, Rossi R. Interventional Radiology. Ed. Thieme; New York, 1990: 300-301
10. A leaflet of Histoacryl. B. Braun Melsungen AG. P.O.B. 11 20, D-34209 Melsungen. Tel (05661) 71-0, Fax (05661) 71-2895

LIPOBLASTIC MENINGIOMA

Patchrin PEKANAN [1], Janjira JATCHAVALA[1], Sawarng CHUAHIRAN[2], Veerasak TEERAPANCHAROEN[3]

ABSTRACT

A case report of a lipomatous meningioma originating from falx cerebri at right frontoparietal convexity, in a 47 year-old female patient was performed. Nonenhanced CT scan showed a low density mass (31 H.U.) . The enhancement was homogeneously dense. A broad-base attachment to the convexity was observed. The surrounding brain edema was minimal.

INTRODUCTION

A lipoblastic or vacuolated meningioma is a variant of meningiomas characterized by the formation of conspicuous vacuolization of the tumor cells.[1,2] It has an unusual histologic appearance which may mimic chordoma, liposarcoma or metastatic adenocarcinoma.

CASE REPORT

A 47 year – old female patient from Bangkok had seizure of left upper extremity for one week. The first episode was 11 months ago, about 8 times for the whole previous year. No loss of consciousness was noted . At physical examination, the patient had good consciousness and was cooperative. Grade IV motor weakness of left extremities were noted and the rest of the examination appeared normal. EEG showed spike wave discharges in both frontal areas.

Plain films of the skull revealed no abnormality. Noncontrast –enhanced CT scan of the brain showed a hypodensity mass(31 H.U.), size 5.5 cm in diameter at high right frontoparietal lobe (Fig.1). Contrast-enhanced CT scan of the mass showed densely and homogeneously enhanced pattern (Fig.2). Broad-base attachment to the right parietal convexity and closely relation to the superior sagittal sinus was shown (Fig.2,3). Mild peritumoral edema was noted and there was 1 cm midline shift to the left.

At operation, the tumor originating from right side of the falx cerebri at right frontoparietal region was noted and total tumor removal was performed with the accidental tearing of the superior sagittal sinus.

At pathology, the specimen consisted of a well encapsulated mass, measuring 5 cm in diameter. The cut surface showed brown and soft surface with yellow foci. At histology, the specimen consisted of collaginous tissues of possible dural mater and admixture of lipocytes and several blood vessels and scattered pleomorphic cells in the stroma. No abnormal mitosis could be identified in any sections. From images, operative findings and histological description, the lipomatous meningioma was compatible. The differential diagnosis includes pleomorphic lipoma, and angiolipoma by histology.

[1] Department of Radiology, Ramathibodi Hospital, Rama 6th street, Bangkok 10400, Thailand
[2] Department of Pathology
[3] Department of Surgery

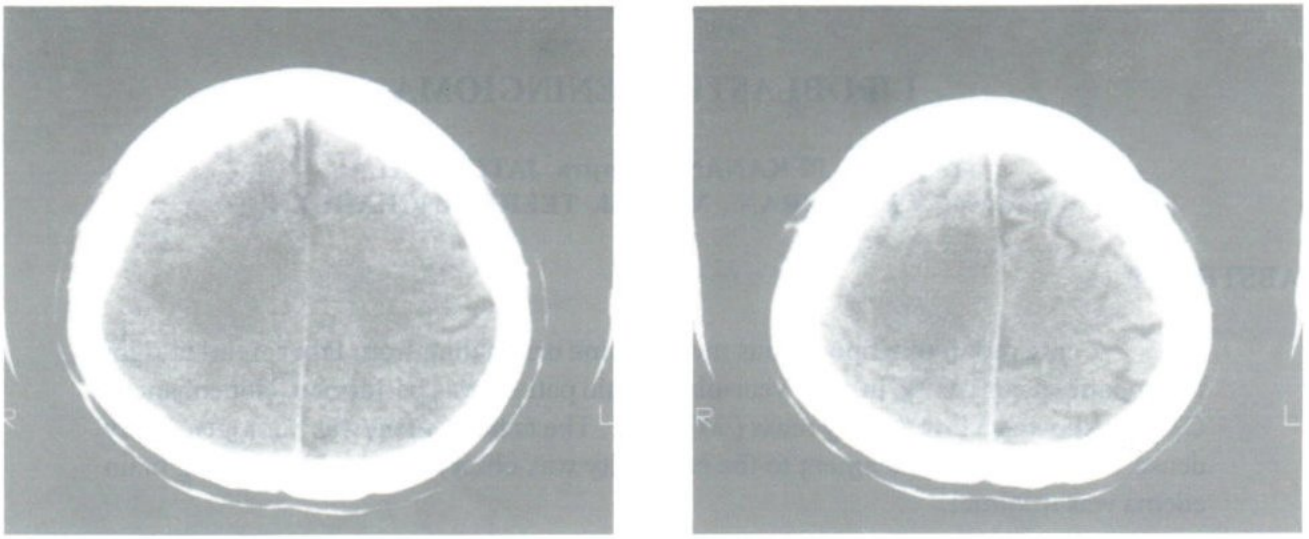

Fig. 1 NCE CT scan of the near vertex of the brain showed an indistinct border low density mass at right frontoparietal lobe, mild pressure on the adjacent falx was shown.

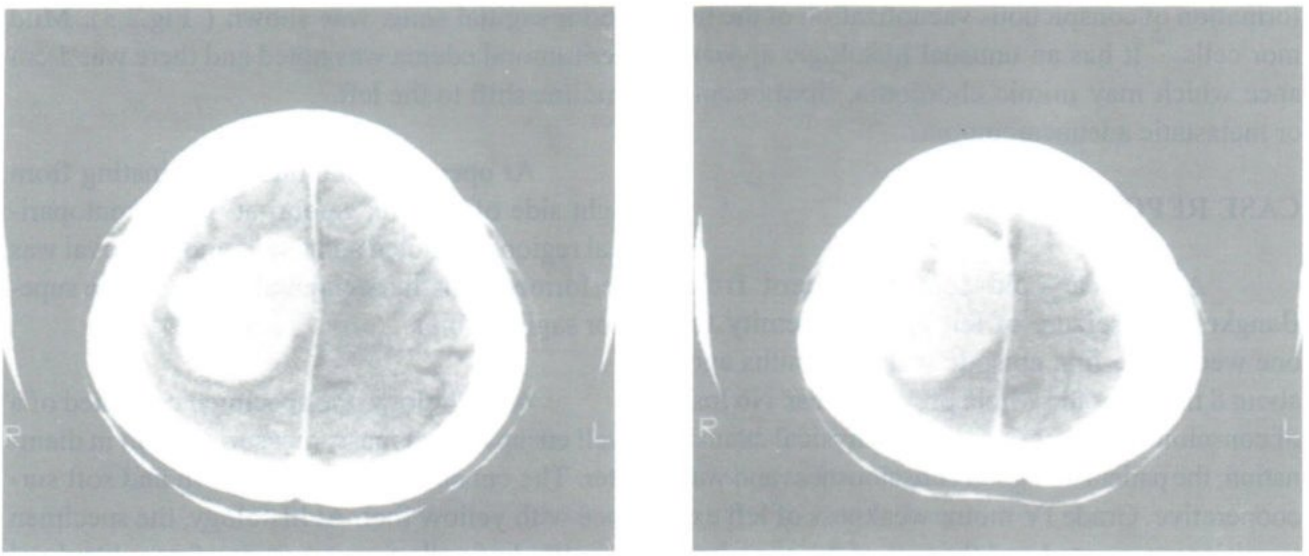

Fig. 2 CE axial CT scan of the brian at the mass showed that the mass was densely and homogeneously enhanced. Part of its borders attached to the right frontoparietal convexity and the falx.

NCE = Noncontrast enhanced.
CE = Contrast enhanced.

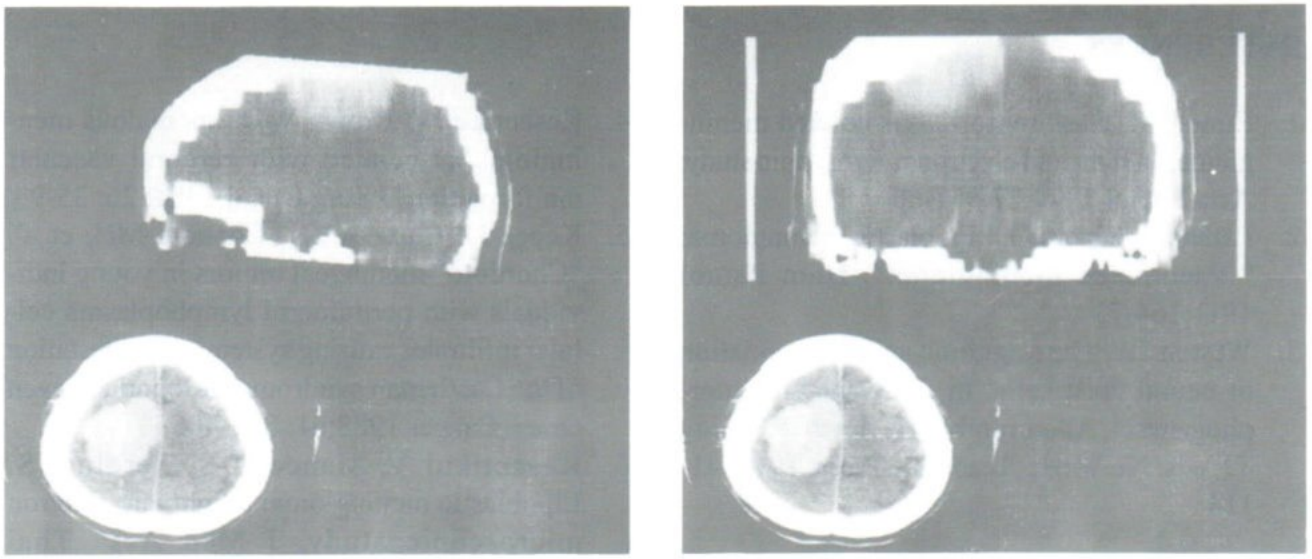

Fig. 3 Reconstructed CT images of the mass in sagittal and coronal view, demonstrating the attachment of the mass to the convexity and the falx.

DISCUSSION

Leptomeninges are derivatives of the neural crest which may differentiate into many cell types including bone, cartilage, and adipose tissue.[3] It is , therefore, not surprising to encounter lipomatous tissue in meningiomas.[4] This type of meningiomas had been reported to occur in the patients of age range between 8 years to 90 years.[5] Most of the patients had good prognosis and no recurrence was observed for 1 to 18 years , post surgery.[2] Kasantikul et al reported a case of lipoblastic meningioma who showed a low density extra-axial mass at right frontal convexity on non-contrast CT scan of the brain and dense homogeneously enhancement post intravenous contrast injection. Another case of lipomatous meningioma, also reported by Kasantikul et al[4] showed a large low density mass in the region of right frontal lobe with surrounding tissue edema. Contrast administration increased the staining around the rim of the mass medially and posteriorly. However, in the latter case ,there was an association with cerebral vascular malformation in the brain nearby. Recognizing this rare variant of meningioma is important because it can prevent an errorneous diagnosis of liposarcoma or metastatic carcinoma particularly when a rapid diagnosis by frozen section is relied on.[6]

Similar findings of the CT images of our case and the two cases of Kasantikul are 1) The location at high right frontoparietal convexity 2) Low density of the entire mass on nonenhanced CT scan (31 H.U. in our case and the measurement of the density was not mentioned in the cases of Kasantikul) 3) Densely enhancement of the mass in two cases(rim enhancement in one case) 4) Mild surrounding brain edema. Reports of such cases in the Radiology-literatures are considered rare.

REFERENCES

1. Eimoto R, Hashimoto K. Vacuolated meningiomas: a light and electron microscopic study. Acta Pathol 1977;27:557-66
2. Latters R, Bigotti G. Lipoblastic meningioma: " vacuolated meningioma". Hum Pathol 1911;164-71
3. Weston TA. The migration and differentiation of neural crest cells. In : Advances in morphogenesis. Abercromble H, Brachet J, King TJ, eds: Ne Work: Academic Press, 1970: 41-114
4. Kasantikul V, Brown WJ. Lipomatous meningioma associated with cerebral vascular malformation. J Surg Oncol 1984; 26: 35-9
5. Kepes JJ, Chen WYK, Connors MH, et al. "Chordoid" meningeal tumors in young individuals with peritumoral lymphoplasma cellular infiltrates causing systemic manifestation of the Castleman syndrome: A report of seven cases. Cancer 1988;61: 391-406
6. Kasantikul V, Maneesri S, Lerdlum S. Lipoblastic meningioma: a light and electron microscopic study. J Med Ass Thai 1995;78(5):276-80

CT SCAN OF INTRACRANIAL AIR EMBOLISM: POST CARDIOPULMONARY RESUSCITATION

Anannit VISUDTIBHAN[1], Patchrin PEKANAN[2], Sirintara PONGPECH[2], Suphaneewan JAOVISIDTH[2], Klaus W PREIDLER[3]

ABSTRACT

A case report of intracranial intravascular air detected by CT scan was performed. The images obtained immediately after the patient expired post failed cardiopulmonary resuscitation in an 11- year-old child who had unknown cause of hepatitis.

INTRODUCTION

Cerebral air embolism has been previously reported in many situations including trauma to the head,[1] cardiothorax[2] and to the cervical spine. Caisson's disease,[3] operations in neurosurgery, in gynecology[4] and in cardiothorax[5] can introduce air to the intracranium. Pneumothorax, percutaneous lung biopsy, lung cancer, arterial or venous catheterization,[6] mechanical positive pressure ventilation,[7] esophagoatrial fistula,[8] intra-aortic balloon pumping catheter insertion,[9] angiography,[10] hemodilution[13] and intravenous transfusion has also been reported as causes of cerebral air embolism.

A pediatric case of massive cerebral arterial and venous air embolism detected by CT scan immediately post cardiopulmonary resuscitation is presented.

CASE REPORT

An 11-year-old girl was admitted for liver biopsy and a detailed investigation due to unknown cause of hepatitis. Physical examination revealed a mildly pale and alert girl with icteric sclera, palmar erythemia, hepatosplenomegaly and eczema at both legs. The liver biopsy was deferred because of the prolonged coagulogram.The hospital course was a grave one. Her consciousness and renal function was deterirorated in a short period of time and she has also fever.No clinical improvement was observed after peritoneal dialysis, antibiotics, intravenous immunoglobulin and D. penicillamine administration. Later she had respiratory distress, hypotensive, fixed dilated right pupil which was not reactive to light .The patient developed cardiac arrest on the way to the CT room. CT scan was performed;however, despite failed cardiopulmonary resuscitation.

Nonenhanced axial CT scan of the brain revealed extensive low density of air in both arteries and veins intracranially. Air was observed in both carotid and vertebrobasilar systems (Fig.1). Both areas of cavernous sinuses were filled with air (Fig.2). Less air was detected in the dural venous sinuses (Fig.3). In addition, a large hematoma was shown in right cerebral hemisphere which extended to the ventricular system.Air was also observed in the anterior part of the intracerebral hematoma (this air should come from the artery which was ruptured) (Fig. 4). Air in the intraorbital vasculature was also seen. No air was detected from plain chest film.

[1] Department of Pediatrics, Ramathibodi Hospital, Rama 6 Street, Bangkok 10400, Thailand
[2] Department of Radiology, Ramathibodi Hospital
[3] Department of Radiology, Karl Franzens university Graz, Graz, Austria

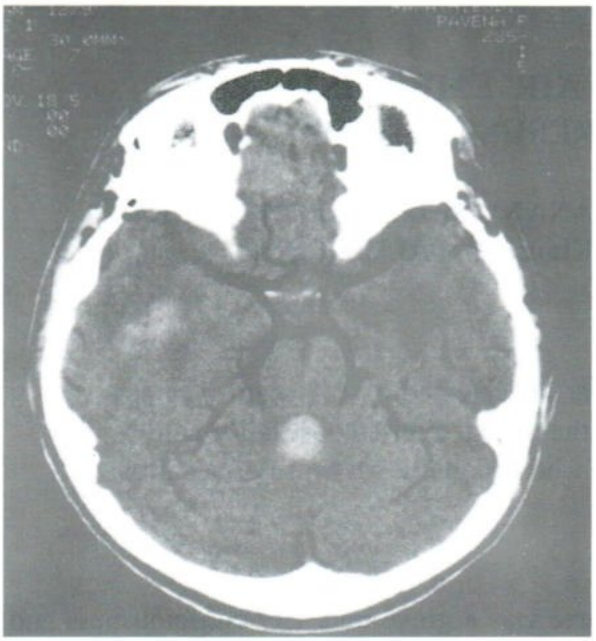

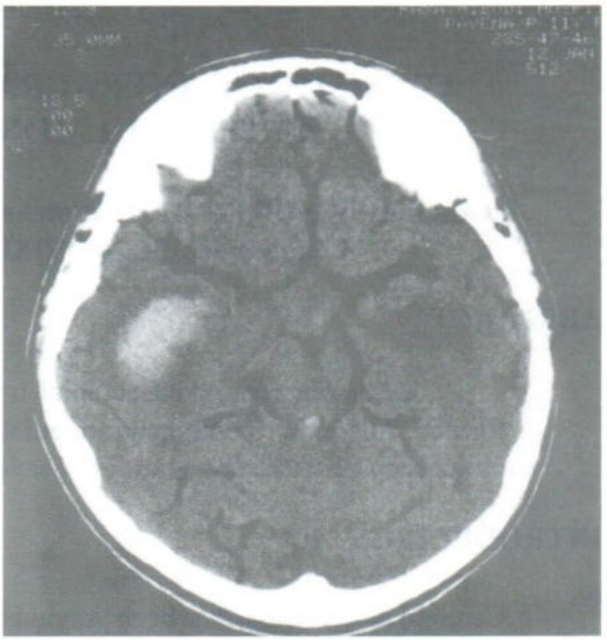

Fig. 1. NCE CT scan of the brain showed air in the arteries of carotid and vertebrobasilar system of both sides, (hematoma is also noted in right temporal lobe, and in the 4th ventricle)

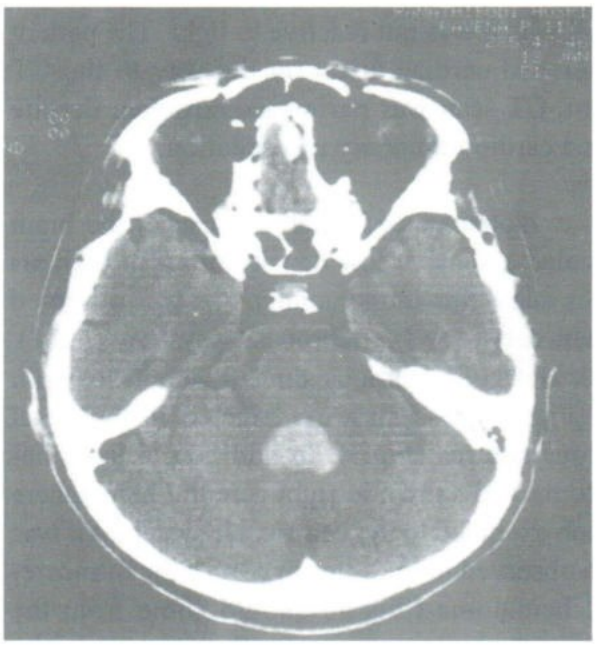

Fig. 2. NCE axial CT scan of the brain showed air in the cavernous sinuses. (The hematoma in the 4th ventricle is observed.)

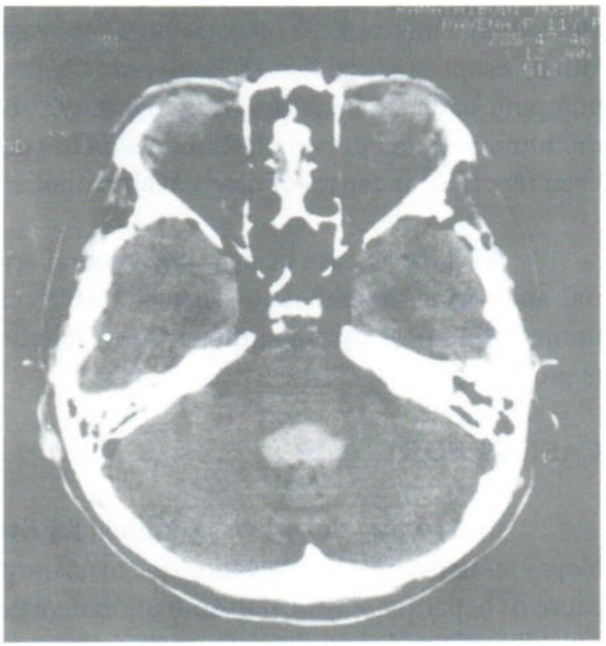

Fig. 3. NCE CT scan of the brain showed less air in the right sigmoid sinus (The hematoma in the 4th ventricle).

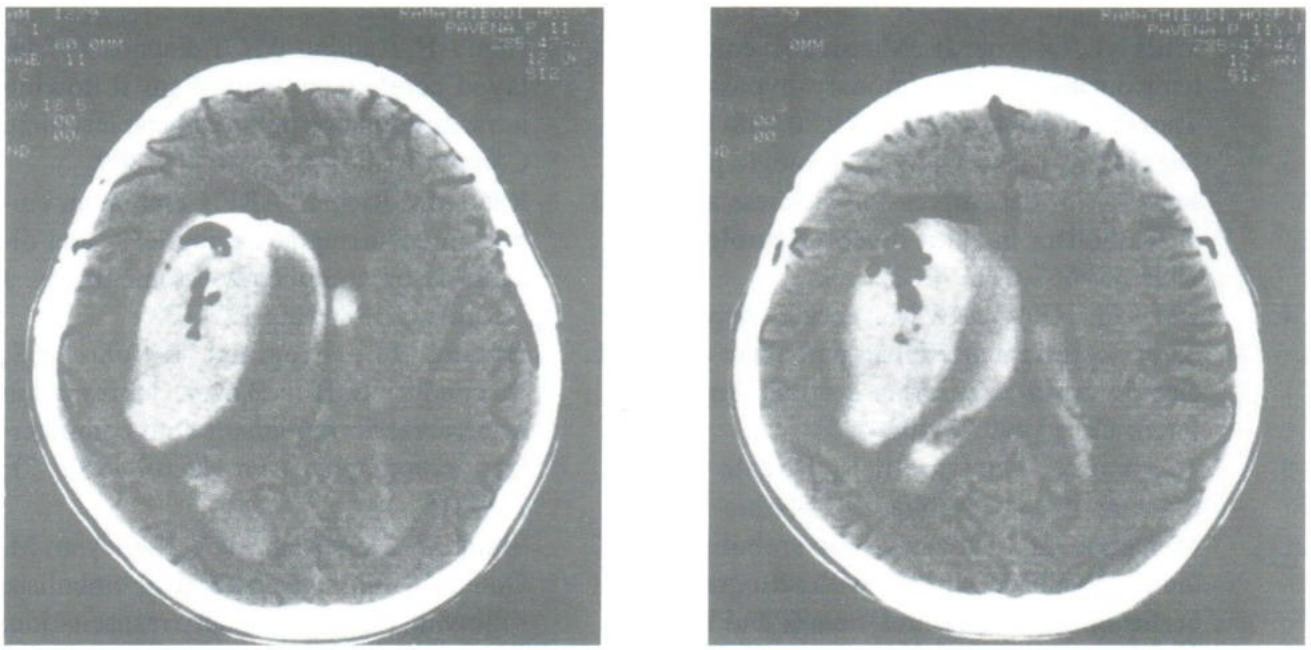

Fig. 4. NCE axial CT scan of the brain showed a large right cerebral hemispheric hematoma, leaking to lateral ventricle. Note the air in the hematoma, probably came from the ruptured artery. (Air in the convexity arteries of both sides were also shown.)

NCE = Non - contrast enhanced.

DISCUSSION

Systemic air embolism is almost invariably iatrogenic except for cases of penetrating trauma to the thorax, lungs,major vessels or in decompression sickness.[11] Shiina et al[12] reported two cases of massive cerebral arterial air embolism associated with postraumatic cardiopulmonary resuscitation.It was proposed that mechanical impact of cardiopulmonary resuscitation resulted in pulmonary barotrauma and pushed massive air into the arterial circulation and the intracerebral arteries.

The mechanism whereby venous air is transferred to the arterial circulation is controversial.[13] Air is able to pass through an existing intracardiac septal defect into the systemic circulation if there Is increase in right heart pressure from pulmonary outflow obstruction.[14] Paradoxical cerebral air embolism could occur without intracardiac septal defects.[15] Certain conditions may allow the passage of venous air to the systemic circulation through the pulmonary arteriovenous barrier.[16]

Detection of air is thought to be dependent on the timing of the CT scan and on the amount of air which initially entered the vessels to the brain; the earlier the initial scan and the greater the quantity of air,the more likely it is to be detected.

REFERENCES

1. Butler BD, Hills BA. Transpulmonary passage of venous air emboli. J Appl Physiol 1985; 59: 543-547

2. Mills NL, Ochsner JL. Massive air embolism during cardiopulmonary bypass. J Thorac Cardiovasc Surg 1980;80:708-717
3. Dick APK, Massey SW. Neurologic presentation of decompression sickness and air embolism in sport divers. Neurology 1985;35: 667-671
4. Davis FM, Glover PW,Maycock E. Hyperbaric oxygen for arterial air embolism occurring during Caesarian section. Anest Intens Care 1990;18:403-405
5. Toscano M, Chiavarelli R, Ruvolo G, Machiarelli A, Serblia G, Marino B. Management of massive air embolism during openheart surgery with retrograde perfusion of the cerebral vessels and hyperbaric oxygenation. Thorac Cardiovasc Surg 1983; 31: 183-184
6. Kearns PJ, Han IK AA, McDonald TW. Homonymous hemianopia due to cerebral air embolism from cerebral venous catheter. West J Med 1984; 40:615-617
7. Michael AM, Milton LP, Ronald BP. Detection of pneumoencephaly secondary to mechanical ventilation in neonates. J Comput tomogr 1981; 5: 328-332
8. Nadjimi M, Schaffer R, Wordartz R. Cerebral arterial air embolism due to an esophago-atrial fistula seen on CT. Neuroradiology 1979;18:103-106
9. Hani AH, Ayming W. CT diagnosis of delayed cerebral air embolism following intraaortic balloon pump catheter insertion. Comput Radiol 1987;10: 307-309
10. Rand MV, Richard ARF. Cerebral air embolism occurring at angiography and diagnosed by computerized tomography. J Neurosurg 1984; 60: 177-178
11. Hwang TL, Fremaux R,Sears ES, MacFadyen B, Hills B,et al. Confirmation of cerebral air embolism with computerized tomography. Ann Neurol 1983; 13: 214-215
12. Shiina G, Shimosegawa Y, Kameyam M, Onuma T. Massive cerebral air embolism following cardiopulmonary resuscitation. Report of two cases. Acta Neurochir (Wien) 1993; 125: 181-183
13. Hirabuki N, Miura T, Mitomo M,et al. Changes of cerebral air embolism shown by computed tomography. The British Journal of Radiology 1988;61: 252-255
14. Ponsky JL, Pories WJ. Paradoxical cerebral air embolism (Letter) . New England Journal of Medicine 1971; 284: 985
15. Kearns PJ, Haulk AA, McDonald TW. Homonymous hemianopia due to cerebral air embolism from central venous catheters. Western Journal of Medicine 1984; 140: 615-617
16. Butlers BD, Hills BA. The lung as a filter for microbubbles. Journal of Applied Physiology 1979; 47: 537-543

TELERADIOLOGY

Supong PEKANAN[1], Patchrin PEKANAN[2]

OVERVIEW

The Teleradiology is a computer application which combines three major areas of computer related technology, which are Digital Image Processing, Data Communication Networking and Database Management System. The objective of system development is to reduce the cost of film development, to solve the problem of film archiving/accessing, to prevent loosing of patient's films, to extend radiological service to districts where experienced radiologists cannot be reached, and to establish a film library as by product of the system.

The Teleradiology system has been developing in foreign countries for many years. There are standards which have been developed such as Digital Imaging Communication in Medicine or DICOM (by American College of Radiology – National Electrical Manufacturer's Association, ARC-NEMA), regulations developed by FDA to be used as guide line in equipment purchasing. There are also commercial products from major manufacturers available such as Picture Archiving and Communication System (PACS) which is a database system for digital image archiving and retrieving, digital radiological devices such as CT, MRI, Ultrasound etc. which include DICOM as standard or optional function.

Though, in theory, the Teleradiology system provides remarkable advantages to public services and radiological studies, implementing the system requires carefully study in technologies, system operation migration and investment. It is obvious that the information technological industry is changing rapidly. For example, the price of a personal computer in 1994 was twice the price in 1995 while the performance and configuration was just half of the one in 1995. This situation continues to today and there is signs that this changing will continue for a decade. The worse is a desktop purchased three years ago cannot run today application without upgrading or repurchasing the whole set. Also, it is hard to find a sparepart. Investing in higher quality computers does not guarantee that the hospitals will not face the same situation. The manufacturers of UNIX based computers have to continue developing their computers to compete with PC industry. Using the UNIX operating system in Thailand is also an unpleasant thing. The solution requires a qualified system integrator to take care. The record shows that a single problem, if luckily, requires at least 1 month to fix. This is because the application software manufacturer is not the operating system manufacturer and in most case there is no conclusion that the problem is of the application software or operating software. The operating system and system software is also changing. Microsoft Windows changes from Windows 3.x to Windows 95, Windows NT changes from NT 3.x to 4.x within five years. These effect application software to be upgraded. System software such as Database management system changes from simple one to Object-oriented database. New features have been included in the software and these new features are available only in a new

[1] Supong @ Ksc11.Th.Com
[2] Department of Radiology, Ramathibodi Hospital, Rama 6 Street , Bangkok 10400, Thailand

version of software which is applicable only for the new operating system. There was a new computer networking technology called Asynchronous Transfer Mode or ATM available in the late 1995 which provided a 155 Mbps trunk speed which is faster but less robust than FDDI. The committed trunk speed will be 622 Mbps and the specification has been developing while manufacturers is introducing proprietary features and put them in a proposed box. The investment in this technology for this project may cost 4 million US$ and may be obsolete within three years if the study is not done carefully enough.

THE COMPONENTS OF TELERADIOLOGY SYSTEM

The Teleradiology system, in general, composes of 5 major components:

- Radiological Devices
- Radiologist Workstation
- Picture Archiving and Communication System
- End-user workstation
- Computer Networking System

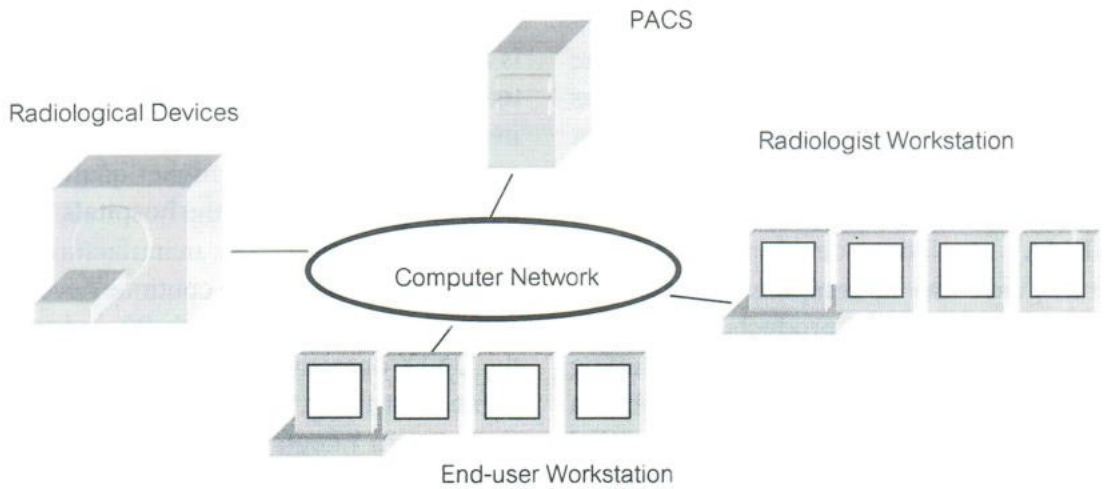

RADIOLOGICAL DEVICES

Radiological devices such as X-Ray, CT, MRI, PET, Ultrasound, Nuclear Medicine etc., in the Teleradiology system must be able to produce digitized images such that the images can be processed and stored in the computer system. Since the Teleradiology system has never been used in the hospitals, most of existing equipments require upgrading by adding DICOM interface modules to those equipments which currently producing digitized images and adding digitizers and DICOM interface modules to those equipments which currently producing analog images.

Is DICOM an essential part? DICOM plays a part in Teleradiology system as the standard protocol in acquiring digitized images from the devices. The hospitals may develop or allow the solution suppliers to develop some kind of control procedure to do the same thing. But this will not guarantee that the system will be able to communicate with other devices to be purchased in future nor provide image-acquiring services to or from the outside systems.

For the devices which produce digitized images, the DICOM interface upgrade will con-

nect the devices to the hospital network, receive requests from other devices, and transmit the images in DICOM standard image format to the requestors. The device operators may issue request to transfer the images from devices to store at PACS. In most cases, the DICOM upgrade modules must be purchased from the device manufacturer, if available.

For devices that do not produce digitized images, an image plate, which can transform X-Ray intensity to digitized images directly, can be used instead of the X-Ray films. This plate connects directly to a workstation, which will process the digitized images and transfer the images into the system.

For the devices that cannot put the plate in, or the devices that do not have DICOM upgrade parts, the films are still be developed and put in an X-Ray film scanner to produce a digitized image.

The CCD camera in the set of the X-Ray digitizing plate or the X-Ray film scanner should be able to produce gray scale image of 1,024 or 2,048 level with optical resolution of 360,000 pixels per square inch. The digitized images may be temporally stored in the workstation or PACS for further reading. The images should be compressed using standard compression method that can be perfectly restored. There is some suggestion that the compression ration should be 2.5: 1.

The result images should contain textual details such as medical reference numbers, the patient's basic data, the date and time of exposure,the laboratory reference numbers, etc., as parts of the images.

THE RADIOLOGIST WORKSTATION

The Radiologist Workstation is used by the radiologists to interpret the images. The software should facilitate the radiologists in various ways such as zooming, panning, image enhancement, filtering etc. The image processing function must not produce distorted images, which causes misinterpretation. It is recommended that the workstation should be equipped with at least 4 display monitors to display 4 images at the same time. The size of each monitor should be at least 18 by 24 inches (around size of largest film) with minimum of 1,024 gray level and 1,728 by 2,304 pixel area. A single keyboard and, a mouse or a pen should control system function.

The software should also allow the radiologists to put on white mark or circle on images easily and let the radiologists organize or format the images in the way that he or she expects the end-users to see. The diagnosis should be tightly binding with the images or image sets.

A film printer (a printer that can print a photographic image on a film) should be attached to the workstation to reproduce output in classical film media. The workstation should be able to work off-line, directly connected to the radiological devices using backup port such that it can produce output when the main system fails for a long time.

PICTURE ARCHIVING AND COMMUNICATION SYSTEM (PACS).

The PACS archives the images and the diagnosis results, searches for requested images and results. For a university hospital, the size of the database will be enormous if it accumulates the images for more than 6 months period. Thus the PACS should be separated into at least 3 subsystems. One for images which are still in use; one for only selected interesting cases and the other for references. The PACS for active cases should store the data in the high-speed, large disk storage/ disk arrays for better performance. The other 2 PACS should store the data in optical media such as compact discs or magneto-optical media to save the cost of storage. It is possible to eliminate the

PACS for archiving interesting cases by setting a WEB servers instead. The PACS for reference images will keep the images for latest 3 years then all optical media will be moved to another library system.

All PACSs must use DICOM as their standard protocol/ interface to communicate with other devices in the system. Since the PACS is one of the two most critical components in the system, the specification of both hardware and software must be carefully considered. Any damage on the PACS will cause the entire health services, which require the diagnosis result to be stopped. This is not acceptable for ER and OR. Thus the design of the hardware system and software for the PACS must provide high reliability and high availability and can operate 24 hours a day. The available PC or PC-base operating system may not be up to specification in this case. The hardware and all relevant software (the operating system, database management system, PACS application) must be designed for a fully fault tolerant service. This includes the backup power supply system, air conditioning system, computer and storage devices and supporting network systems. The system should have 3 redundant equipment sets operating in a hot-standby mode or the backup system should be ready for service within 3 minutes. Since the system will operate 24 hours a day, the database backing up system must be done during service (online backup) and must be able to do the backup in both entire database backup and incremental backup mode. In case of database failure, the database restoration mechanism should allow the undamaged part of the database to be usable.

The user interface of the PACS database administration system must be easy to use and understand. The developer of the PACS should design the UI, hiding the complicate SQL or system commands, making use of the GUIs to simplify the system operation, use clear messages and consistence choice of operation to communicate with the system administrators.

Since the PACS is the core of the entire system and will serve the users in many departments within the hospital as well as the entire university and outside health care units. The system must be a high-throughput system using huge redundant single server or clusters of smaller server. The PACS must also be designed ready to interface with other systems of the hospital such as the 'Patient Registration System' or the 'Hospital Management System'. The authentication system must be able to protect the system from accessing by unauthorized users and must have access logging mechanism, which can alert to the system administrators when abnormal accessing occurs.

END-USER WORKSTATION SYSTEM

The End-User Workstation System can be divided into 3 types,a single display monitor – workstation system for general use,a multiple display monitor - workstation system for special examination area, asecured multiple display monitor system for ER, OR.

The workstation using in ER and OR should be designed similar to the "wheel box" which can be moved to anywhere within the room. The keyboard and pointing device should be specially designed such that the unit can be cleaned by a standard cleaning procedure of the room. The networking device should be of type infrared or RF to minimize the cable use. The box must be sealed to prevent toxic gas generated by electric short circuit from diffusing into the air. An UPS system and an alternate network port should be installed for use in case of power system failure or network device failure. The workstation system should contain at least 4 display monitors controlled by a single keyboard and pointing device. Each monitor should be 18 x 18 inches and should be able to display an entire film without scrolling.

All workstation should be designed using the same user interface and communicate with the PACS via DICOM standard protocol.

COMPUTER NETWORKING SYSTEM

The network system for the Teleradiology System must be a high bandwidth network. Most of the data transferring between each node in the network are image pixels, which is around 233 Mbytes per largest uncompressed image or 72 Mbytes per 2.5:1 compressed image (calculation is for 18 x 18 inches film at 600 dpi, 1024 level gray scale image). The 10 Mbps LAN with 2 Mbps throughput can transfer the images within 290 seconds or 4.8 minutes while the 100 Mbps circuit completes the same job within 29 seconds. Multiple of 100 Mbps or higher bandwidth circuits should be used along with balancing the number of an active mode per circuit. The switch device such as Fast Ethernet Switch should be applied to filter the irrelevant traffic from the port.

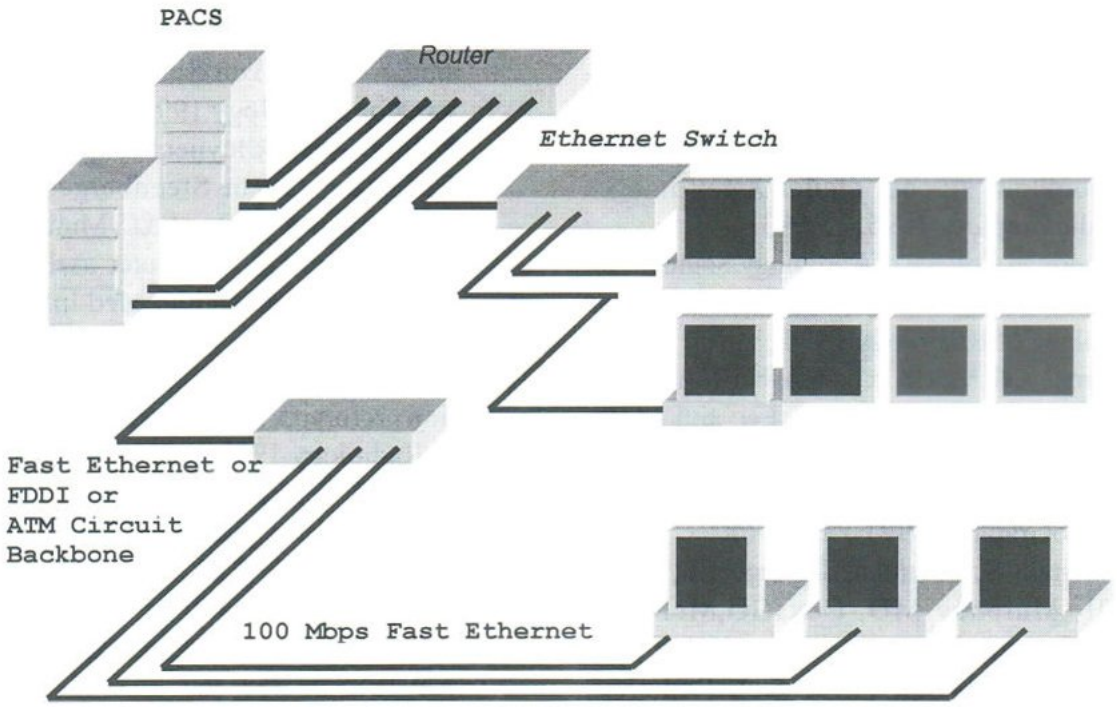

Since the system must be a high-availability system, the network must be a fault tolerant network. All devices and cabling system must be redundant including power supply to all connected networking devices. All devices and control software must be able to switch to alternate route automatically when a device or cable failure occurs. A network management system must be installed for fast failure locating and network monitoring. Any serious fault should be reported to system administrator automatically via red alert on network management station or paging system.

By connecting the network to the Internet will allow accessing to the Teleradiology System from outside the hospital. In such case, a "Fire Wall" must be installed to prevent unauthorized accessing since the images are private to patients. Setting up terminal server also allows accessing the system from limited origins. The hospital may install a secured WEB server connecting to the PACS to provide accessing images using Web Browser as displaying tool.

SUGGESTED REFERENCES

1. Arenson RL,Chakraborty DP,Seshadri SB,et al.The digital imaging workstation. Radiology 1990;17b:303-315
2. Ackeman LV, Gitlin JN, ACR-NEMA. Digital imaging communication standard: demonstration of RANA '92 InfoRad. Radiology 1992;195-394
3. Ackerman SJ, Gitlin JN, Gayler RW, Flagle DC, Bryan RA. Receiver operating characteristic analysis of fracture and pneumonia detection:comparison of laser digitalized workstation images and conventional analog radiographs. Radiology 1993;186:-263-268
4. Antonuk LE,et al.Real-time ,flat-panel, amorphous silicon, digital X-ray imager. RadioGraphics 1995; 15:993
5. American College of Radiology.Standard for Teleradiology.Reston,Virginia: American College of Radiology 1994
6. Barnes GT,Morin RL, Staab EV.InfoRad: computers for clinical practice and education in Radiology. Teleradiology: fundamental considerations and clinical applications. RadioGraphics 1993;13:673-682
7. Batnitzky S, Rosenthal SJ,Siegel EL, Wetzel LH, Murphey MD, Cox GG,McMillan JH,Templeton AW, Dwyer SJ III Teleradiology: an assessment. Radiology 1990;177:11-17
8. Bidgood WD,Horii SC.Introduction to the ACR-NEMA DICOM standard. Radio Graphics 1992;12:345-355
9. Brody WR,Johnston GS.Computer applications to assist radiology, SCAR '92 Symposium for computer assisted radiology. Available from Symposia Foundation, PO Box 2107 Carlsbad CA 92008
10. Binkhuysen FHB,et al.Remote expert consultation for MRI procudures by means of teleradiology. EUR J Radiol 1995;19:147
11. Baum S,Caplan A. Teleradiology:friend or foe? Radiology 1996;201:16
12. Baxter KG,Wetzel LH, Murphy MD, Rosenthal SJ, Haines JE,Batnitzky S, Caresio JF, Templeton AW, Dwyer SJ III.Wide area networks for teleradiology .J Digit Imag 1991;4:51-59
13. Bidgood WD, Jr, Horii SC.PACS mini refresher course: introduction to the ACR-NEMA DICOM standard. RadioGraphics 1992;12:345-353
14. Beard DV, Hemminger BM,Perry JR, Mauro MA, Muller KE, Warshauer DM, Smith MA, Zito AJ. Interpretation of CT studies: single –screen workstation versus film alternator. Radiology 1993;187:565-569
15. Bellon E,van Cleynenbreugel J, Suetens P,Marchal G,van Steenbergen W, Plets C,Oosterlinck A, Baert AL. Multimedial E-mail systems for computer assisted radiological communication. Med Inf 1994;19:-139-148
16. Chang PJ. MR multiband viewing workstation prototype. RSNA conference 1992:416 or Radiology 1992;185(suppl):416
17. Coons T. Teleradiology: The practice of Radiology enters Cyberspace. Radiologic Technology 1995;67(2):125-140
18. Carey LS. Teleradiology: part of a comprehensive telehealth system. Radiol Clin North Am 1985;23:357-362
19. Cawthorn MA,et al. Preliminary assessment of computed tomography and satellite teleradiology from operation Desert Storm. Invest Radiol 1991;10:854-857
20. Casarella WJ. Benefits of teleradiology. Radiology 1996;201:16
21. Carson GC, Fath SJ,et al. IMAGEnet: wide area teleradiology network. Emergency Radiol 1994;1:32
22. Caramella D. Teleradiology: state of the art in clinical environment/Eur J Radiol 1996;-22:197

23. Caramella D, Lencioni R, Mazzeo S, Bartolozzi C. Transmission of radiological images using broadband communications. Eur Radiol 1994;4:377-381
24. Caramella D,Del Sarto M, et al.Diagnostic image management and transmission systems: the experience of the University of Pisa. Radio Med 1995:89:136-142
25. Cradduck TD. The wide world of Internet. J Nucl Med 1994;35:30N-34N
26. De Simone DN, et al. Effect of a digital imaging network on physician behavior in an intensive care unit. Radiology 1988;169:41-44
27. DoVan M,et al Initial experience with asynchronous transfer mode for use in a medical imaging network. J Digit Imaging 1995;8:-43-48
28. Don S, Albertina MJ, Ammann DL, Evens RG, Siegel MJ.soft-copy computer radiology in neonatal and pediastric intensive care units:cost savings analysis. Radiology 1995;197:501-505
29. Dwyer SJ III, Templeton AW, et al. Teleradiology: costs of hardware and communications. AJR 1991;156:1279-1282
30. De Corato D, Kagetsu N, Ablow R.Off-hours interpretation of radiologic images of patients admitted to the emergency department: Efficacy of teleradiology. AJR 1995;1293-1296
31. Dohrmann P. Low cost teleradiology for Australia. Australian and New Zealand Journal of Surgery 1991;61:115-117
32. Frank MS. Opinion: a prototype for a computerized national mammography registry and tracking system using telecommun-cations and the Internet. J Digit Imaging 1995;8:127-131
33. Franken EA, et al. Teleradiology for rural hospitals: analysis of a field study/J Telemedicine and Telecare 1995;1:202-208
34. Fisk NM,et al. Fetal telemedicine: interactive transfer of realtime ultrasound and video via ISDN for remote consultation. J Telemedicine and Telecare 1995;1:38-44
35. Franken EA Jr, et al. Teleradiology for a family practice center. JAMA 1989;3014-3015
36. Gitlin JN. Teleradiology. Radiol Clin North Am 1986;24:55-68
37. Goldberg MA, et al. New high resolution teleradiology system: prospective study of diagnostic accuracy in 685 transmitted clinical cases. Radiology 1993;186:429-434
38. Gray JF. Use of SMPTE test pattern in picture archiving and communication systems. JUI 1992;5(1):54-58
39. Goldberg MA,et al. Making global telemedicine practical and affordable: demonstrations from the Middle East. AJR 1994;163:1495
40. Goldberg MA. Teleradiology and telemedicine. Radiol Clin North Am 1996;34:647
41. Giger ML, et al An "intelligent" workstation for computer-aided diagnosis. RadioGraphics 1993;13:647-656
42. Gold RH, et al. Teleconferencing for cost-effective sharing of radiology educational resources: potential and technical development. AJR 1993;160:1309-1311
43. Huang HK, Tecotzky RH, Bazzil T. A fiber-optic broadband CT/MR video communication system. J Digit Imaging 1992;5:20-25
44. Huang HK,et al. Asynchronous transfer mode technology for radiologic image communication. AJR 1995;164:1533-1536
45. Hemminger BM, et al. Introduction to perceptual linearization of video display systems for medical image presentation. Digital Imag 1995;8:21
46. Huda W,et al.Computed radiography and film digitizer inputs to an intensive care unit teleradiology system:image quality comparison. Acad Radiol 1996;3:110
47. Ho B,et al. Data clustering and other archive retrieval stratefies for teleradiology and picture archiving and communication systems. J Digital Imag 1995;8:180

48. Hare W. Teleradiology.Australian and New Zealand Journal of Surgery 1991;61:89
49. Haynor DR, et al. Hardware and software requirements for a picture archiving and communications system's diagnostic workstations. J Digital Imag 1992;5:1070117
50. Ho B,et al. Design and implementation of full-frame. Bit-Allocation image-compression hardware module. Radiology 1991;-179:563-567
51. Ishigaki R, et al. Clinical evaluation of irreversible image compression: analysis of chest with computed radiography. Radiology 1990;175:739-743
52. Kagetsu NJ,et al. Clinical trial of digital teleradiology in the practice of emergency room radiology. Radiology 1987;165:551-554
53. Kline TJ,et al. Radiologists, communication, and resolution 5: a medico-legal issur. Radiology 1992;184:131-134
54. Kassirer JP. The next tansformation in the delivery of health care.N Engl J Med 1995;-332:52-53
55. Kahn CE.Artificial intelligence in radiology: decision support systems. RadioGraphics 1994;14:849-861
56. Lear JL, et al. Ultrahigh-speed teleradiology with ISDN technology. Radiology 1989;-171:862-863
57. Laehde S,et al. Low-cost digital teleradiology. Eur J Radiol 1995;19:226
58. Lee CD. Teleradiology. Radiology 1996;-201:15
59. Meredith G,et al. Modeling and simulation of a high performance PACS based on a Shared File system architecture. SPIE Medical Imaging VI 1992;1654:169-179
60. MacMahon H,e tal. Data compression: effect on diagnostic accuracy in digital chest radiography. Radiology 1991;178:175-179
61. Marglin S, et al. Preliminary experience with portable digital imaging for intensive care radiography. J of Thoracic Imaging 1990;5-(1):49-54
62. MacMahon H, et al. Portable chest radiography techniques and teleradiology. Radiol Clin North Am 1996;34:1
63. Mezrich RS,et al. Radiology on the information superhighway. Radiology 1995;195:-73-81
64. Meyer-Ebrecht D. Digital image communication. Eur J Radiol 1993;17:47-55
65. Mattheus R. European standardization efforts: an important framework for medical imaging. Eur J Radiol 1993;17:28-37
66. Nerger SB,et al. Medical-legal issues in teleradiology. AJR 1996;166:505
67. O'Hare NJ ,et al. Specification and initial evaluation of a multiple application teleradiology system. Br J Radiol 1996;69:735
68. Orphanoudakis SC, et al. Technological advances in teleradiology. EUR J Radiol 1996;22:205
69. Partovi S.RIP: Radiology Internet Protocol. RadioGraphics 1996;16:1495
70. Ravin CE. Initial experience with automatic image transmission to an intensive care unit using picture archiving and communications system technology. J Digit Imag 1990;3:195-199
71. Richardson ML, et al.An on-line digital internet radiology teaching file server. AJR 1994;162:1239-1242
72. Stewart DA. The radiologist as communicator :assessments and impressions. Radiology 1995;196:37A-42A
73. Stewart BK, Dwyer SJ III, et al. Design of a high-speed, high-resolution teleradiology network. J Digit Imaging 1992;5:144-155
74. Scott WW,et al. Interpretation of emergency department radiographs by radiologists and emegency medicine physicians: teleradiology workstation versus radiolograph raeadings. Radiology 1995;195:223-229
75. Scott WW,et al.Subtle orthopedic fractures: teleradiology workstation versus film interpretation. Radiology 1993;187:811-815

76. Siegel EL, et al. Image data compression using a new-floating point digital signal processor. J Digit Imaging 1991;4:188-195
77. Shih-Chung I, et al. Compression of radiological images with 512,1024, and 2048 matrices. Radiology 1986;161:519-525
78. Schilling RB, et al. Inforad:computers for clinical practice and education in Radiology, Teleradiology, information transfer, and PACS:implications for diagnostic imaging in the 1990s. RadioGraphics 1993;13:683-686
79. Stewart BK, et al. Functionality of gray scale display workstation hardware and software in clinical radiology. RadioGraphics 1994;-14:657
80. Stewart, et al. Clinical utilization of gray scale workstations. IEEE, Engineering in Medicine and Biology 1993;86-102
81. Sagel S,et al.Digital mobile radiography. Journal of Thoracic Imaging 1990;5(1):36-48
82. Sayre J, et al. Subperiosteal resorption: effect of full-frame image compression of hand radiographs on diagnostic accuracy. Radiology 1992;185:599-603
83. Templeton AQ, et al. Digital image management networks: current status. Radiology 1988;169:193-199
84. Templeton AQ,et al.A dial-up digital teleradiology system: technical considerations and clinical experience. AJR 1991;-157:1331-1336
85. Wilson AJ,et al. Digitized radiographs in skeletal trauma: performance comparison between a digital workstation and the original film images. Radiology 1995;196:565
86. Wilson AJ. Is teleradiology the solution to after-hours emergency radiology coverage? RadioGraphics 1996;16:939
87. Yoshino MR, et al. Diagnostic performance of teleradiology in cervical spine fracture detection. Invest Radiol 1992;27:55-59

บริษัท คงศักดิ์เอ็กซเรย์การแพทย์อุตสาหกรรม จำกัด
KONGSAK X-RAY MEDICAL INDUSTRY COMPANY LIMITED
212/1 PHAHONYOTHIN SOI 55 BANGKHEN BANGKOK 10220
TEL. 5213214, 5511794 CABLE: KELEX FAX: 5523744

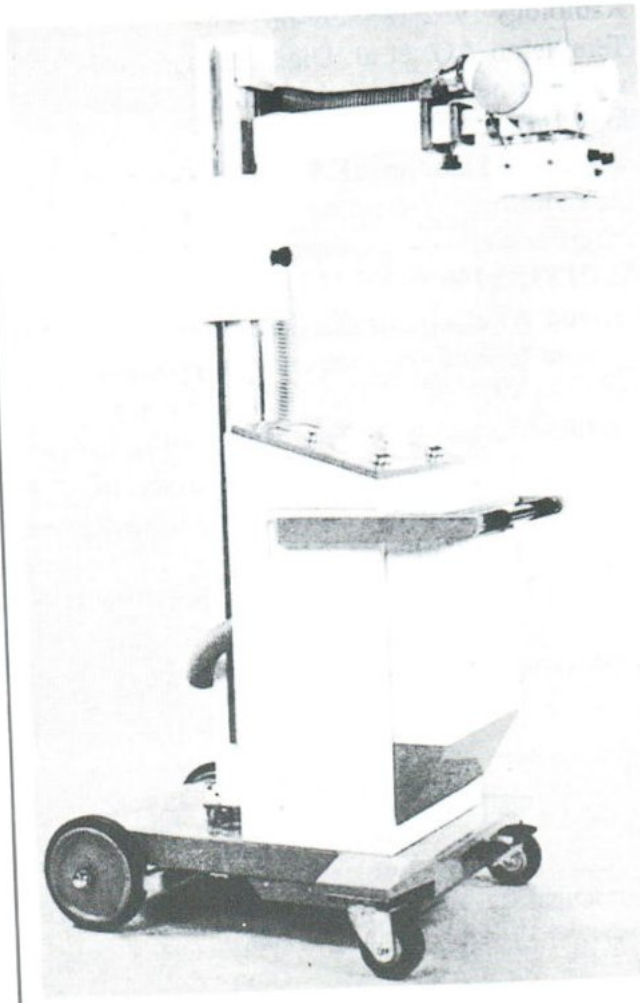

KELEX
50 mA 100 KV MOBILE TYPE DIAGNOSTIC X-RAY UNIT MODEL MD 50-99

- # เหมาะสำหรับคลินิคเอกชนและโรงพยาบาลทั่วไป
- # มีช่างผู้ชำนาญให้การบริการ ตลอดอายุการใช้งาน
- # พร้อมทั้งจำหน่ายอุปกรณ์เอ็กซเรย์

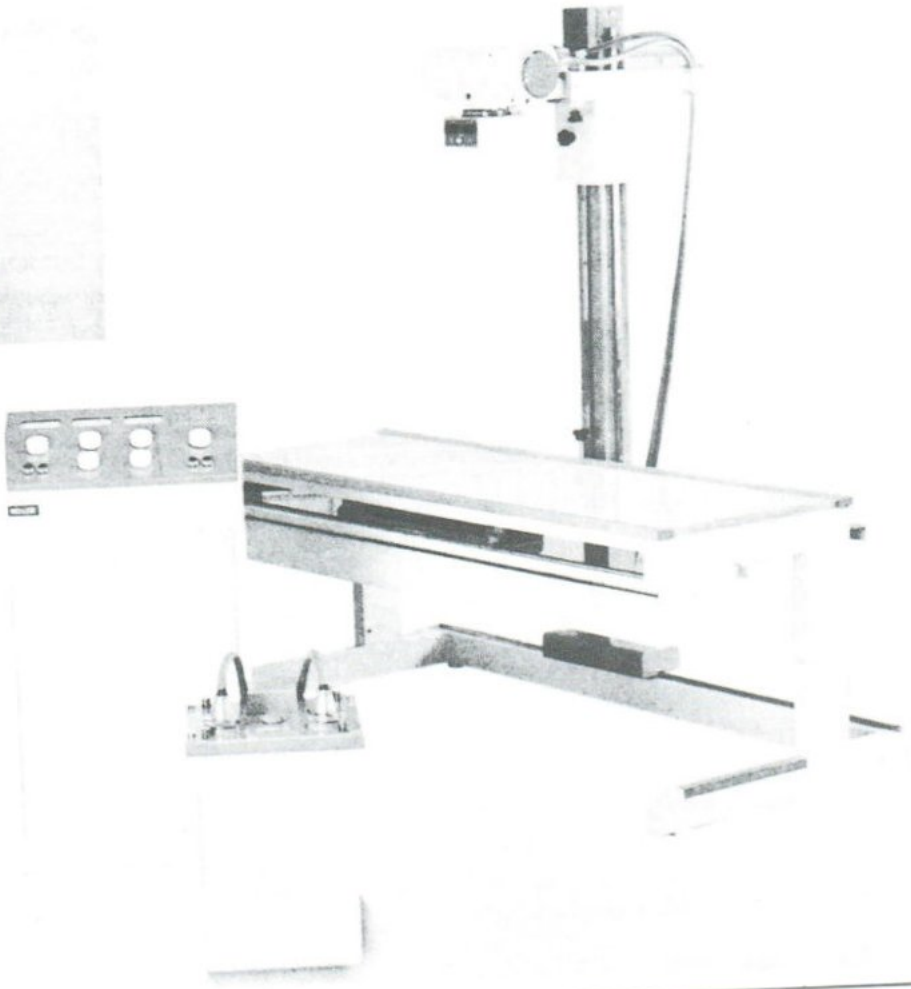

KELEX
MD 100-99 X-RAY SYSTEM
FULL WAVE 100 MA 100 KV

ULTRASOUND AND NUCLEAR SCAN IN THE DIAGNOSIS OF BILIARY ATRESIA IN PERSISTENTLY JAUNDICED INFANTS

Beverly HERCEDA-LAZARA[1], Jonas Francisco Y. SANTIAGO[2], Benigno R. SANTI II[1], Willie N. LAGDAMEO[3] and Orestes P. MONZON[2].

ABSTRACT

This review of cases aims to evaluate the sensitivity and specificity of ultrasonography (US) and hepatobiliary scintigraphy (HBS) in the diagnosis of biliary atresia in persistently jaundiced infants. Thirty-four (34) patients (age 1 to 11 months, 11 females and 23 males) underwent surgery for correction of biliary atresia diagnosed by ultrasound and/or hepatobiliary scintigraphy between January 1981 to December 1995 at the Clinical Division of Santo Tomas University Hospital. All patients had tissue sent for histopathological examination. There were 26 patients with both ultrasound and scintigraphic studies, six (6) with scintigraphic studies only, and one (1) with ultrasound only. Using Fisher's Exact Probability Test, hepatobiliary scintigraphy showed a better sensitivity (83.3%) than ultrasound (68.8%) ($p < 0.05$). However, ultrasound has a better positive predictive value (84.6%) compared to hepatobiliary scintigraphy (75%) in the diagnosis of biliary atresia in persistently jaundiced infants. The study recommends that ultrasound should be used as the initial imaging modality of choice in evaluating biliary atresia in persistently jaundiced infants.

INTRODUCTION

Biliary atresia (BA) is a serious disease of very young infants. It is an obstructive condition of the bile ducts causing neonatal jaundice. The obstruction is of unknown etiology but results from a progressive obliterative process of variable extent. In the majority of patients, the entire extrahepatic biliary tree is obliterated. However, others may have only partial obliteration. The symptoms are evident between 2 to 6 weeks after birth. A slight female predominance is noted but there is no racial predilection.[1] The typical patient is a few months old with intractable jaundice, acholic stools, and deep yellow urine.

BA has to be differentiated from neonatal hepatitis which presents with similar clinical features, laboratory findings and histopathological characteristics. The pathogenesis of BA and neonatal hepatitis may be the same. It has been suggested that an initial insult leads to an inflammatory process at any level of the hepatobiliary tract. If it is the hepatocyte, it results in neonatal hepatitis and if it is at the extrahepatic bile ducts, it results in BA.[2]

The two most important tests in the evaluation of BA are ultrasound (US) and hepatobiliary scintigraphy (HBS). These diagnostic tests aim to provide an early and accurate answer to a specific question: Is the patient's cholestasis due to

[1] Division of Radiological Sciences,
[2] Section of Nuclear Medicine,
[3] Department of Pediatric Surgery, Santo Tomas University Hospital Espana, Manila, Philippines

neonatal hepatitis or BA? Is the patient a surgical (biliary atresia) or a medical (neonatal hepatitis) case ?

Ultrasound is always utilized as the initial diagnostic modality in the evaluation of children with jaundice.[3] The advantages of US include low cost, ease of use, versatility and availability. Limitations include presence of bowel gas, obesity, and the necessity for fasting for four to six hours prior to the procedure.

Absent or small gallbladder is a frequent finding in BA; therefore, nonvisualization of the gallbladder or a small gallbladder on sonography favors this diagnosis.[4] The ultrasonic demonstration of a normal gallbladder (normal length > or = 1.5 cm) supports the diagnosis of neonatal hepatitis and is less commonly seen in BA. The presence of the gallbladder , however, does not necessarily rule out the diagnosis of BA. Contraction of the gallbladder after a fatty meal militates against BA.[5] In addition, some researchers claim that the visualization of triangular or tubular echogenic density in the vicinity of the portal vein (triangular cord sign) is specific for BA.[6]

Majority of patients with BA will not have sonographically depictable bile ducts. But occasionally there will be atresia of only portions of the bile ducts with dilatation of the segments proximal to the atretic area.[4] In these cases, it is possible to demonstrate the biliary tree.

HBS is the other modality usually requested to differentiate between BA and neonatal hepatitis. The technetium-99m iminodiacetic acid derivatives (Tc99m-IDA) are rapidly extracted from the blood by the hepatocytes and are excreted into the bowel through the biliary ducts.[7] Most of the intravenously injected tracer is seen in the liver within 30 minutes. When there is hepatocellular disease there is delayed uptake; with biliary obstruction , the materiai accumulates in the liver, but none appears in the bowel. Complete biliary tract obstruction is diagnosed when the gallbladder and intestines are not visualized plus the presence of a "liver scan"-appearing liver.[8]

A delay in management of the obstructed neonate may result in cirrhosis, portal hypertension and pancreatitis. Previous reports showed better prognosis when surgery is done before ten weeks of age.[9]

This study aims to evaluate the sensitivity and specificity of US and hepatobiliary scintigraphy and their predictive values in the diagnosis of BA in persistently jaundiced infants.

METHODOLOGY

The records of patients *who underwent biliary surgery from January 1981 to December 1995* at the Clinical Division of Santo Tomas University Hospital (STUH) were reviewed. Patients who satisfied the following criteria were entered into the study: 1. those who had radionuclide hepatobiliary imaging and/or ultrasonography before the surgery; and, 2. those who were not more than 12 months of age. Thirty-four subjects met the above criteria and were included in the study. The age ranged from 1 - to 11 months old. There were 11 females and 23 males. All patients had tissue sent for histopathological examination. There were 26 patients who had both US and scintigraphic studies, six with scintigraphic studies only and one with US only. A short history and physical examination were obtained from the chart. Pertinent laboratory and imaging procedures were noted. The histopathological report was also documented.

Non-visualization of the gallbladder and biliary tree was considered as positive US findings suggestive of BA. The presence of a normal gallbladder was considered as a negative US finding.

Positive scintigraphic findings were noted

in those cases which had no gallbladder visualization and no radioactive tracer excreted into the intestines up to 24 hours after the administration of the radiopharmaceutical. In addition, the liver had to be well-visualized with intense tracer uptake.

Data was tabulated using Microsoft Excel program. Statistical analysis with Fisher's exact probability test was done using Kwikstat (Texasoft, Texas, USA).

RESULTS

The 34 patients included in the study were typical. The cases were a few months old with recognized jaundice since birth. Acholic stools were frequent but not seen in all. Abdominal enlargement was seen infrequently. The initial workup of a jaundiced infant included a complete blood count and liver function tests. Bilirubin levels were also obtained.

Table 1 shows the laboratory exam results of the subjects. There were 11 females and 23 males. Worthy of note were the elevated values for SGOT, SGPT, total, indirect and direct bilirubin.

Table 2 shows the US, HBS, and histopathological diagnosis of the 34 subjects. Histopathological diagnosis was done by the pathologists of STUH. Worth mentioning was the one case diagnosed to have choledochal cyst by US which was later proved correct by histopathologic exam.

US and HBS versus histopathological diagnosis were analyzed via a 2 x 2 contingency table as seen in **Table 3 and 4.** Hepatobiliary scintigraphy was correct in 25 out of 33 patients (76%). The sensitivity and specificity of HBS were 83.3% and 66.7%, respectively. The positive predictive value was 75% and the negative predictive value was 76.9% ($p<0.005$). Ultrasonography was correct in 20 out of 27 patients (74%). The sensitivity and specificity of US were 68.8% and 81.8%, respectively. The positive predictive value was 84.6% and the negative predictive value was 64.3% ($p<.05$).

Table 5 shows the distribution of the 26 patients with both US and HBS and whether they have BA or not by pathology ($p<0.05$). In eight patients who were diagnosed to have BA by US and HBS, all of them (100%) had BA by histopathology. However, 2 out of 7 patients (28%) who had negative findings by both US and HBS had positive histopathologic result for biliary atresia; 5 out of these 7 patients (72%) who had negative findings by both US and HBS had no BA. On the other hand, 3 out of 7 patients (43%) who had positive HBS and negative US findings were correctly diagnosed to have BA; hence, 4 out of these 7 patients (57%) were incorrectly diagnosed to have BA. In 4 patients who had negative HBS and positive US findings 2 of these patients (50%) had BA and also 2 of these patients (50%) had no BA on histopathology. Out of these 26 patients who had both HBS and US examinations, 13 patients (50%) were correctly diagnosed to have biliary atresia. A cause of concern were the 2 patients (7.7%) with negative US and HBS findings but have biliary atresia on histopathology; both had no GB by US although the biliary ducts were seen in one. With HBS the liver was faintly visualized in both which makes nuclear physicians wary of diagnosing biliary obstruction since extensive liver damage could cause the same picture and is admittedly one of the causes of false positive exams.

Table 1
Laboratory Data of the 35 Cases in the Study

Name	Sex	Age	SGOT	SGPT	TB	b1	b2
		months	u/l	u/l	mg/dl	mg/dl	md/dl
			8 to 33	5 to 40	.1 to 1.2	.1 to 1	.1 to 1
J.P	f	3		83			
E.C.	m	2		326	7	1.76	5.1
A.D	f	9	143	62		0.76	9.6
J.A.	m	3	136	95	6.4	2.6	3.76
K.O.	f	3			17	2.1	14.7
R.D.	m	2		125	7.2	3.4	7.36
J.B.	m	3					
J.C.	m	4					
J.T	m	2.5					
BH	m	2					
RB	f	4	500	300	15	1.7	14
BR	m	2	29		12	4	8
CL	f	9			18	6.58	12
CD	f	4.5		47.5	6.4	6.8	6.1
ML	f	2.5			5.7		4.8
KC	m	3.5		30.5	1.3	4.1	1.3
W.B.	f	3			11.7	5	6.2
C.J.	f	1.5	41	23	5	0.4	4.7
R.B	m	11			29.5	7.3	22.1
W.M.	m	3	600	350	7.7	5.2	2.5
B.Q.	m	2	100	58	7.6	5.2	2.4
R.D.	m	5	380	250	7.2	5	2.2
V.C.	m	2.5	210	300	8.7	6.1	2.6
M.S.	m	3	800	250	6.6	5.8	0.8
R.M.	m	3	680	580	10.8	6.8	4
K.V.	f	3	120	98	7.5	4.8	2.7
R.F.	m	4	580	460	8.6	6.6	2
K.S.	f	6	540	290	16.8	3.9	12.9
D.L.	m	4	400	350	5.8	3.9	1.9
J.C.	m	2	720	600	12	10.2	1.8
J.K.	m	2	580	340	16.3	12.7	3.6
R.B.	m	1	600	400	23.6	20.4	3.2
R.C.	m	1.5	110	80	23.4	15	8.4
A.R.	m	3	250	200	11.8	8.4	3.4
mean		3.56	375.95	237.42	11.31	5.95	6.00

Table 2
Imaging Results and Histopathological Findings

PATIENT	ULTRASOUND	SCINTIGRAPHY	HISTOPATHOLOGY
J.P	n gb, n bt	gb, si not seen	biliary atresia
E.C		gb, si not seen	neonatal hepatitis
A.D	n gb, n bt		biliary atresia, chronic cholecysitis, portal fibrosis
J.A		gb, si not seen, hepatitis	neonatal hepatitis
K.O	gb not seen, intrahep duct not dilated	gb, si not seen, hepatomegaly	biliary atresia
R.D		gb, si not seen	biliary atresia, portal , central fibrosis
J.B		gb, si not seen	biliary atresia
J.C		gb ,si not seen	biliary atresia,chronic cholecystitis, portal fibrosis
J.T		gb, si not seen, hepatitis	biliary atresia with fibrosis
BH	gb not seen	gb si not seen	biliary cirrhosis, stenotic, fibrotic cbd
RB	gb not seen, diffuse liver disease	gb, si not seen, liver not seen	biliary atresia
BR	gb not seen, diffuse liver disease	gb, si not seen, hepatomegaly	biliary atresia
CL	n gb, n liver	gb,si not seen, hepatomegaly	biliary atresia
CD	n gb, n liver	gb, si not seen, faint liver	biliary atresia, chronic cholecystitis
ML	n gb, n liver	gb, si not seen	biliary atresia, chronic inflammation of the liver
KC	gb not seen	gb, si not seen	biliary atresia, chronic inflammation of the bt
W.B	gb not seen	gb, si not seen	biliary atresia, chronic cholecystitis
C.J	gb not seen, diffuse liver disease	gb not seen, si seen	biliary atresia, liver cirrhosis, chronic inflammation of gb
R.B		gb, si not seen	neonatal hepatitis
W.M	n gb, n liver	gb,si seen	neonatal hepatitis
D.Q	n gb, n liver	gb,si seen	neonatal hepatitis
R.D	n gb, n liver	gb,si seen	neonatal hepatitis
S.D	gb, bt not seen	gb,si seen	neonatal hepatitis
M.S	gb, bt not seen	gb,si seen	neonatal hepatitis
R.M	gb, bt not seen	gb,si not seen	biliary atresia
K.J	gb, bt not seen	gb,si not seen, faint liver, hepatomegaly	biliary atresia
R.F	gb, bt not seen	gb,si not seen	biliary atresia
K.S	gb, bt not seen	gb,si not seen	biliary atresia
D.L	choleduchal cyst	gb, si not seen	choledochal cyst
J.C	n gb, bt seen	gb, si not seen, intense liver tracer uptake,hepatomegaly	neonatal hepatitis
J.K	n gb, bt seen	gb,si not seen	neonatal hepatitis
R.B	n gb, bt seen	gb, si not seen	neonatal hepatitis
R.C	n gb, bt seen	gb, si not seen, faint liver	neonatal hepatitis
A.R	n gb, bt seen	gb, si not seen, faint liver	neonatal hepatitis

gb=gallbladder; **bt**=biliary tract; **si**=small intestine; **n**=normal; **cbd**=common bile; **chd**=common hepatic duct

Table 3
Hepatobiliary Scintigraphy and Histopathologic Findings

	Histopathological Diagnosis		
	(+) biliary atresia	(-) biliary atresia	Total
(+) scintigraphy	15	5	20
(-) scintigraphy	3	10	13
Total	18	15	33

$p < 0.005$
Sensitivity = 83.3 %
Specificity = 66.7 %
Positive Predictive Value = 75.0 %
Negative Predictive Value = 76.9 %

Table 4
Ultrasound and Histopathologic Findings

	Histopathological Diagnosis		
	(+) biliary atresia	(-) biliary atresia	Total
(+) ultrasound	11	2	13
(-) ultrasound	5	9	14
Total	16	11	27

$p < 0.05$
Sensitivity = 68.8 %
Specificity = 81.8%
Positive Predictive Value = 84.6 %
Negative Predictive Value = 64. 3 %

Table 5. Hepatobiliary Scintigraphy and Ultrasound vs. Histopathologic Findings

	(+) HBS (+)US	(-) HBS (-)US	(+) HBS (-) US	(-) HBS (+)US	Total
(+)BA	8	2	3	2	15
(-)BA	0	5	4	2	11
Total	8	7	7	4	26

BA=biliary atresia; **HBS**=hepatobiliary scintigraphy; **US**=ultrasound

$p<0.05$

DISCUSSION

There are different types of biliary atresia. The most common variants include: 1) complete obliteration of the extrahepatic ducts; 2) patency of the distal biliary tree (gallbladder, cystic duct and common bile duct) with proximal obliteration; and 3) proximal hilar bile cyst (formerly considered the "correctable" type).[1]

It is associated with neonatal hepatitis and choledochal cyst in a disease spectrum which Landing in 1974 called "infantile obstructive cholangiopathy".[10] Some hypotheses as to the etiology includes 1) viral infection with reovirus type 3, 2) blood supply catastrophe, 3) abnormal bile acid metabolism, 4) genetic influences and 5) developmental anomaly.[2] Reovirus type 3 in particular, persists in the murine liver and shows BA-like effects in offspring of infected pregnant mice.[11]

Two patients with neonatal hepatitis studied by Park et al had marked dilatation of the endoplasmic reticulum and mild mitochondrial alterations without the cytoplasmic biliary necrosis of bile canalicular injury.[2] These two patients later proved to be cases of BA reinforcing the idea that early pathological changes of BA are similar to neonatal hepatitis.

Without surgery BA is a progressive disease which results in cirrhosis. Liver cirrhosis may be a pre-cancerous lesion although no causal relationship has been elaborated satisfactorily. However, the association between chronic hepatic disease and hepatoma is even stronger in children than in adults.[12]

Biliary atresia is diagnosed histopathologically when there is intrahepatic bile duct degeneration and lymphocytic infiltration of portal areas and biliary epithelial cells.[13] In addition, the porta hepatis is encased in fibrous tissue. In the development of the fetus, there is failure of the remodeling process at the hepatic hilum, with persistence of fetal bile ducts poorly supported by mesenchyme. An intense inflammatory reaction results as bile flow increases perinatally which culminates in biliary tree obliteration.[14]

With an incidence of as high as 1 in 15,000 and a possible role for reovirus type 3, BA may, in fact, be even more prevalent in developing and population-dense countries. It is difficult to generate incidence data for BA in the Philippines, for example, because of poor patient follow-up, low autopsy rate, and the relative unpopularity of the

surgical intervention indicated for the condition (Kasai portoenterostomy and liver transplantation).

The work-up of jaundiced infants varies little from the diagnostic work-up of jaundiced adults. Blood exams and US are standard owing to their accessibility and inexpensiveness. In infants, jaundice beyond two weeks warrants, aside from serum and urine bilirubin measurements, imaging to immediately rule out a potentially surgically-correctable cause. Some authors recommend that HBS should be the first imaging modality given its high sensitivity and specificity (90 - 95 % for both).[15] In the neonate, delay in the definitive management causes a marked decline in survival rates. In a study by Oh et al in 1995, 35 out of 42 (83.3 %) BA patients who had surgery before two months of age were still alive during the study. Contrast this with 6 out of 17 (35.3 %) living biliary atresia patients who had surgery after the "golden period" of two months. Delay in surgery also results in more complications like portal hypertension and growth retardation.[9]

Hepatobiliary imaging is not without its variations. It started originally with the use of iodine-131 Rose Bengal. Later, it was replaced by the technetium-based radiopharmaceuticals exemplified by the iminodiacetic acids IDA.[16] Advances in the field have yielded agents with higher hepatic extraction and lower renal excretion. Diisopropyl-IDA (DISIDA) exhibits faster hepatic transit and higher gallbladder-to-liver ratio. The problem with highly jaundiced patients (as high as bilirubin levels of 30 mg/dl) is surmounted.[7] To increase the sensitivity of the test, neonates are "primed" with phenobarbital a few days prior to the procedure. Morphine is used in adults in order to lessen the investigation period to a few hours without sacrificing sensitivity.[17]

The sample of patients in the study were highly selected patients. The patients had intractable jaundice since birth and many had acholic stools. There were more male infants affected. Laboratory examinations such as liver function tests, were elevated. The sensitivity of hepatobiliary scintigraphy (HBS) for diagnosing biliary atresia in persistently jaundiced infants was 83.3%, which is higher compared to US (68.8%). On the other hand, the specificity of US was 81.8% while HBS has 66.7% specificity. US has 84.6% positive predictive value which was better than HBS (75.0%). The data on table 5 shows that if HBS was positive and US was negative for biliary atresia, the chances of the patient to have BA was <50% while if the HBS was negative and US was positive, the chances of the patient to have BA was 50%. When both HBS and US were positive, 100% positive predictive value was noted. However, it was observed that when both HBS and US were negative, 28% of these patients may still have a false negative result.

CONCLUSION

Persistently jaundiced infants pose problems to clinicians in differentiating between a medical and surgical case despite good clinical evaluation and laboratory examinations. This study shows that ultrasonography is a useful initial imaging modality in the diagnosis of biliary atresia in persistently jaundiced infants compared to HBS given the better positive predictive value of ultrasound.

The study also shows that if HBS and US have both positive findings for biliary atresia, the positive predictive value of the procedures increase.

The other role of US is in the identification of other causes of biliary obstruction such as choledochal cyst, determination of hepatic size, and to provide information about the liver parenchyma.

REFERENCES

1. Karrer FM, Lilly JR, Hall RJ. Biliary Tract Disorders and Portal Hypertension. Pediatric Surgery. 2nd ed. 1993.
2. Park W, Kim S, Park K, Choi S, Lee H, and Kwon KY. Electron microscopic study of the liver with biliary atresia and neonatal hepatitis. Journal of Pediatric Surgery 31: 367-374,1996.
3. Fleischner AC, James,Jr EA. Diagnostic Sonography: Principles and Clinical Applications. c 1989.
4. Gates G, Sinatra F, and Thomas D. Cholestatic syndromes in infancy and childhood. American Journal of Roentgenology 134:1141, 1980.
5. Donaldson J, Gore, Levine and Lauffer. Textbook of Gastrointestinal Radiology. WB Saunders 1st ed., 1994.
6. Lee H, Taegu K, Kim JS, Woo S, Choi SO, Park WH, Suh S. Triangular cord sign: a diagnostic sonographic feature of biliary atresia. Journal of Pediatric Surgery 1996.
7. Torres,Jr JF, and Obaldo JM. Radionuclide studies of the hepatobiliary system and their significance in clinical practice. Unpublished, 1995.
8. Majd M, Reba RC, Altman RP. Hepatobiliary scintigraphy with Tc99m-PIPIDA in the evaluation of neonatal jaundice. Pediatrics 67: 140-145, 1981.
9. Oh M, Hobeldin M, Chen T, Thomas DW, Atkinson JB. The Kasai procedure in the treatment of biliary atresia. Journal of Pediatric Surgery 30: 1077-1081, 1995.
10. Torrisi JM, Haller JO, Velcek FT. Choledochal cyst and biliary atresia in the neonate:Imaging findings in five cases. American Journal of Radiology 155:1273-1276, 1990.
11. Parashar K, Tarlow MJ, McCrae MA. Experimental reovirus type 3—induced murine biliary tract disease. Journal of Pediatric Surgery 27: 843-847, 1992.
12. Kohno M, Kitatani H, Wada H, Kajimoto T, Matuno H, Tanino M, Nakagawa T, Takarada A. Hepatocellular carcinoma complicating biliary cirrhosis caused by biliary atresia: Report of a case. Journal of Pediatric Surgery 30: 1713-1715, 1995.
13. Ohya T, Fujimoto T, Shimomura H, and Miyano T. Degeneration of intrahepatic bile duct with lymphocyte infiltration into biliary epithelial cells in biliary atresia. Journal of Pediatric Surgery 30: 515-518, 1995.
14. Tan CE, Driver M, Howard ER, Moscoso GJ. Extrahepatic biliary atresia: a first trimester event? Journal of Pediatric Surgery 29: 1994.
15. Wagner H, Szabo Z, Buchanan J. Prin ciples of Nuclear Medicine. 2 ed. 1995.
16. Klingensmith III WC, Spitzer V, Fritzberg A, Kuni CC. The normal fasting and postprandial diisopropyl-IDA Tc 99m Hepatobiliary Study. Radiology. 141: 771-776, 1981.
17. Fink-Bennett D, Balon H, Tsai T. Morphine-augmented cholescintigraphy: Its efficacy in detecting acute cholecystitis. Journal of Nuclear Medicine 32: 1231-1233, 1991.

EDUCATION

Asian-Oceanian Seminars on Diagnostic and Interventional Radiology

1 9 9 8

Emergency Radiology
April 16-18
Subic, Philippines
Programme Leader:
A. Tingcungco

Imaging of the Digestive System: Current Status & Future Direction
June 6-8
Beijing, China
Programme Leaders:
G.N. Liu
J.P. Dai

Radiology in Obstetrics & Gynaecology
October 15-17
Lahore, Pakistan
Programme Leader:
M.A.J. Siddiqui

BRACCO
INTERNATIONAL

For further information please contact:
Bracco International B.V.
47 Hill Street, #06-05
S.C.C.C.I. Building
Singapore 179365
Tel: ++65-337 1880
Fax: ++65-337 7576
E-mail: singapore@braccoint.com.sg
http://www.bracco-group.com

GASTRIC VOLVULUS

Panida MUKDEEPROM[1]

ABSTRACT

Gastric volvulus is a rare but important cause of high intestinal obstruction.Three cases of gastric volvulus were presented, one organoaxial and two mesenteroaxial volvulus. Radiographic findings in these three cases were typical. It is essential that the radiologists recognize the radiographic features of gastric volvulus since prompt corrective surgery is vital in proper management of these patients.

Gastric volvulus is a rare condition defined as an abnormal anterior or posterior rotation of part or all of the stomach about either the saggital or coronal plane of the gastric body. The two main types of volvulus are the organoaxial volvulus - the stomach is twisted around its long axis or coronal plane - and the mesenteroaxial Volvulus where the stomach is twisted around the axis joining the lesser and greater curvature (saggital plane). Volvulus can be complete or partial and can occur in the abdomen or be intrathoracic. The diagnosis of this category can be made by plain film and contrast study of the gastrointestinal tract.

CASES REPORT

Case I

A 42-year-old woman complained of intermittent dull pain and fullness of the epigastrium. The physical examination revealed some vague tenderness over the epigastrium without definite rigidity or guarding. A plain film of the abdomen showed multiple air pockets superimposed on the cardiac shadow and a small amount of air in gastric fundus (fig 1). The upper gastrointestinal study revealed organoaxial volvulus of the stomach (fig 2). During the operation, herniation of the colon through the Morgagne foramen was found and the stomach was twisted around its longitudinal plane due to retraction of the gastrocolic ligament.

Case II

A 4-year-old boy was brought in after experiencing nausea, vomiting and pain at the epigastrium for 1 day. On physical examination, he appeared to be acutely ill and his abdomen was moderately distended. A plain film of abdomen showed a spherical distended fluid-filled stomach and a slight elevation of the left hemi-diaphragm. The upper gastrointestinal study showed mesenteroaxial volvulus of the stomach (fig.3,4). He was transferred to the operating room where it was revealed that the stomach was twisted around its mesenteric axis. Detorse procedure was performed with fixation of the stomach. The post-operative course was uneventful.

[1] Department of Radiology, Saraburi hospital

Case III

A 67-year-old man came to the hospital after having fallen from a significant height. The Physical examination and chest film revealed multiple rib fractures on the left side with elevation of the left diaphragmatic shadow. There was a large air pocket at the left lower lung field. A traumatic diaphragmatic hernia was suggested. An upper gastrointestinal study showed an upside down stomach with a complete obstruction at the distal end (Fig.5). During the operation a large rupture of the diaphragm was found. The stomach was twisted around the saggital axis and herniated into the thoracic cavity. Reduction of the volvulus and herniated stomach was done and the diaphragm was repaired. The post-operative course was uneventful.

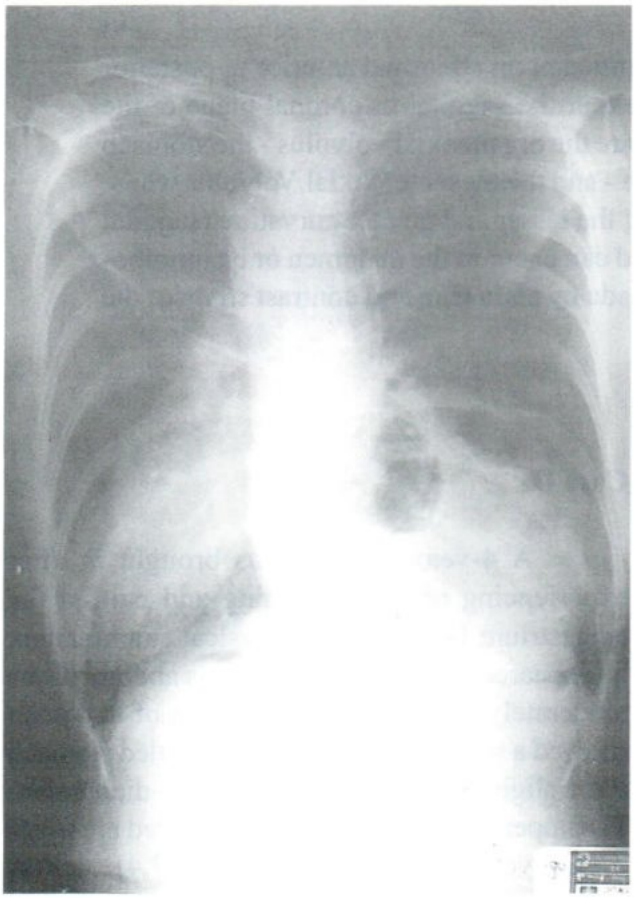

Fig. 1 Multiple air pockets at retrocardiac area, small amount of air in gastric fundus.

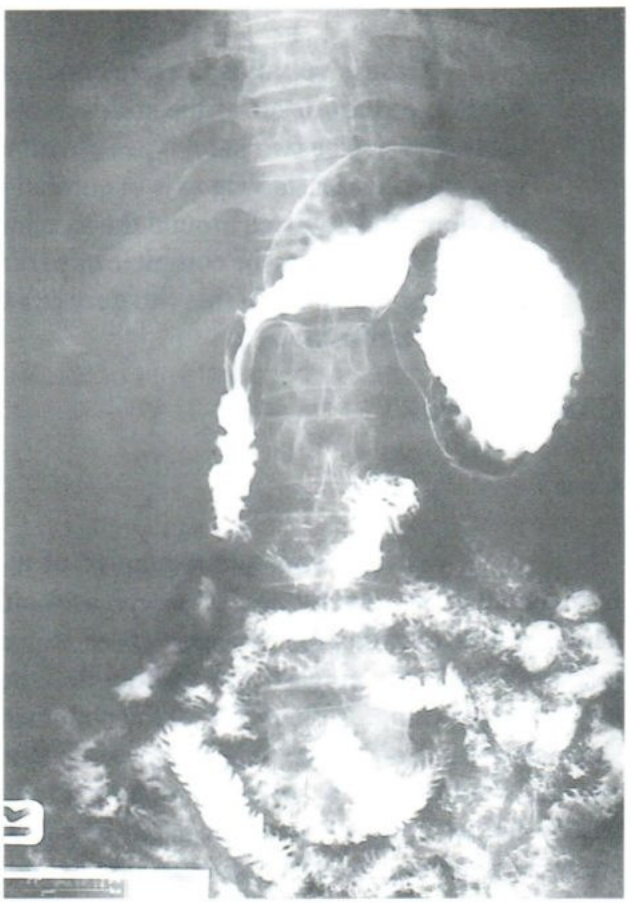

Fig. 2 Organoaxial volvulus : Transverse position of the stomach with greater curvature rotated upward, the pylorus and duodenum pointed downward.

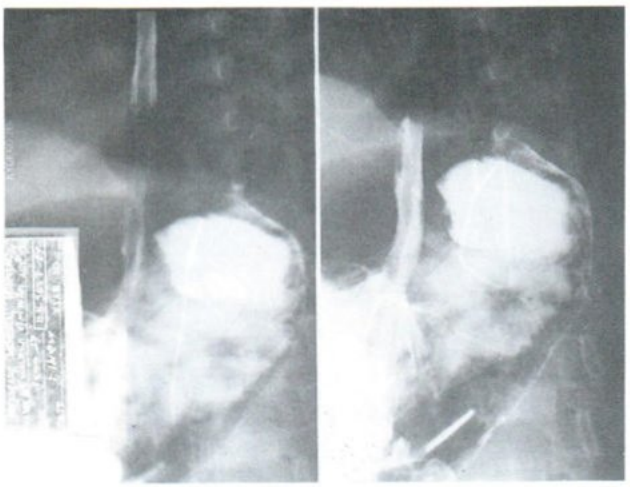

Fig .3 Case II Mesenteroaxial volvulus: The E-G junction lied inferior to the antrum which rotated above and to the left of the fundus, creating upside-down stomach.

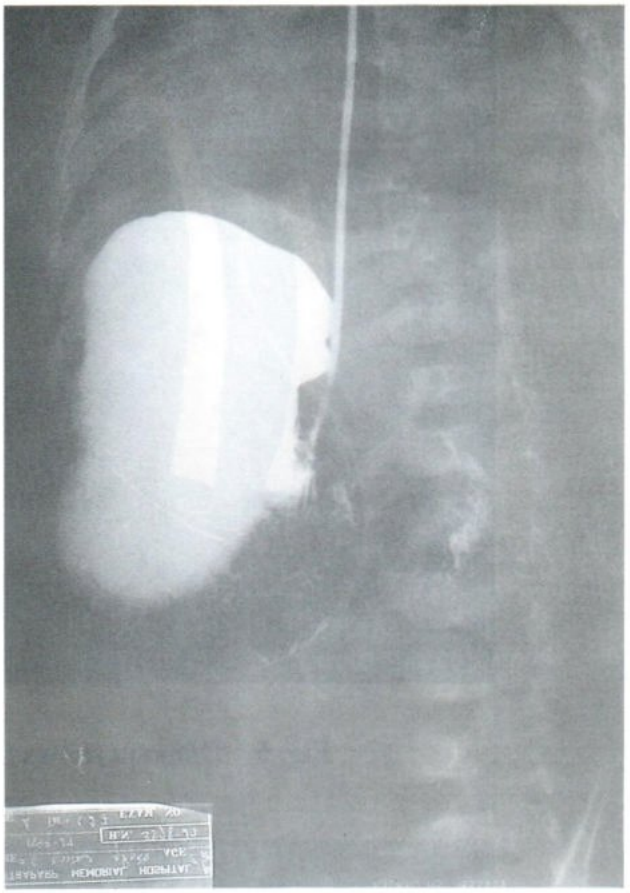

Fig. 3

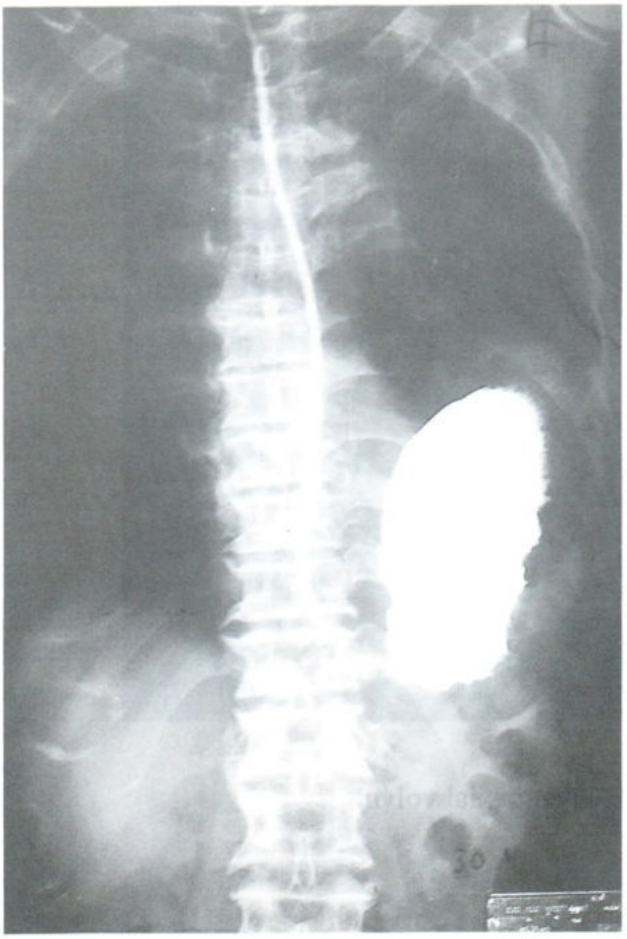

Fig. 4 Upside-down stomach with complete obstruction, mesenteroaxial volvulus.

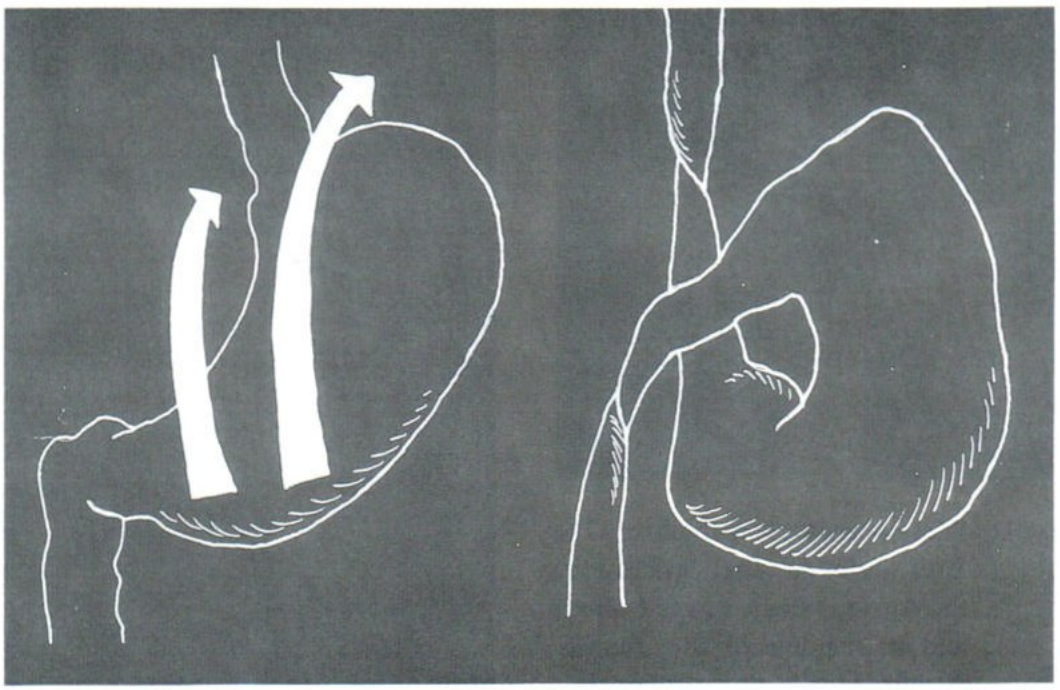

Fig. 5 Diagram shows : **A.** Mesenteroaxial volvulus.

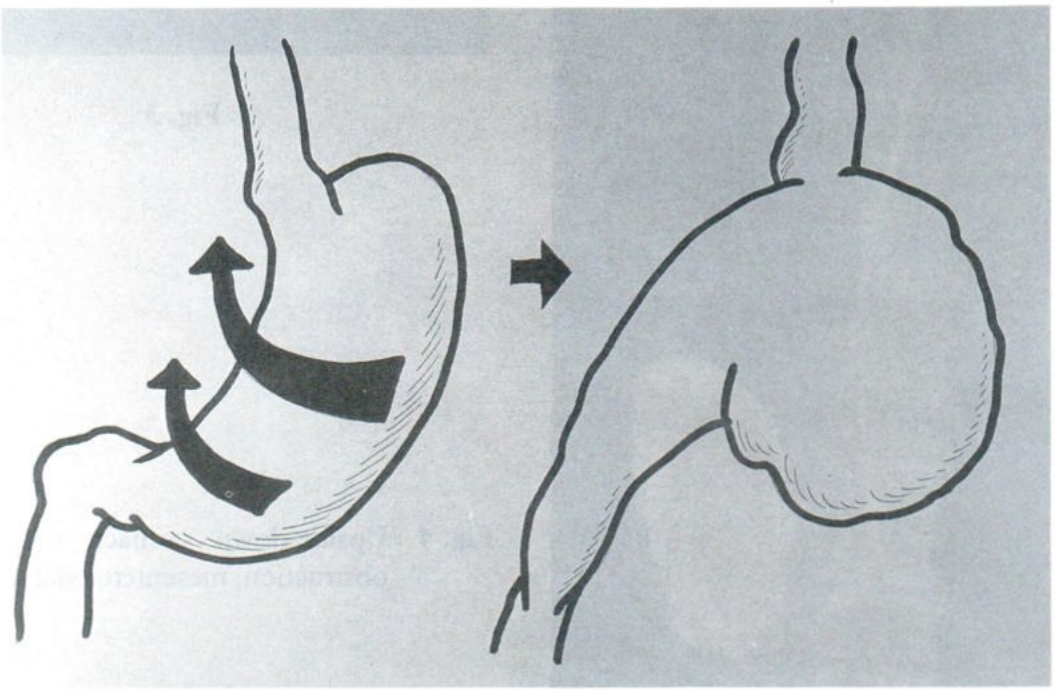

Fig. 5 Diagram shows : **B.** Organoaxial volvulus.

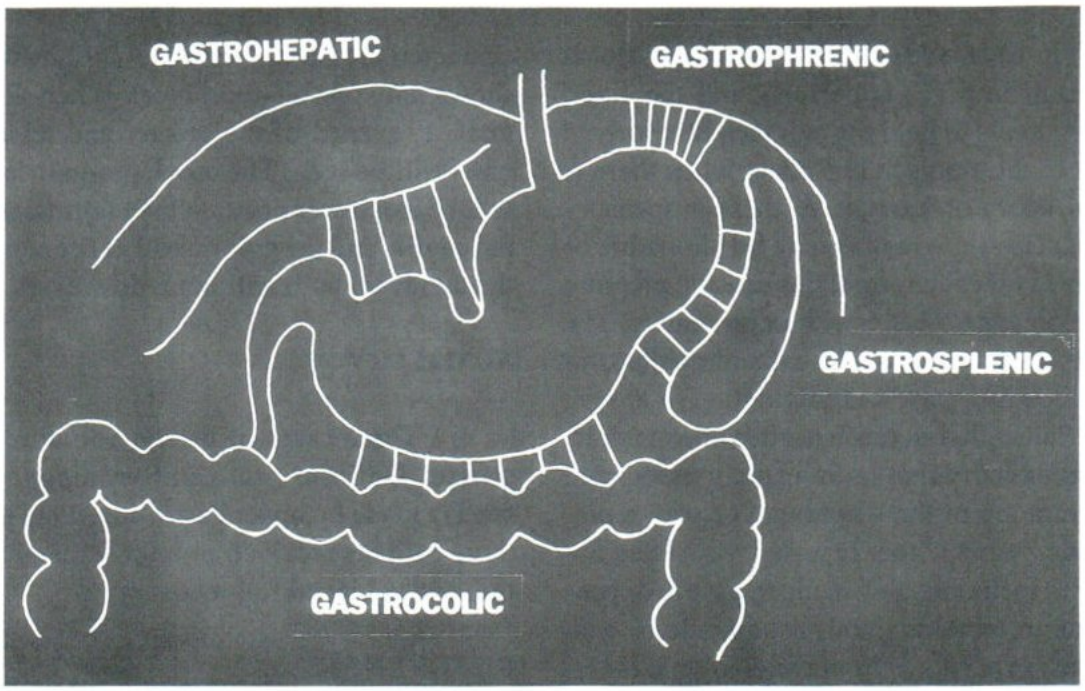

Fig. 6 Four supporting ligaments of the stomach.

Table I Anatomical classification of gastric volvulus

Classification	Description
Location:	
Abdominal	Entire volvulus in abdominal cavity; most commonly associated with eventration of left hemidiaphragm
Thoracic	Entire rotated stomach in intrathoracic position
Direction (fig 5)	
Organoaxial	Stomach rotates along longitudinal axis
Mesenteroaxial	Stomach rotates in axis of mesentery perpendicular to longitudinal axis
Extent:	
Complete	Entire stomach involved in the twist
Segmental	Most commonly involves segmental twist of distal stomach

DISCUSSION

Gastric volvulus is a rare condition. Several types (Table I) are recognized[3]

The stomach is an irregularly shaped viscus that expands and contracts several times daily. In normal circumstances, the stomach is not likely to undergo volvulus because it is suspended relatively securely by the gastric ligaments. These include the gastrohepatic ligament along the lesser curvature, the gastrocolic and gastrosplenic ligaments along greater curvature, and the gastrophrenic ligament along the posterior aspect of the

fundus (Fig 6) In addition, the esophagus holds the stomach in place superiorly and the fixed duodenum tends to hold the stomach inferiorly.[4,6] Volvulus of the stomach can occur when there is abnormal laxity or absence of these suspensory ligaments. Gastric volvulus may be idiopathic or secondary to other abnormalities causing pressure or retraction upon the stomach or mesentery. The mesenteroaxial volvulus is usually idiopathic, although cascading gastric configuration or atonic, a dilated fluid-filled stomach is often encountered. The organoaxial volvulus is usually associated with eventration of the diaphragm or with a diaphragmatic hernia. Other reported associated abnormalities including gastric ulcer, gastric or pancreatic tumor, phrenic paralysis, colonic or gastric distension, cast syndrome and colonic diverticulum.[1,2,3,4,7,8]

A radiographic study should readily substantiate the clinical suspicion of gastric volvulus. In mesenteroaxial volvulus, the distended stomach appears spherical on a supine film. There is often a double fluid level, the inferior one lies in the fundus and the superior one lies in the antrum. On upright films and occasionally on supine films, a characteristic "beak" sign is produced by a gaseous distension of the inverted antrum, pylorus and proximal duodenum. An upper gastrointestinal study confirms volvulus and documents the degree of obstruction. The pyloric end of the stomach will have rotated to the left either anteriorly or posteriorly. The greater curvature will be above the lesser curvature. The pyloric end may rise above the proximal end creating an upside down stomach.[1,6,7]

The diagnosis of organoaxial volvulus on plain films is not easy. Although an upper gastrointestinal study can confirm the diagnosis, it may be missed if careful attention is not paid to the position of the esophagogastric junction which is lower than normal. UGI also shows that the stomach is positioned horizontally, there is no characteristic "beak" and the upright film often shows only one air-fluid level. When volvulus is total, a reversal of the greater and lesser curvatures will be seen. The esophago-gastric junction will be in a lower position than normal relative to the cardia, and the pyloric end of the stomach and the duodenal bulb will point downward.[1,3,4,6]

SUMMARY

Three cases of gastric volvulus were reported. Definite preoperative diagnosis were readily made by upper gastro-intestinal study. All three patients received prompt surgical intervention and achieved full recovery.

REFERENCES

1. Myerson DA, Myerson PJ, Lawson JP: Antral infracolic volvulus of the stomach. J Can asso Radiologists 1975;26:128-131.
2. Campbell JB, Rappaport LN, Skerker LB: Acute mesentero-axial volvulus of the stomach. Radiology 1972;103: 153-156.
3. Menuck L: Plain film findings of gastric volvulus herniation into the chest. Am J Roentgenol 1976;126: 1169-1174.
4. Campbell JB: Neonatal gastric volvulus. AJR 1979;132:723-725.
5. Dagher M, Terry DO, MacMath L, Seger DL: Mesenteroaxial gastric volvulus in children. Southern Medical Journal 77:-768-770.
6. Ziprkowski MN, Teele RL: AJR 1979;-132:921-925.
7. Kilcoyne RF, Babbitt DP, Sakaguchi S: Volvulus of the stomach, A case report. Radiology 1972;103: 157-158.
8. Ashby ME, Balfour GW, Cambell JA: Acute gastric volvulus mimicking the cast syndrome, A case report. The Journal of Bone and joint Surgery 59A: 1001-1002, 1977.

ACUTE TRAUMATIC ABDOMINAL WALL HERNIA DIAGNOSED BY ULTRASONOGRAPHY: A CASE REPORT.

Panida MUKDEEPROM[1]

ABSTRACT

A traumatic abdominal hernia is a rare clinical entity despite an overall increase in blunt abdominal trauma. Early recognition of the injury is important for this condition is often associated with other intra-abdominal organ injury. The diagnosis can be made by physical examination alone. Plain film, computed tomography and ultrasonography have also proven useful. This paper reports a case of acute traumatic abdominal wall hernia diagnosed by ultrasonographic examination following a motorcycle accident.

CASE REPORT

A 18-year-old man was brought to the emergency department after he was involved in a motor-vehicle accident. He described that his bicycle ran over a stone and he was thrown forward and was hit in the lower abdomen region by the handlebar. On initial examination, the patient was in good conscious and alert and his vital signs were normal. There was a swollen area with ecchymosis at the point of impact approximately 10 cm. in diameter. The patient complained of a marked tenderness over this area. Acute abdominal series disclosed no free air or free fluid in the abdomen. The bowel pattern was normal. The patient underwent an ultrasonographic examination in order to evaluate for solid organ injury. It showed normal appearance of the liver, gall bladder, spleen and both kidneys. There was no free fluid in the abdomen. A scan over the swollen area using a 7.5 MHz linear transducer showed discontinuation of the rectus muscle and rectus sheet just inferior to the umbilicus with bowel loops protruding through. The bowel loops lied in the subcutaneous tissue of the anterior abdominal wall. (Fig.1) Motion of the herniated bowel was clearly revealed. A diagnosis of blunt abdominal trauma with traumatic abdominal wall hernia was made. The patient was transferred to the operating room where the operation was performed through a midline incision. There was transverse and vertical tear of the peritoneum, rectus sheet and rectus muscle with herniation of the bowel loops which were parts of the jejunum through the defect. The bowel was contused and there was a small perforation. Bowel resection with end to end anastomosis was done. The post operative course was uneventful.

[1] Department of Radiology, Saraburi hospital

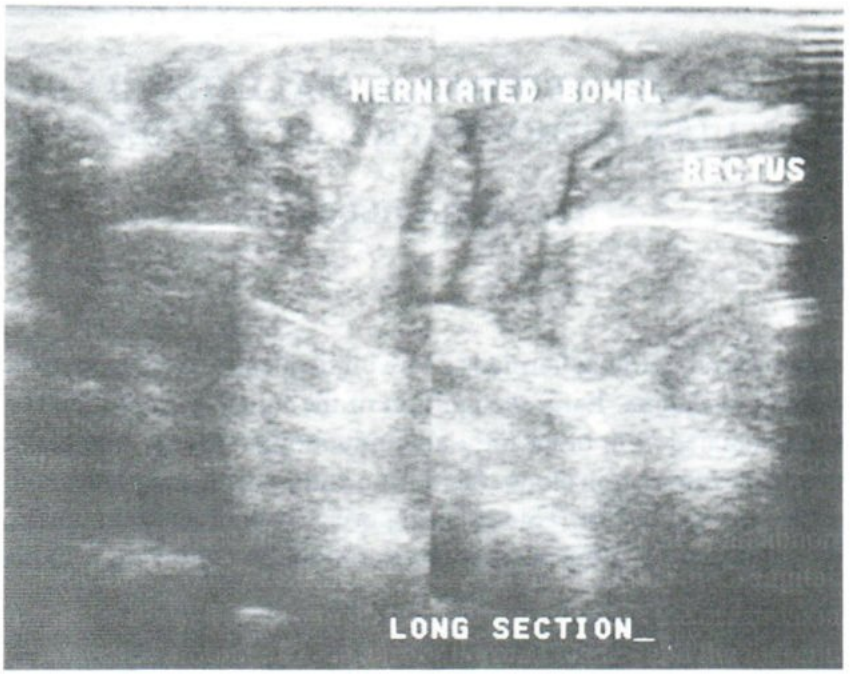

A.

B.

Fig.1 Scan over the mass in both longitudinal(A) and transverse(B) view disclosed discontinuation of the rectus sheet and rectus muscle with herniation of bowel loops through the defect.

DISCUSSION

Blunt trauma of the abdomen is increasing as a consequence of traffic accidents. However, hernia involving anterior abdominal wall following trauma is rare. Guly[1] divided traumatic abdominal wall hernia into two categories, those caused by avulsion of the muscles and tendons from the bone by a shearing force that are distributed across the bony prominence of the pelvis or lower thoracic cage and others occurring through the injuries in muscle or aponeurosis after a direct blow. Metzdorff et al.[2] in 1984 collected only 38 cases of blunt traumatic rupture of the anterior abdominal wall musculature described in literature. Reports in the literature have recorded avulsion of both recti muscles, single rectus muscle, avulsion from the left costal arch, from the ileac crest and pubic bone.[3] Associate injuries were reported in 30 percent of cases.[4] Imaging modalities are needed to evaluate the extent and detail of injury after blunt abdominal trauma. Conventional plain abdominal radiographs, contrast studies or both also are obtained in an effort to diagnose the specific problem. In a certain number of patients, more sophisticated imaging is ultimately required. The development and continued improvement of non invasive cross-sectional imaging modalities have greatly facilitated the diagnosis of many acute abdominal conditions. Ultrasonography (US) is a useful imaging modality to demonstrate free fluid and solid organ injuries. US has several advantages over other diagnostic modalities such as magnetic resonance imaging (MRI) or computed tomography (CT). Real time ultrasonography is a dynamic test that permits the visualization of the structural detail and motion. It can be performed regardless of breathing motion. With other cross-sectional imaging modalities, the patient is asked to lies motionless on an examination table and is then left alone in the scanning room while the examination is performed. The patient is rarely given the opportunity to explain his or her problems. The interactive nature of real time sonography provides advantages for obtaining clinical information important to the diagnosis of the patient's problem during the examination. Recently, high frequency linear array transducers (7.5 and 10 MHz) have become available. These permit much greater insight of the superficial structure and small parts of the body. The technique of directing "ultrasonography palpation" permits the radiologists to establish the area of concern rapidly. In this case, US can demonstrate tear of the rectus muscle and sheet as well as bowel loops that herniated through the injury. The absent of ionizing radiation, short examination time, low cost relative to other modalities, non-invasive character and patient's comfort are the other advantages. It is advisable to integrated US in the line of investigation in case of abdominal trauma.

SUMMARY

A rare case of traumatic abdominal wall hernia caused by blunt abdominal trauma was report. Diagnosis of this condition was made by ultrasonographic examination, which proved to be a convenient and useful imaging modality.

REFERENCES

1. Guly HR, Stewart IP. Traumatic hernia. J Trauma 1983;23:250-252.
2. Metzdorff MT, Miller SH, Smiley P, et al. Blunt traumatic rupture of the abdominal wall musculature. Ann Plast Surg 1984;-13:63-66.
3. Quasim O, Quasabi A, Tandon RC. Traumatic hernia of the abdominal wall. J. Trauma 1988;28:875-876.
4. Chanvitan A, Traumatic abdominal wall hernia: A case report. J Med Ass Thailand 1986;69:343-345.

5. Damschen DD, Landercasper J, Cogbill TH, Stolee RT. Acute traumatic abdominal hernia: case reports. Journal of trauma 1994;36(2):273-6.
6. Dimyan W, Robb MB, MacKay C. Handlebar hernia. J Trauma 1980;20:812-813.
7. Dreyfuss DC, Flancbuam L, Krasna IH, Tell B, Trooskin SZ. Acute trans-rectus traumatic hernia. J Trauma 1986;26:1134-1136

PELVIMETRY BY IMAGING - CURRENT STATUS

[1]BJJ ABDULLAH, [2]S.RAMAN, [3]J..MAHADEVAN, & [4]D. CHIEN.

ABSTRACT

The role of pelvimetry in the management of complicated pregnancy warrants investigation. There is probably agreement that there is a role in the assessment of a breech pregnancy where vaginal delivery is contemplated. Conventional pelvimetry is still carried out in many centers throughout the world. The radiation dose to the fetus and mother has caused concern leading to changes such as the use of intensifying screens, air gap technique, computed tomography (CT) pelvimetry, digital pelvimetry and now magnetic resonance imaging (MRI) pelvimetry. The advantages of MRI have been the absence of radiation, shorter duration of examination and the absence of distortion of measurements from magnification. The ability to define the soft tissue may also be important though this has not yet been determined. One of the major limitations of MRI was the question of cost but this was based on the older longer sequences. Presently with the availability of newer shorter sequences, the examination could be carried-out much faster and therefore should be really cost-effective.

The role of pelvimetry in the management of complicated pregnancy is still uncertain.[1-4] Krishnamurthy et al[4] found that 66% of patients with radiologically inadequate pelvises delivered the next pregnancy vaginally without any problems and that X-ray pelvimetry cannot reliably effectively identify women who cannot delivery vaginally. There needs to be a distinction made between pelvimetry for vertex and breech presentations. It no longer considered to be of any value in the cephalic presentation, where a trial of labour can be allowed in all cases as it is felt that the foetal head is the best pelvimeter.[5] The most important indication is probably in the management of breech deliveries where vaginal delivery is indicated.[6] There may also be a minor role for the assessment of pelvic deformity secondary to trauma or metabolic bone disease.[7] This is in contrast to a resurgence to clinical pelvimetry alone even in breech deliveries[8] though here the subjectivity may be even more than be of practical value[2]. Pelvimetry can either be done antepartum, intrapartum or postpartum. There are several different types of pelvimetry available e.g. clinical, ultrasound, X-ray, computed topographic (CT) and Magnetic Resonance Imaging (MRI). We will discuss only the latter types of radiological pelvimetry.

The first imaging modality used in pelvimetry was film screen X-ray pelvimetry to assess the dimensions of the maternal pelvis. This is still by far the most commonly used modality because of the simplicity, easy access and low cost. Further the relationship of the presenting part to the maternal pelvis is better assessed unlike with CT or MR pelvimetry. The lateral view is the single view done antepartum while the two views (AP

[1,3]DEPARTMENTS OF RADIOLOGY & [2]OBSTRETRICS AND GYNAECOLOGY, FACULTY OF MEDICINE, UNIVERSITY OF MALAYA, & [4]SIEMENS LTD., HONG KONG

Address correspondence to:
BJJ ABDULLAH DEPARTMENT OF RADIOLOGY, UNIVERSITY OF MALAYA MEDICAL CENTER, JALAN UNIVERSITI, 50603-KUALA LUMPUR MALAYSIA TELEPHONE NO 03-7502069 FAX NO 603-7581973

& lateral) are done postpartum. The major disadvantage of X-ray pelvimetry is the presence of ionizing radiation.[9] There is however no threshold to carcinogenesis by ionizing radiation and that the fetus is not less radiosensitive in the third trimester compared to the first.[10] X-ray pelvimetry is a major contributing of ionizing radiation to the foetus. The dose is dependent to a great extent on the radiographic technique e.g. the radiographic exposure factors, area of exposed film as well as the focus film distance. The total dose has been reduced by the use of strict collimation, fast film-screen combinations, as well as the use of a gridless technique. The air-gap technique has been shown to give a similar dose to the average CT lateral scanogram and is potentially a reliable low dose technique.[11] It is also easy to perform with simpler positioning. This may be the choice in patients who may be too large for the CT or MR gantry or places where CT is not available. The interspinous and intertuberous distances measured on the AP views may not be accurate[5] but these differences are not significant. The conjugate diameter appears to be longer during pregnancy than post- or ante-partum. This difference is significant and averages around 5%.[5] The clinical relevance however is questionable. There is also a feeling that the minimum dimensions for X-ray pelvimetry may be too conservative. X-ray pelvimetry is unable to define the soft tissue. There are also inaccuracies of the measurements compared to the sectional imaging modalities especially the bispinous diameter.[5,12] This is caused by numerous factors including rotation of the patient, poor definition of bony landmarks, inaccuracies in correcting for magnification, operator errors in making and recording the measurements. Morever this examination is quite uncomfortable for the patients soon after delivery especially if surgery has been carried out.

Digital X-ray pelvimetry has also been advocated with some centers reporting very low doses.[13] This is dependent on the ease in which to position the patient plus the need for specialized equipment which at the present moment is not easily available.

The next evolution in pelvimetry was the use of CT. This reduced the radiation dose by approximately two-thirds but is still significant.[14,15] This generally requires the use of AP and lateral scouts, the former to measure the anteroposterior dimensions while the latter is used to measure the transverse dimensions. The CT lateral scout gives on the average 25% of the dose compared to a conventional X-ray pelvimetry. The use of axial slices to measure the bispinous diameter is only done when necessary and this contributes to almost the entire dose (approx. 90%). There is therefore no justification for routine use of this view though using very low tube current and a bone algorithm images for measurement may be acquired with a significant reduction in dose (about 20 fold).[11] Another way to avoid using axial images is to correct for magnification of the bispinous diameter on the AP scout when possible.[16] This may be time consuming and require some training. Visibility of the ischial spines on the AP scout can be improved by tilting the CT gantry caudally.[16] In addition the typical location of the ischial spines on the axial is assumed to be at the level of the fovea of the femur though this is not the case in 16% to 35% of cases[11,17] and results in a significant difference in measurements. Thus review of the axial images by the radiologist while the patient is still in the gantry is advised. If the ischial spines are not visible on that slice then a further image needs to be acquired 10mm caudal.

There is also an increased fetal dose from an AP scout which is probably caused by the fetus lying in the direct beam. The radiation dose can be kept to the barest minimum by using a PA scout instead and keeping the milliamperes (X-ray tube current) to the lowest levels[18] since there is a correlation between the energy imparted to patient and the total mAs given.[19] The speed of

table movement also appears to affect the total dose with higher doses with slower speeds i.e. the patient dose from the scouts is inversely related to the table speed.[11] Thus CT is a low dose technique provided that the total mas for the scouts is kept low. This in fact means that CT scanners with slow couch speed and or high mAs may result in similar doses to that of conventional pelvimetry. In addition the accuracy of measurements taken off the scout views need to be verified by using a uniform grid. The other disadvantage is greater cost and sometimes decreased accessibility. Even then the other advantages of CT pelvimetry are that it is more comfortable for the patient, requires a shorter time as well as allowing direct measurements off the console with less distortion.

Ultrasound is a tool widely used in obstetrics. It has the advantage that there is no radiation involved and the safety has been well established. Transvaginal ultrasound pelvimetry has been performed and the cephalopelvic index of diameter (CID) defined as the mean diameter of the mid-pelvis and the foetal biparietal diameter (BPD) seems to be a good predictor of outcome.[19] Although still in the preliminary stages together with the problems of obtaining good measurements in all cases this promises to be an alternative worth considering.

With the greater availability of MR machines, MR pelvimetry is now being increasing used. This modality does not use radiation which is its major advantage. MRI is not advised in the first trimester of pregnancy even though there is no data to suggest that there is any adverse effects to the fetus to the static magnetic fields, the gradient magnetic fields or the radiofrequency pulses.[20] This is not an absolute contraindication and may be carried out if a radiographic procedure would have to be done to reach a diagnosis. In addition its multiplanar capability allows scanning in any plane with the patient lying supine plus its superior soft tissue contrast to identify both bone and soft tissues. Obesity is not a problem with MR pelvimetry unlike x-ray pelvimetry. Further patient positioning is not critical as the scan planes can be adjusted if there is any rotation of the patient. The technique is easy to perform and can be carried out by the radiographers with minimal training. The radiologists only needs to be present in the difficult cases. This is thus a cost-effective strategy.

The measurements can be done straight from the console for all the planes without having any problems with magnification resulting in greater accuracy.[12] MR pelvimetry is also useful when the fetus, cervix, placenta (placental abruption or placenta praevia) or uterus need to be assessed.[21,22] There may also be a role for the assessment of pelvic masses during pregnancy. In addition rather than a small bony pelvis being the cause of failure of progress of labour soft-tissue dystocia seems to be the major factor in obstructed labour.[23] Most of the studies done comparing the value of pelvimetry have used the dimensions of the bony pelvis.[1,2,4-8,13-15,18] In a study done[24] there is a difference of 4.1% to as high as 27.0 % between the soft tissue to soft tissue dimensions to that of bone against bone. The greatest variation is for the transverse and bispinous diameters. MR pelvimetry in conjunction with the ultrasound estimation of fetal weight may play a role in the assessment of soft tissue dystocia.

The disadvantages of MR pelvimetry have been the cost, accessibility (due to the already increasing demands made by the other clinical specialties), availability and the contraindications like the presence of prosthetic heart valves, cardiac pacemakers, etc.. The latter disadvantage is not a major problem in this group of patients. The cost of the examination is partly dependent on the time taken to do the examination and if it can be completed in less than 5 minutes then the cost calculated based solely on time will be approximately 65 US Dollars in our setting. Therefore the actual

cost of MR pelvimetry is not much higher than that of x-ray pelvimetry with the other added benefits especially the absence of radiation and ease of performing.

Review of the literature shows that the scan times are between 5-20 minutes and these were base on gradient echo-sequences and the older spin-echo sequences.[5,12] However with the newer sequences using[24] the fast turbo spin-echo, tru-fisp and 2D gradient echo the total examination time can be reduced to less than 5 minutes with the actual scanning only taking about a minute at the most. The fast spin-echo seems to be the best overall in performance in terms of the presence of artifacts, superior contrast resolution, scanning times as well as the ability to define the cortical bone. This was despite using just the body coil without the use of any relaxants. The sequences used previously have been the T1 Spin echo[5] and T1 weighted gradient echo.[12] Claustrophobia is frequently quoted disadvantage but this has been partly overcome by placing the patient feet first into the bore of the magnet. Large female patients may not be able to get into the bore of the magnet. Another potential source of error which is not clinically important may be related to the inability to identify the junction between the sacrum and first mobile coccygeal segment This is also a problem with X-ray pelvimetry and CT.

Melchert et al[25] have used computer aided simulation of the vaginal delivery from MRI images using finite analysis to understand the dynamics of delivery. Pelvimetry as it is used presently does not reflect the actual dynamics of delivery and does not consider moulding of the fetal head, space requirements of maternal soft tissues, mobility of the pelvic joints (sacroiliac joints and symphysis pubis). They suggest computer aided simulation of the vaginal delivery from MRI images using finite analysis which allows evaluation of pelvimetric data with regards to birth dynamics.

REFERENCES

1. Parsons MT & Specally WN. Prospective randomized study of X-ray pelvimetry in the primigravida. Obstet Gynaecol 1985; 66:76-79
2. Thubisi M, Ebrahim A, Moodley et al. Vaginal delivery after previous caesarean-section: is X-ray pelvimetry necessary? Br J Obstet Gynaecol 1993;100:421-424
3. Morrison JJ, Sinnatamy, Hackett GA, et al. Obstetric pelvimetry in the UK: an appraisal of current practice. Br J Obstet Gynaecol.1995;102:748-750
4. Krishnamurthy S, Fairlie F, Cameron AD et al. The role of postnatal X-ray pelvimetry after caeserian section in the management of subsequent delivery. Br J Obstet Gynaecol 1991;98:716-718
5. van Loon AJ, Mantingh A, Thijn CJP et al. Pelvimetry by magnetic resonance imaging in breech presentation. Am J Obstet Gynecol 1990;163:1256-1260
6. Flanagan TA, Mulchahey KM, Korenbrot CC et al Management of term breech presentation. Am J Obstet Gynaecol 1987; 156:1492-1499
7. Compton AA. Soft tissues and pelvic dystocia. Clin Obstet Gynaecol 1987;30:69
8. Biswas A & Johnstone MJ. Term breech delivery. Aust NZ J Obstet Gynaecol 1993; 33:150-153
9. Boice JD & Land CE. Ionizing radiation. In: Schottenfeld D, Fraumeni JF, eds. Cancer epidemiology and prevention. Philadelphia: WB Saunders, 1982:137-238
10. Mole RH. Childhood cancer after prenatal exposure to diagnostic X-ray examinations in Britain. Br J Cancer 1990;62:171
11. Badr I, Thomas SM, Cotterill D, Pettett A, Oduko JM, Fitzgerald M & Adam EJ. X-ray pelvimetry - Which is the best technique? Clinical Radiology 1997;52:136-141

12. Wright AR, English PT, Cameron HM et al. MR pelvimetry- A Practical alternative. Acta Radiologica 1992;33:582-587
13. Wright DJ, Godding L, Kirkpateick C. Technical note: Digital radiographic pelvimetry - a novel, low dose, accurate technique. The British Journal of Radiology 1995;68:528-530
14. Kopelman JN, Duff P, Karl RT et al. Computed tomography in the evaluation of breech presentation. Obstet Gynacol 1986; 68:455-458
15. Raman S, Samuel D & Suresh K. A com parative study of X-ray pelvimetry and CT pelvimetry. Aust NZ J Obstet Gynaecol 1991;31:217-220
16. Davidson R. CT pelvimetry: a two view approach. Radiograph 1986:33;62-6
17. Federle MA, Cohen HA, Rosenwein MF, Brant-Zawadzki MN, Cann LE. Pelvim etry by digital radiography: a low dose examination. Radiology 1982:143;733-5
18. Weisen EJ, Crass JR, Bello EM et al Improvement in CT pelvimetry. Radiology 1991;178:259
19. Bian XM, Zhuang J, Cheng X. Pelvic measurements by transvaginal ultrasound. Chinese J Med 1991;71:453-454
20. National Radiation Protection Board: Lim its on patient and volunteer exposure dur ing clinical magnetic resonance procedures. Documents of the NRPB, vol 2, no. 1. Her Majesty's Stationary Office, Lon don 1991.
21. McCarthy SM, Filly RA, Stark SM, et al Obstetrical magnetic resonance imaging. Fetal anatomy. Radiology 1985;154:427
22. McCarthy SM, Stark SM, Filly RA, et al Obstetrical magnetic resonance imaging. Maternal anatomy. Radiology 1985;154: 421-426
23. Campbell JA. X-ray pelvimetry. J Natl Med Assoc 1975:68;514-520
24. Abdullah BJJ, Mahadevan J, Raman S & Chien D. Comparison of the various new MRI sequences in pelvimetry (Abs). Advances in MRI-Second I nternational Magnetom Vision User Conference, Rotterdam, June 13-14, 1997
25. Melchert F, Wischnik & Nalepa E. The prevention of birth trauma by means of computer aided simulation of the delivery by means of the nuclear magnetic resonance imaging and finite element analysis. J Obstet Gynaecol 1995;21:195-207

Message from

Professor Dr. Kawee Tungsubutra

Editor-in-Chief, The Asean Journal of Radiology.

This is the fourth year of the Asean Journal of Radiology.

We have another 2 years to prove that we have the co-operation among radiologists from all countries in Asia and outside Asia to maintain the quality of the Journal.

In this volume we have a variety of the topics covering all sub-specialities of Radiology from Thailand, Malaysia and Philippines.

We hope, we will be accepted to be in the Index Medicus after the end of the fifth year.

Kawee Tungsubutra
January-April 1998.

AAR Journal of Radiology
for Authors

Instructions

1. The AAR Journal of Radiology publishes the papers on Radiological Sciences, such as research work, review articles, case reports, innovations in Medical Sciences related to all branches of Radiology, and letters to the editor. The aforementioned materials can be written in English only.

2. The authors have to submit 2 copies of the manuscript and a diskette: **to Prof. Dr. Kawee Tungsubutra,** 318 Kaweevej Hospital, Tarksin Road, Dhonburi, Bangkok 10600, Thailand. **or to the Associate Editors** at the Radiological Society of Malaysia, Indonesia, Philippine, Singapore and Brunei. The names and adresses of the Associate Editors in each country were published in the front page of this Journal.

3. The original copy to be submitted must be typed in a double space on one side of the page of 8.1/2"x 11.1/2" paper.

4. The format of the article must include :

a. Title page and address of the author (s)
b. Abstract
c. Introduction (Background)
d. Material and Method
e. Results and discussion (Tables and Illustrations)
f. Acknowledgement (if any)
g. References (Follow the Vancouver style developed by ICMJE)

5. We will provide 25 copies of reprints for the author (s) who submit (s) an article for publication in the AAR Journal.

6. The illustrations and tables must be clearly prepared with legends in English as they are the art works to be reproduced.

7. The authors are responsible for the contents of the article as to its facts and findings.

8. Ethics.

Paper reporting studies which might be interpreted as human experimentation (e.g. controlled trials) should conform to the standards of the Declaration of Helsinki (see British Medical Journal 1964:2:177) and should indicate that, approval that such studies may proceed, has been granted by the local or hospital Ethics Committee.

When reporting experiments on animals indicate whether the institution's or the National Research Council's guide for, or any national law on, the care and use of laboratory animals was followed.

บริษัท กรุงสิทธิวรรณ จำกัด
SONGSITTIVAN CO.,LTD.
TEL. 585-3233, 587-5292, 910-1888, 910-1999 FAX. 587-2084, 910-1888